UNIVERSITÉ DE MONTRÉAL

A PRACTICAL APPROACH TO MODEL PREDICTIVE CONTROL (MPC) FOR SOLAR COMMUNITIES

HUMBERTO QUINTANA

DÉPARTEMENT DE GÉNIE MÉCANIQUE

ÉCOLE POLYTECHNIQUE DE MONTRÉAL

MÉMOIRE PRÉSENTÉ EN VUE DE L'OBTENTION

DU DIPLÔME DE MAÎTRISE ÈS SCIENCES APPLIQUÉES

(GÉNIE MÉCANIQUE)

JUIN 2013

UNIVERSITÉ DE MONTRÉAL

ÉCOLE POLYTECHNIQUE DE MONTRÉAL

Ce mémoire intitulé:

A PRACTICAL APPROACH TO MODEL PREDICTIVE CONTROL (MPC) FOR SOLAR COMMUNITIES

présenté par : QUINTANA Humberto

en vue de l'obtention du diplôme de : Maîtrise ès sciences appliquées

a été dûment accepté par le jury d'examen constitué de :

M. BERNIER Michel, Ph.D, président

M. KUMMERT Michaël, Ph.D., membre et directeur de recherche

M. SIBBITT Bruce, M.A.Sc., membre

To my mother and mis abuelitos

ACKNOWLEDGEMENTS

It is curious that this page is the first one with prose when in the actual chronological order it is the last one. This is the personal touch that takes the mind away from the technical facts and allows remembering the path that has been followed and the people who were there for guiding, sharing, cheering or just observing. Please grant me the licence to be a bit informal on this page.

First of all, a Big Thank You to my supervisor Michaël Kummert for the opportunity to work with him, his knowledge and positive attitude are inspiring (and his feedback very much needed). Same Big gratitude goes for Professor Michel Bernier; it has been an honor to be part of his group on Mécanique de Bâtiments (MecBat) at Polytechnique-Montréal. I also want to thank to Professor Alberto Teyssedou, Professor Oumarou Savadogo and Jean-François Desgroseillers, also from Polytechnique, for their advice and teachings.

Thanks to the SNEBRN research network for the funding for this research, and to John Kokko (Enermodal) and Bill Wong (SAIC-Canada) for making available all the needed documentation. At Natural Resources Canada, my appreciation goes to Doug McClenahan and Bruce Sibbitt for the interest on the development of this work; without the data, documents and feedback they provided, this research would have been impossible to carry out. I'm also grateful to Angela, David, Matt, Tim and Jeff from TESS for looking after me during my internship at their headquarters.

A special recognition to my hard-working colleagues in the MecBat team for their openness, cooperation and professionalism: Ali, Antoine, Aurélie, Benoit, Chiara, Katherine, Marilyne, Massimo, Mathieu(s), Mathilde, Roman, Parham, Yannick, and Vivien. Thanks to my brother, the family artist, for his help with certain figures. Special hugs travel the distance to reach my mother, my sisters, and my cousins, aunts and uncles; your love is very important in my life. Anna, Denise, Emmanuelle, Lidia, Maria Elena, Milena, Mónica, Verónica, Daniel, Edwin, Enrique, Harold, Juan Carlos, Ricardo, Sebastian and Thibaut; your support was also part of me achieving this goal.

Finally, a thankful smile to all those persons that may be never read this document but that directly or indirectly influenced my decisions, my thoughts and my motivation. In the same way, I hope this work will eventually have a positive influence in society.

RÉSUMÉ

Les réseaux de chaleur solaire (SDH pour Solar District Heating) font partie des solutions pour réduire la consommation d'énergie et les émissions de Gaz à Effet de Serre (GES) dues aux besoins de chauffage. Ce type d'installation permet de profiter des effets d'économie d'échelle et des avantages d'avoir un système centralisé qui facilite l'intégration de l'énergie solaire pour réduire la dépendance aux carburants fossiles. Un système SDH est un concept éprouvé qui peut être complémenté avec l'ajout de stockage à long terme de l'énergie thermique pour compenser le décalage dans le temps entre l'offre d'énergie solaire et la demande de la charge de chauffage. Ces systèmes sont surtout déployés en Europe; au Canada, la seule installation de SDH est la communauté solaire Drake Landing (DLSC pour Drake Landing Solar Community). Ce projet, qui comprend du stockage saisonnier (BTES pour Borehole Thermal Energy Storage), a été un grand succès, il a atteint 95% de fraction solaire à la cinquième année d'opération.

Un système SDH ne peut être complet sans un système de commande qui coordonne le fonctionnement et l'interaction des composants de l'installation. Le contrôle est basé sur un ensemble de règles qui prennent en considération l'état interne du système et les conditions extérieures pour garantir le confort des occupants avec un minimum de consommation de combustibles fossiles. Ce projet de recherche se concentre principalement sur la conception et l'évaluation des nouveaux mécanismes de commande visant à l'augmentation de l'efficacité énergétique globale des systèmes SDH. L'étude de cas est le projet DLSC, et les stratégies de commande proposées sont basées sur l'application pratique des concepts de la Commande Prédictive basée sur des Modèles (MPC pour Model Predictive Control).

Un modèle calibré de DLSC qui inclut les stratégies de commande a été développé dans TRNSYS, en s'appuyant sur le modèle utilisé pour les études de conception. Le modèle a été amélioré et de nouveaux composants ont été créés. Le processus de calibration a montré un très bon accord pour les indices annuels de performance énergétique (2% pour la consommation de gaz et pour la partie solaire de l'énergie thermique livrée au réseau de chaleur et, 5% pour la consommation d'électricité).

Les stratégies de commande proposées ont été conçues pour modifier quatre aspects du système du commande actuel: les paramètres qui définissent l'interaction entre le stockage de court terme

(STTS pour Short-Term Thermal Storage) et le BTES ont été optimisés pour faire en sorte que le STTS maintient un niveau plus élevé de charge lorsque le système est en mode *hiver*; une deuxième stratégie de contrôle oblige la décharge du BTES lorsque les conditions météorologiques prévues indiquent une forte charge de chauffage et/ou un rayonnement solaire réduit; les deux dernières stratégies ciblent la consommation d'électricité dans la boucle solaire et la boucle BTES en modulant la vitesse des pompes. Les résultats montrent que l'efficacité énergétique peut être améliorée d'environ 5% lorsque ces stratégies de commande sont utilisées avec des prévisions météorologiques *parfaites*.

ABSTRACT

Solar district heating (SDH) systems are part of the solution to reduce energy consumption and GHG emissions required for space heating. This kind of installation takes advantage of the convenience of a centralized system and of solar energy to reduce dependency on fossil-fuels. An SDH system is a proven concept that can be enhanced with the addition of long-term thermal energy storage to compensate the seasonal disparity between solar energy supply and heating load demand. These systems are especially deployed in Europe. In Canada, the only SDH installation is the Drake Landing Solar Community (DLSC). This project, which includes seasonal storage (Borehole Thermal Energy Storage-BTES), has been a remarkable success, reaching a solar fraction of 97% by the fifth year of operation.

An SDH system cannot be complete without an appropriate supervisory control that coordinates the operation and interaction of system components. The control is based on a set of rules that must consider the system's internal status and external conditions to guarantee occupant comfort with minimal fossil-fuels consumption. This research project is mainly focused on conceiving and assessing new control mechanisms aiming towards an increase of SDH systems' overall energy efficiency. The case study is the DLSC plant, and the proposed control strategies are based on the practical application of Model Predictive Control (MPC) theory.

A calibrated model of DLSC including the supervisory control strategies was developed in TRNSYS, building upon the model used for design studies. The model was improved and new components were created when needed. The calibration process delivered a very good agreement for the most important yearly energy performance indices (2 % for solar heat input to the district and for gas consumption, and 5 % for electricity use).

Proposed control strategies were conceived for modifying four aspects of the current control: the parameters that define the interaction between the Short-Term Thermal Storage (STTS) and the BTES have been optimized so the STTS keeps a higher level of charge in winter-mode operation; a second control strategy forces the BTES discharge when anticipated weather conditions indicate a high heating load and/or reduced solar irradiation; the last two strategies target electricity consumption in the solar loop and the BTES loop by modulating the pumps speeds. Results show that energy efficiency when these control strategies are applied altogether can be improved by about 5% when using *perfect* forecasts as model's input.

CONTENTS

LIST OF TABLES

LIST OF FIGURES

LIST OF APPENDICES

NOMENCLATURE AND ABBREVIATIONS

ACL	See STTS ACL
ATES	Aquifer Thermal Energy Storage
BTES	Borehole Thermal Energy Storage
CLO	Closed-Loop Optimization
CSHP	Central Solar Heating Plant
CSHPDS	Central Solar Heating Plant with Diurnal Storage
CSHPSS	Central Solar Heating Plant with Seasonal Storage
CSHPxS	Central Solar Heating Plant with no Storage
CTBO	Continuous Time Block Optimization
CWEC	Canadian Weather for Energy Calculations
Delta T (ΔT)	Temperature difference between collectors' inlet and outlet
DLSC	Drake Landing Solar Community
DLSP	District Loop Set Point
DST	Duct Ground Heat Storage model
FLL	Future Load Limit
FRC	Force BTES discharge
GenOpt	Generic Optimization software
GHX	Ground Heat Exchanger
HVAC	Heating, Ventilation, Air Conditioning
MaxLoad	Maximum (District) Load threshold
MinUE	Minimum Usable (Solar) Energy threshold
MPC	Model Predictive Control
SF	Solar Fraction

SDH	Solar District Heating
SDHW	Solar Domestic Heat Water
STD	Current control strategy for DLSC
STES	Seasonal Thermal Energy Storage
STTS	Short-Term Thermal Storage
STTS ACL	Short-Term Thermal Storage Absolute Charge Level
TRNSYS	TRaNsient SYStems software
WGTES	Water-Gravel Thermal Energy Storage
WSF	Weighted Solar Fraction
WTES	Water Thermal Energy Storage

CONTROL STRATEGIES TERMINOLOGY

Table 0.1: Control strategies terminology

Brief description	Added/Modified Control Parameters	Applied in chapter
STD		
Reference (standard) control strategy		5
STD+		
STD with optimized control parameters	Winter BTES Charge Factor, Winter BTES Discharge Factor	5
FRC		
Force BTES discharge for extreme weather conditions	Thresholds to force BTES discharge: Min. Usable Solar Energy (*minUE*), Max. District Load (*maxL*) for six scenarios	5
FRC+		
Combines STD+ and FRC	Parameters of both STD and FRC	5, 6
Solar loop		
Set different values for the temperature difference (Delta T), between collector's inlet and outlet, that modulates pump speed	Four cases for *Delta T* based on STTS status (STTS ACL)	6
BTES loop pump		
Pump speed proportional to STTS status (STTS ACL). Two different conditions depending whether forecast load is normal/moderated or very high	Two cases based on forecast load for *ACLmin* and *ACLmax*	6

INTRODUCTION

In 2010, residential and commercial space heating accounted for 16% of total energy consumption in Canada and 14 % (66.4 Mt CO_2) of the country's greenhouse gas emissions (Natural Resources Canada, 2012b). To achieve a significant reduction of these contributions, energy efficiency measures must be supplemented with on-site renewable energy conversion.

Solar thermal energy is one of the promising technologies to achieve a high fraction of renewable energy in the built environment, but capital cost represents a significant barrier to its wider deployment in new and existing buildings.

Solar district heating (SDH) systems can deliver economies of scale for equipment and control systems and bring solar heat to individual buildings for space heating and domestic hot water. Unfortunately, solar energy, as other alternative energy sources, suffers a lack of synchronization between demand and supply; more specifically, for space heating the demand is higher during winter months when solar irradiation is lower. A high solar fraction (high share of solar energy in the total heat delivered to the buildings) can only be achieved by using seasonal thermal energy storage – to store the *excess* of solar thermal energy during summer time – and by the implementation of advanced control strategies for better system management.

The potential of SDH systems and the challenges in implementing them have been recognized by the International Energy Agency Solar Heating and Cooling programme (IEA-SHC), which oversees Task 45, a large Research and Development effort about large solar heating/cooling, seasonal storage and heat pumps "to assist in the development of a worldwide strong and sustainable market of large solar heating and cooling systems by focusing on cost effectiveness, high performance and reliability of systems" (Nielsen, 2012). In Canada, considerable research in the area is supported by the Smart Net-zero Energy Building Research Network (SNEBRN) with its research themes III (Mid-to Long-Term Thermal Storage for Buildings and Communities) and IV (Smart Building Operating Strategies) (SNEBRN, 2013).

SDH systems have been deployed successfully throughout the world with already more than one hundred systems operating in European countries; a complete list can be found in the website of the Solar District Heating (SDH) organization (SDH, 2013). Under the leadership of Natural Resources Canada, the first Canadian system is the Drake Landing Solar Community (DLSC)

located in Okotoks, Alberta (Wong et al., 2007). The DLSC plant is the case study for this research.

Problem definition

Besides selecting the appropriate component sizes, improving energy performance relies to some extent on an effective supervisory control system designed to manage, among others, the interactions between the Short-Term Thermal Storage (STTS) and the long-term seasonal storage (Borehole Thermal Energy Storage, BTES). In the case of the DLSC control strategy, STTS-BTES control follows an indirect approach for estimating current and near-future heating needs based on current temperature and time of day. Nevertheless, very low ambient temperatures (or a rapid temperature drop), low solar irradiation periods, and low BTES temperatures can lead to cases when the STTS is unable to supply all the needed heat to the district loop.

Another characteristic of the current control is the priority given to solar fraction which basically translates to a diminution of gas consumption. Under some circumstances – related to energy prices and/or CO_2 emissions reduction – priority could be shifted to reduce electricity consumption rather than gas usage.

The paragraphs above lead to the following research questions:

- Can the long-term system performance be improved if the STTS-BTES control strategy is able to anticipate extreme weather events and to adapt the charge/discharge operation accordingly?
- Is it possible for the control strategy to take into account the electricity consumption in addition to the (heat-based) solar fraction so that operating costs (or CO_2 emissions if that is desired) can be optimized?
- Can MPC principles be integrated at different levels in SDH systems (supervisory control, local pump speed control)?

Objectives and scope

The objectives of the project are:

- Develop a calibrated model of DSLC suitable for MPC studies

- Develop new control strategies based on Model Predictive Control (MPC) to increase the energy performance of solar communities and reduce their operating costs.
- Assess the potential of MPC to optimize the supervisory control strategy managing the short-term and long-term thermal storage.
- Assess the potential of MPC to further reduce operating costs by controlling variable speed pumps.

The supervisory control system consists of rules, parameters and set-points for the different system components and fluid circuits. The introduction of new control strategies was limited to the components and circuits being perceived as the ones having a direct impact on reaching the aforementioned objectives.

Methodology

Initial steps consisted of gathering and understanding all possible information about the case study (DLSC); this included articles, reports, schemas, internal documents and most importantly: monitored data for five year of operation and an out-dated – but very useful and instructive – system model implemented in TRNSYS.

The collected documents and data allowed to calibrate the community's TRNSYS model and to provide the measured weather and heating load to simulations. After this process, potential improvements to the control strategy were identified and alternative controls with predictive features were devised. The method used to build on the existing controller rules and take into account the predicted system behaviour is explained in Chapter 3.

The conceived control strategies were first tested by trial and error to validate their relevance and to identify the control parameters suitable for optimization. In a second step, optimization and tune up of the predictive strategies was performed using measured data as *perfect* forecasts for weather and heating load. The generic optimization tool GenOpt was employed to evaluate the control strategies parameters that minimize the combined consumption of gas and electricity for different periods of simulated system operation. In the last step, two different MPC approaches were implemented to optimize the control strategies altogether.

Thesis outline

There are six chapters in this thesis. The first one is a literature review oriented to covering the topics of solar district heating, seasonal storage and control methods, especially Model Predictive Control. The second chapter presents the system used as case study, the Drake Landing Solar Community (DLSC). The third chapter presents the methodology and briefly introduces the proposed control strategies and the concepts applied during the different phases of the project. Chapter four details the process followed to obtain a calibrated TRNSYS DLSC model starting from the original model; this included the development of two new TRNSYS components. Next two chapters introduce and discuss the results of using Model Predictive Control (MPC) for the new control strategies intended to increase overall energy performance during system operation; chapter five describes a control add-on (FRC) that forces the discharge of the seasonal storage in order to have thermal energy more readily available for heating needs; chapter six shows the integration of this add-on with control strategies aimed to reduce pump electricity consumption.

CHAPTER 1 LITERATURE REVIEW

This chapter describes the concept of *solar communities*, also known as *solar heating districts*, and explores the developments for seasonal storage and supervisory control for such systems. Model Predictive Control theory and applications are also especially reviewed to illustrate its potential and limitations.

1.1 Solar Communities / Solar District Heating Systems

A district heating system provides heat from a centralized point to residential or commercial areas to satisfy the demands for space heating and/or hot water. The heat production can be from different sources: gas, biomass, solar, geothermal, co-generation or any combination of them. District heating systems have some advantages over individual heating systems, especially for high density areas or buildings. When using co-generation the energy efficiency of the overall plant is increased due to the utilization of the waste heat for the district (District Heating, 2013).

The oldest systems for heat distribution can be traced to the ancient Romans; they used underground tunnels called hypocausts to circulate hot air to heat homes. In modern times, it was in 1877 that the engineer Birdsill Holly conceived the first heating district for Lockport (New York); the system drew a lot of attention and it was soon followed with more plants in the U.S. In Europe, the development of heating districts started as early as 1921 in Hamburg; the system was so successful that by 1938 it was expanded to provide 30 times the initial heat. Similar growth was observed in other countries (Turping, 1966). Nowadays, there are district heating systems in Asian, European and North-American cities, such as the one in downtown Montreal (operating since 1947), which serves 20 large buildings including commercial, residential and institutional customers (Dalkia, 2010).

In the case of solar communities, also known as Solar District Heating (SDH) systems or Central Solar Heating Plants (CSHP), one if the heat sources is obviously the sun's radiation. The Solar District Heating organization (http://www.solar-district-heating.eu) lists in its European database only the larger plants consisting of more than 500 m^2 of solar collectors' area.

The first SDH projects emerged at the end of the 70's in Sweden, The Netherlands and Denmark. Some of the systems were intended for research purposes so to set the foundations for further projects. In the 90's, Germany and Austria grew more interested in these kinds of systems and

more than 100 plants have been built since. In 2010, there were more than 130 SDH systems worldwide, 240 000 m^2 of solar collectors, with Sweden and Germany leading. Putting these numbers in context, they only represent 1% of the total of solar collector area installed for solar thermal systems (Dalenback, 2009).

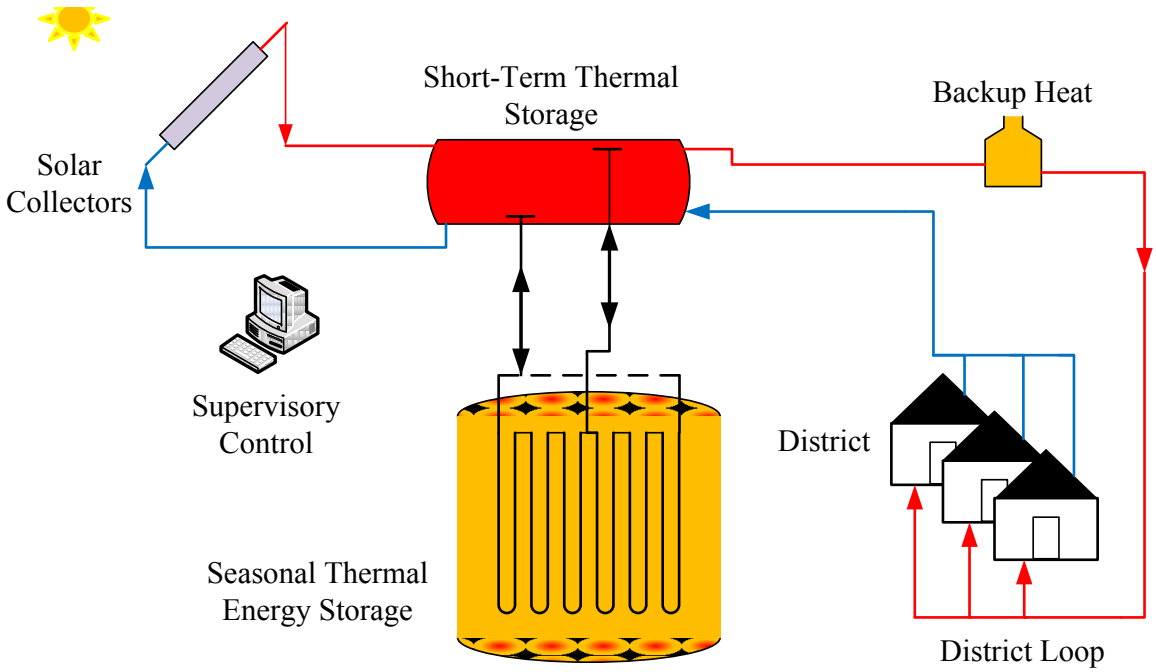

Figure 1-1: SDH system components

The main components of a SDH system are depicted on Figure 1-1:

Heating district: It is the *raison d'être* of the system. It can consist of individual homes or blocks of apartments. District dwellings are fed with hot water for space heating and/or domestic hot water needs.

Solar Collectors: Capture and transfer solar radiation to a heat carrier fluid which is flowing between them and the short-term storage. In the Northern Hemisphere, to get the best solar irradiation conditions through the year, they are usually oriented towards the south, and tilted the same amount of degrees as the location's latitude. They can be installed on the roofs or in a separate parcel of land if available. In the latter case, they can also serve other purposes, for example as a sound barrier, as seen in some projects in Germany.

Short-Term Thermal Storage (STTS): It is a temporary storage of thermal energy coming from the collectors on the way to the users and/or to long-term storage (if available). When heating needs arise in the district, the STTS retrieves thermal energy from the long-term storage when its own state of charge in not enough. The STTS is an optional thermal buffer typically used when the long-term storage exhibits low heat transfer rate or when there is no long-term storage (e.g. systems with a low solar fraction).

Seasonal (long-term) Thermal Energy Storage (STES): It is an optional component that allows increasing solar energy performance by storing the excess of solar energy during the summer and shoulder months to make it available through the winter time. Solar Heating Districts including this component are called Central Solar Heating Plants with Seasonal Storage (CSHP**SS**). More details about seasonal thermal energy storage will be presented in section 1.2.

Backup heat: It is activated when the temperature of the water going to the district is not enough to fulfill the heating needs. In Figure 1-1 a centralized gas boiler is depicted.

District Loop: It is the heat distribution network that carries hot water to the homes and brings back the colder water to the plant. In some installations it is used as an alternative means of diurnal storage.

Supervisory Control: It is the *brain* of the plant. It controls the operation by adjusting pumps and valves to transfer thermal energy among the components according to system status and heating needs. Further description and review of the Control component is available in section 0.

1.1.1 Solar Fraction

To quantify solar energy performance in solar districts, the most common measure is the Solar Fraction (SF), usually defined as the ratio between the amount of solar energy delivered to the district and the total energy consumption for district needs. When SDH systems do not have seasonal storage (CSHP**xS**), or only have diurnal storage (CSHP**DS**), the SF is usually low (between 10% - 20%), because collected solar thermal energy in winter cannot cope with the increased heat consumption. On the other hand, CSHPSS plants can attain 70% of solar fraction the cases where they are built to provide space heating and domestic hot water (Fisch, Guigas, & Dalenbäck, 1998). Solar fraction can be even higher (more than 90%) for CSHPSS's designed for

space heating only (Sibbitt et al., 2012). It is important to mention that initial costs also increase when seasonal storage is considered for the plant.

1.1.2 SDH in Europe

Most solar district heating systems are found in Europe. A complete list is available at the Solar District Heating organization database (SDH, 2013). From that list, a few plants in Denmark, Germany and Sweden will be described shortly. Here, the focus is on those having what is known as Borehole Thermal Energy Storage (BTES), the same type of seasonal storage as used in the case study. BTES details of two of these systems are listed along with the case study in Table 1.1.

A review of existing projects in Denmark can be found in Heller (2000). The following comparison shows the evolution of these systems:

Saltum (operates since 1988): With 1 000 m^2 of solar collectors, it is the oldest plant installed in Denmark (and one of the oldest in Europe) still operating. Its solar fraction is very low (4%) in part due to the lack of seasonal storage.

Marstal I (since 1996): 18 300 m^2 of solar collectors and diurnal storage. The system reached 12% of solar fraction before being upgraded.

Marstal II (upgrade in 1998): Includes a Water Thermal Energy Storage (WTES) as seasonal storage. Solar fraction is increased to 25%.

Brædstrup (since 2007, upgraded in 2012): Its collectors area of 18 600 m^2 is the largest in Europe. The expected share of heat load is 20% (Brædstrup SolPark, 2012); with a projected BTES storage the target is a long-term solar fraction of 50% (PlanEnergi, 2010).

Information for most of Denmark's plants, including current status, operational and economic data can be found online at http://solvarmedata.dk.

In the case of Germany, Bauer et al. (2010) compare the most important plants with seasonal heat storage. The installations with BTES storage are:

Neckarsulm (since 1977): 5 570 m^2 of solar collectors and a solar fraction (SF) close to 40%.

Crailsheim (since 2003): 7 300 m2 of solar collectors. SF is planned to be 50% in the long-term, currently it is 36% (Nussbicker & Druck, 2012).

In Sweden, the district of Anneberg is operating since 2002. The collector array's area is 2 400 m^2 and seasonal storage is of BTES-type. Solar fraction was projected to be 70% in 5 years (Lundh & Dalenbäck, 2008); however, it has stayed around 40% (Heier et al., 2011).

1.1.3 SDH Worldwide

The case study, Drake Landing Solar Community (DLSC) in Okotoks (Alberta, Canada), with a collector array of 2 300 m^2 and BTES storage, reached more than 95% SF in its 5th year of operation (Sibbitt et al., 2012). Chapter 1 gives more details about the case study, its operation and modelling.

Solar heating district projects are not limited to Europe and Canada. In South Korea, a feasibility study for a CSHPSS project in Cheju Island was conducted by Chung, Park & Yoon (1998); more recently, in 2011, a 1 000 m^2 array plant started operations, providing hot water to a hospital (http://www.solarthermalworld.org/content/south-korea-hospital-receives-1040-m2-large-scale-collectors).

In China, some cities, including Beijing, are passing laws mandating Solar Domestic Heat Water (SDHW) systems for new residential blocks (of up 12 floors) where no waste heat is employed for heating water (http://www.solarthermalworld.org/content/china-beijing-mandates-solar-hot-water-systems).

In 2012, Saudi Arabia inaugurated what is the biggest solar plant as of March 2013: 36 000 m^2 of collectors (almost double as much as Brædstrup) for providing domestic hot water to 40 000 students in the *Princess Noura Bint Abdul Rahman* University campus in Riyadh (http://www.solarthermalworld.org/content/saudi-arabia-worlds-biggest-solar-thermal-plant-operation).

1.2 Seasonal Thermal Energy Storage (STES)

For solar district heating in countries north or south of tropical latitudes, STES is fundamental to overcome the seasonal imbalance between heating needs and amount of solar radiation. With seasonal thermal storage, it is possible to provide in winter some of the heat stored during the summer. In Europe, 21 out of 86 solar heating districts have seasonal storage (SDH, 2013).

Hadorn (1988) is considered as a seminal reference for seasonal storage; he presents heat storage principles and types along with analytical and numerical methods for modelling and design. The heat storage categories are:

Sensible heat storage: There is no phase change in the substance used for storage, e.g. hot water. It is the simplest and most common way to store heat. All the European plants with seasonal storage listed in the Solar District Heating organization database (SDH, 2013) have some variant of this category.

Latent heat storage: There is a phase change when heat is stored or recovered. They have much higher energy density than the sensible heat type (100-200 times), but their implementation is more difficult due to hysteresis in the phase change cycle and slower thermal energy transfer. A study about using ice slurry as latent storage material can be found in Tamasauskas et al. (2012)

Chemical heat storage: Uses reversible chemical reactions where there are virtually no heat losses. The energy density is even higher, – about 10 times that of latent heat storage. There has been some research in the field but no practical applications at district level were found.

The most commonly employed technologies for solar seasonal storage are underground systems based on the principle of sensible heat, using water and/or earth. Pavlov & Olesen (2011) compare and summarize the results from different European CSHPSS systems, with focus in the seasonal storage role. Schmidt et al. (2004) present and define the following types identified in Figure 1-2:

> "Hot-water heat storage (also known as Water Thermal Energy Storage-WTES, or simply Water Tank Storage): The water-filled tank construction of usually reinforced concrete is totally or partly embedded into the ground.
>
> Gravel-water heat storage (also known as Water-Gravel Thermal Energy Storage-WGTES or Water Gravel Pit Storage): A pit with a watertight plastic liner is filled with a gravel–water mixture forming the storage material.
>
> Aquifer heat storage (also known as Aquifer Thermal Energy Storage-ATES): Aquifers are below-ground widely distributed sand, gravel, sandstone or limestone layers with high hydraulic conductivity which are filled with groundwater.

Duct heat storage (also known as Borehole Thermal Energy Storage-BTES): Heat is stored directly into the ground. Heat is charged or discharged by vertical borehole heat exchangers which are installed into a depth of 30 - 100 m below ground surface."

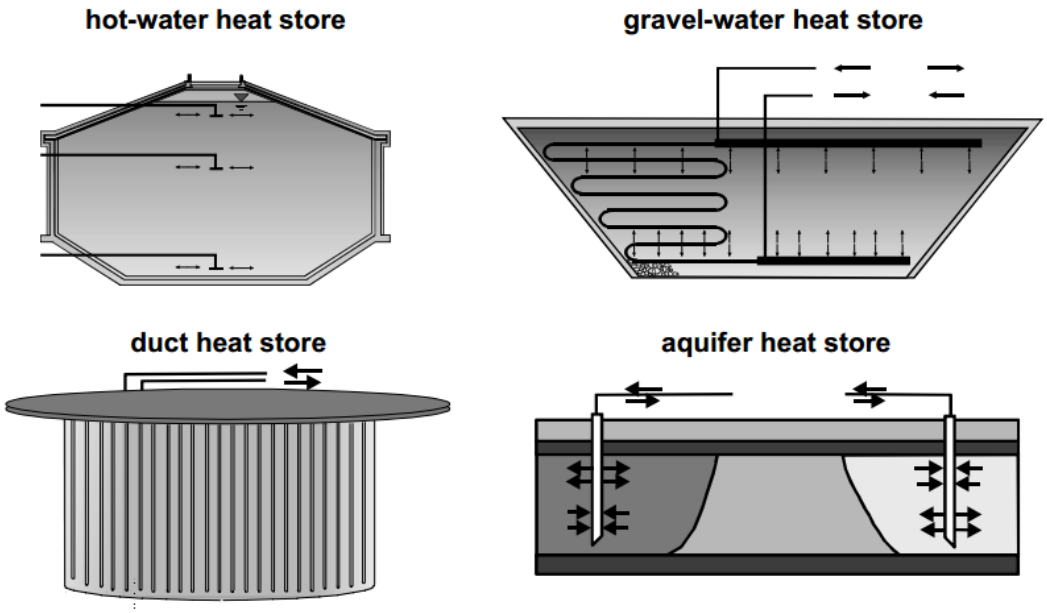

Figure 1-2: Underground thermal energy storage types (Schmidt et al., 2004. With permission from Elsevier)

ATES and BTES systems cost less but they require additional components (e.g. Buffer storage) and depend on geological conditions (Schmidt & Miedaner, 2012). Roth (2009) stresses the impact of seasonal storage size: storage capacity increases linearly with volume, while thermal losses depend only on area.

1.2.1 Borehole Thermal Energy Storage (BTES)

This type of storage uses the ground (soil) as the sensible heat storage medium. It is based on the concept of Geothermal Heat Exchanger (GHX) where a fluid circulating through buried pipe(s) exchanges (delivers or absorbs) heat with the surrounding earth. A typical borehole in a vertical GHX can be seen in Figure 1-3 (left). The pipe(s) inside the boreholes can be placed in different configurations depending on the design (Figure 1-3, right – note that the layout of supply and return pipes can be different). Single U-pipe is the technology employed in Drake Landing.

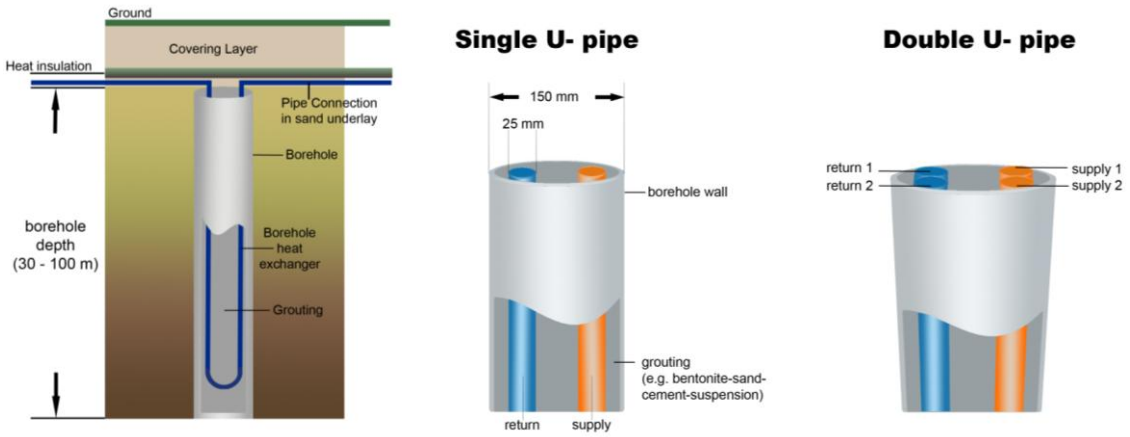

Figure 1-3: Vertical section of borehole heat exchangers (left) and common types (right)

In seasonal storage configurations with single U-pipe, borehole pipes are usually serially connected by horizontal pipes from the center to the edge, in order to induce a thermal stratification from the centre to the periphery. The whole storage volume consists of several of these serial branches arrange in a radial way. The charge process circulates water from the center to the edge, making the center hotter than the periphery. During the discharge process the flow is reversed and water from the edge becomes warmer when going through the center (Figure 1-4).

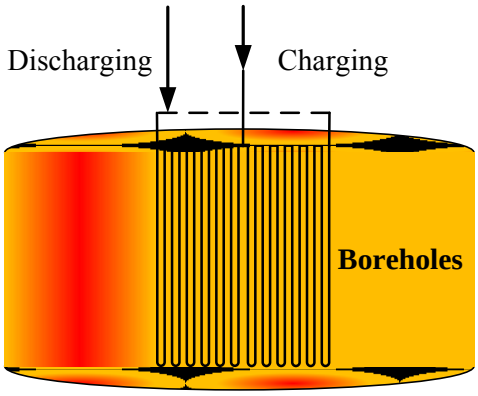

Figure 1-4: BTES flow and boreholes connection

Verstraete (2013) and Verstraete & Bernier (2013) propose and evaluate a double U-pipe storage for solar communities based on the Drake Landing case. As seen in Figure 1-5, there are 2 independent circuits, one connected to the solar collectors for charging the BTES and the other to

the district loop for the heating load. One of the advantages of this configuration is the absence of a Short-term thermal storage (STTS) leading to simplified control rules.

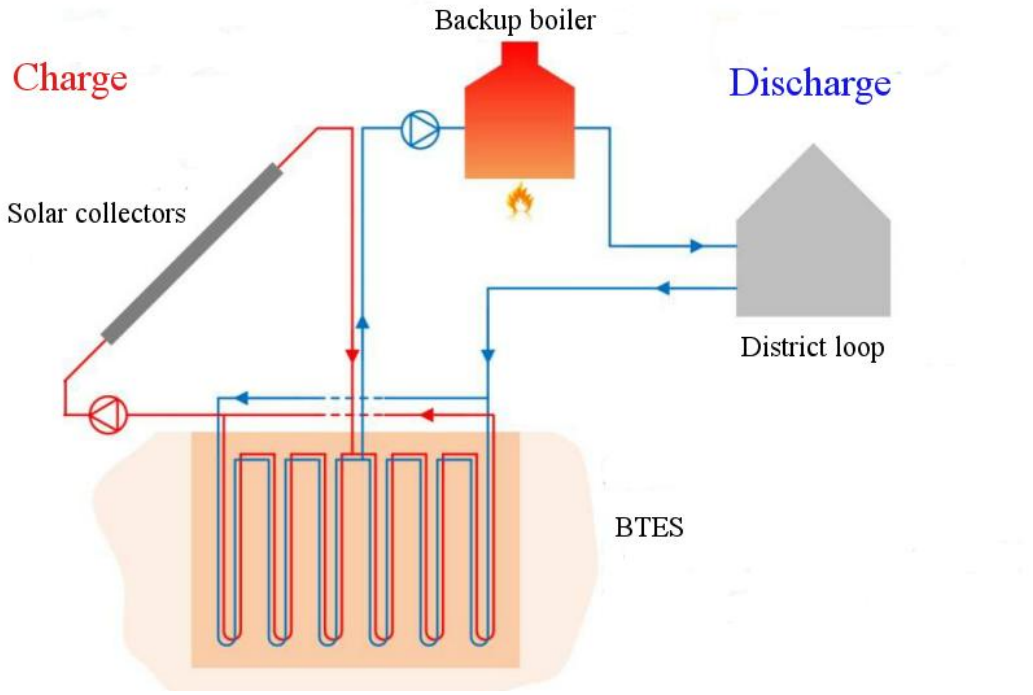

Figure 1-5: BTES with double U-Pipe (Adapted from Verstraete, 2013)

1.2.1.1 Models

The physical phenomena governing these systems have been studied and modelled by different authors. According to the review by Yang, Cui & Fang (2010) the heat transfer analysis has to consider two regions: inside and outside the borehole. For the heat transfer inside the borehole there are one-dimensional, two-dimensional and quasi-three dimensional models. For conduction outside the borehole, they list the following main models:

Kelvin's infinite line source (Ingersoll et al., 1950) is the simplest one. It represents the borehole as one infinite line source where only the (one-dimension) radial heat conduction process is considered. The model is very simple and fast to compute but it is limited to applications within short-time intervals.

Cylindrical Heat Source (CHS) (Carslaw & Jaeger, 1959; Ingersoll et al., 1950) models the borehole as an infinite cylinder within a homogeneous medium. The interaction between the

borehole and the surroundings is also one-dimensional and limited to heat conduction only. This model is more complex to solve and, as the Kelvin's model, it is less accurate for boreholes operating over long-time intervals.

Finite line source model (Carslaw & Jaeger, 1959) considers the influence of the ground surface as a boundary and approximates the borehole to a finite line source. This model is satisfactory for analyzing the long-term operation of the boreholes.

Eskilson's model (Eskilson, 1987) introduces more refinement: a numerical model, the spatial superimposition to account for multiple boreholes in the same field, and the non-dimensional g-functions which give the temperature response at the borehole wall for different configurations of the borehole field. The computer implementation requires pre-calculating the g-functions database.

Duct Ground Heat Storage (DST), introduced by Hellström (1989): "The storage volume has the shape of a cylinder with vertical symmetry axis. The ducts are assumed to be uniformly placed within the storage volume. There is convective heat transfer in the ducts and conductive heat transfer in the ground". The temperature at any point in the ground is obtained from the superposition of three parts: A global temperature process (a heat conduction problem between the storage and the surrounding ground), a local thermal process (around each duct), and a steady-flux part (slow redistribution of heat during injection/extraction). The DST model is implemented in TRNSYS; as a result of calibrating the DLSC TRNSYS model, McDowell & Thornton (2008) found an "excellent [agreement] for both [BTES] charging and discharging operations". The main limitation of the DST model is that it can only model fields where boreholes are evenly spaced in a configuration that can be approximated by a cylinder (e.g. large square field, but not a narrow rectangular configuration).

To overcome the existing DST model limitations, Chapuis (2009) develops and validates a new model based on the finite-line source method and, spatial and temporal superposition techniques: "it allows the study of borefields where the spatial position of each borehole is defined by the user and where two independent borehole networks can be modeled (one working in charge mode while the other one is in discharge mode, for example)".

Bernier, Kummert & Bertagnolio (2007) define and execute a set of test cases to compare CHS, DST, the Eskilson's model and the Multiple Load Aggregation Algorithm (MLAA) (Bernier et al., 2004) –a technique of temporal superposition based on CHS.

1.2.1.2 BTES installations

The following table compares BTES storage parameters and performance for similar plants.

Table 1.1: BTES comparison for different SDH systems

	Drake Landing-Okotoks, year 5 (Sibbitt, 2012)	**Anneberg, year 5 (Heier et al., 2011)**	**Crailsheim design (Nussbicker & Drück, 2012).**
Number of dwellings	52	50	260 + school and gymnasium
Application	Space heating	Space heating and domestic hot water	Space heating and domestic hot water
Volume (m^3)	35 000	60 000	37 500
Number of boreholes	144	100	80
Deep of boreholes (m)	35	65	60
Short-term Storage (m^3)	240	0.75 – 1.5/sub-unit	480
Heat pump	No	No	Yes
Total heat demand (MWh/yr)	588	565	4 100
Collected Solar Energy (MWh/yr)	1 230	1 075	2 700
Energy delivered to BTES (MWh/yr)	700	720	1 135
Energy extracted from BTES (MWh/yr)	252	333	830

1.3 Supervisory Control

The objective of supervisory control for buildings is to keep a balance among occupant comfort and energy conservation. A review of control systems for building environment by Dounis & Caraiscos (2009) includes legacy technologies such as thermostats and PID controllers (proportional - integral – derivative); more elaborate methods using Computational Intelligence (CI) (fuzzy logic, neural networks, evolutionary algorithms, etc.); and Model-based Control strategies: optimal, predictive and adaptive. According to Clarke et al. (2002), Model-based control should be preferred to CI; the latter need a training period, they ignore the physical

underlying system phenomena and their control decisions are not tractable. Another advantage of Model-based control is that it is better suited to be considered during the early stages of building design as it is proposed by Petersen & Svendsen (2010).

Henze, Dodier & Krarti (1997) present three conventional thermal storage control strategies for cooling applications in buildings: chiller-priority, constant-proportion and storage-priority. They state that some of these can also be applied for other types of thermal storage. The first 2 methods are mainly based in current system and weather conditions, but storage-priority implies some level of load prediction. More advanced methods, such as optimal control, allow taking advantage of the passive building thermal storage to time-shift peak electrical load and reduce electricity costs (Braun, J., 1990). De Ridder et al. (2011) describe a dynamic programming algorithm for a long term storage coupled to a heating, ventilation and cooling (HVAC) system.

For the general case of district heating systems, Saarinen (2008) explains how the common method for controlling supply temperature, called *Feed-Forward Control,* can be improved by using a dynamic algorithm for load prediction.

1.3.1 Control for Solar District Heating

The design of the control system for a SDH plant always meets "conflicting targets" as enumerated by Schubert & Trier (2012): "Avoidance of stagnation of the solar system, optimal use of heat storages, minimization of heat losses in collectors, pipes and storages; minimal electricity consumption of pumps, minimum requirement of human intervention, optimal use of other heat sources like heat pumps, boilers, waste heat"

This is confirmed by Wong et al. (2007) regarding Drake Landing: "Optimizing the control strategy was a significant challenge, developing into a balancing act between the two primary goals of assuring occupant comfort and maximizing the solar fraction."

In a SDH plant with no seasonal storage, there are mainly two circuits to control: the charge circuit which includes the collectors and the short-term storage, and the discharge circuit (of the short-term storage) for supplying heat to the district. In the charge segment, the concept of variable flow rate is applied to the circuit pump whether using *collector temperature measurement* or *collector irradiation measurement* (Schubert et al., 2012). The Marstal plant employs the *temperature measurement* method (Heller, 2000). Another alternative consists in

modulating the pump speed to maintain a predefined temperature difference between the solar collectors' inlet and outlet ports (Wong et al., 2007).

The short-term thermal storage (STTS) discharge circuit is activated when the district demands thermal energy from the plant. According to Wong et al. (2007), "the biggest challenge with the District (discharge) Loop was to ensure the greatest temperature drop through the system", this ensures "efficient operation of the STTS by maintaining stratification" and increases the "efficiency in the solar collectors by maintaining the lowest inlet water temperature."

When there is a seasonal storage, two additional circuits, for its charge and discharge, need to be controlled. The seasonal storage is mainly charged from the STTS during summer, besides building the thermal energy reserve, another objective is to make sure that the short-term storage is able to collect the daily solar radiation. The discharge is essentially started for winter periods where the buffer storage has not enough charge to conveniently feed the district loop. No detailed information was found about how these processes are controlled in plants other than Drake Landing; this case will be described in Chapter 2.

1.4 Model Predictive Control (MPC)

As its name states, this control method is based on a model of the actual physical system and predictions of external conditions (or disturbances). With these two elements, MPC is able to determine the best control input to the system so its output is the closest as possible to the expected output.

The following MPC theory is based on the book by Rossiter (2003). The initial concept is that a system model can be represented using the concept of transfer function or state-space matrices. The latter representation is preferred because it is more convenient and less complicated than the former one for the cases of multiple-input, multiple-output (MIMO) systems. In the case of a Linear Time Invariant (LTI) system the state-space matrices (**A**, **B**, **C**, **D** and **F)** are constant – because there is no time dependency– and the model is given by

$$\mathbf{x}(k+1) = \mathbf{A}\mathbf{x}(k) + \mathbf{B}\mathbf{u}(k) + \mathbf{F}\mathbf{d}(k) \tag{1.1}$$

$$\mathbf{y}(k) = \mathbf{C}\mathbf{x}(k) \tag{1.2}$$

where, **x** is the state vector, **y** is the system's outputs vector, **u** vector is the controller input to the system, **d** is the disturbances vector, and (k, k+i) indicate consecutive discrete time samples – commonly used in MPC applications. Future system status and outputs can be predicted for each time sample over a horizon of length *p* by using the above equations on a recursive fashion:

$$\mathbf{x}(k+2) = \mathbf{A}\mathbf{x}(k+1) + \mathbf{B}\mathbf{u}(k+1) + \mathbf{F}\mathbf{d}(k+1) = \mathbf{A}(\mathbf{A}\mathbf{x}(k) + \mathbf{B}\mathbf{u}(k) + \mathbf{F}\mathbf{d}(k)) + \mathbf{B}\mathbf{u}(k+1) + \mathbf{F}\mathbf{d}(k+1)$$

$$\mathbf{y}(k+2) = \mathbf{C}\mathbf{x}(k+2)$$

...

$$\mathbf{x}(k+p) = \mathbf{A}^{p}\mathbf{x}(k) + \mathbf{A}^{p-1}\mathbf{B}\mathbf{u}(k) + \mathbf{A}^{p-2}\mathbf{B}\mathbf{u}(k+1) + \ldots + \mathbf{B}\mathbf{u}(k+p-1) + \mathbf{A}^{p-1}\mathbf{F}\mathbf{d}(k) + \mathbf{A}^{p-2}\mathbf{F}\mathbf{d}(k+1) + \ldots + \mathbf{F}\mathbf{d}(k+p-1)$$

$$\mathbf{y}(k+p) = \mathbf{C}\cdot\mathbf{x}(k+p) \qquad (1.3)$$

What equations 1-3 mean is that the system's output at the time sample *k*+*p* can be predicted by using the system's state at the current time sample (**x**(k)), the accumulated control inputs (**u**(k) to **u**(k+p-1)) and the predicted disturbances for the horizon (**d**(k) to **d**(k+p-1))

If the expected system's output for any time sample is written as $\hat{\mathbf{y}}(i)$, the difference between the actual output and the expected output is $\mathbf{e}(i) = \hat{\mathbf{y}}(i) - \mathbf{y}(i)$, and a control performance index over a the period can be written as :

$$J = \sum \| \mathbf{e}(i) \|^2 + \sum \lambda \, \|\Delta\mathbf{u}(i)\|^2 \; ; \; i=k+1 \text{ to } k+p \qquad (1.4)$$

where, λ is a weight factor to account for big changes in **u**.

Applying MPC consists in solving equations 1.3 to find the optimal control for each time sample (**u**(i)) so the performance index or cost function *J* is minimized. In other words, the optimization algorithm considers predicted disturbances (**d**) and system's output to determine the set of control inputs that would allow the system to reach the intended output or reference trajectory ($\hat{\mathbf{y}}$) over the entire prediction horizon (Figure 1-6). At each iteration, only the first calculated control inputs (**u**(k+1)) are applied to the real system and a new optimization for the next time sample is performed taking into account the resulting system's state and updated disturbances forecasts. The period (p) over which the control inputs are estimated is called receding horizon because it keeps moving forward after each iteration so it is never reached.

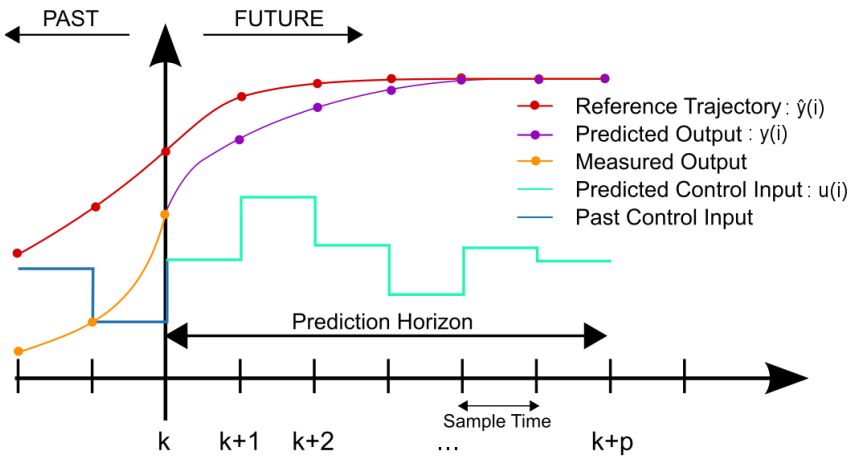

Figure 1-6: Model Predictive Control by Martin Behrendt (2009). Made available under Creative Commons Licence.

1.4.1 Online and offline MPC

1.4.1.1 Online MPC

The general MPC description is also known as *online* MPC; it is called this way because the physical system and the model-based control are tightly coupled. Figure 1-7 illustrates how MPC control continuously takes the decisions for modifying control settings based on feedback from the actual system and disturbances forecast.

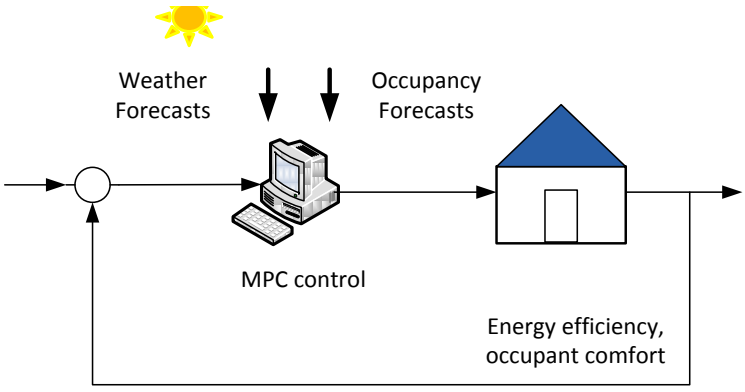

Figure 1-7: Online MPC

There are multiple MPC variants with different optimization algorithms but all of them share the main features: being based on a model of the actual physical system, computing the control signal using disturbances prediction and the receding horizon concept (Maciejowski, 2002); e.g., Robust MPC controllers account for model and/or disturbances uncertainty (Jalali, 2006).

Applying optimal control one interval at a time and then using the system output to repeat the process is called Closed-Loop Optimization (CLO). This is not the only way of implementing MPC, another approach is Continuous Time Block Optimization (CTBO) (Henze et al. 2004). It is different from CLO because the whole block of optimal control values found for the period is applied to the system. In this approach the next optimization is done for the period starting in k+p. Figure 1-8 compares the two options using (purple and blue) solid lines to indicate the extent of the optimal control input applied in each case.

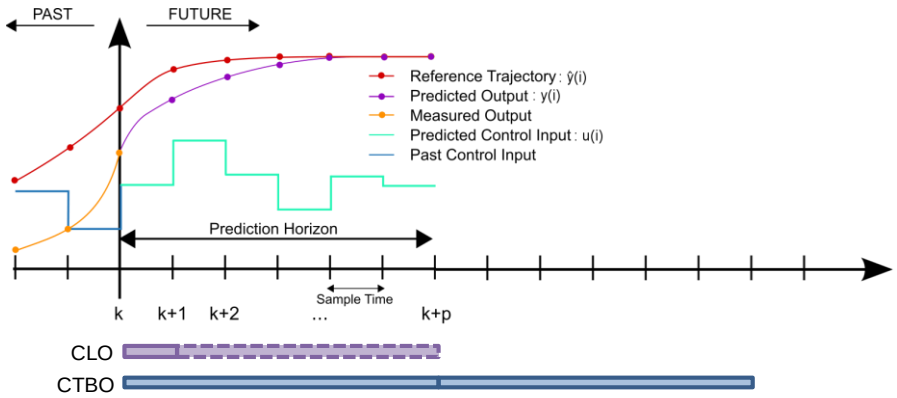

Figure 1-8: CTBO and CLO

1.4.1.2 Offline MPC

As an alternative to online MPC, the concept of offline MPC can be employed for certain situations when either online MPC is not feasible and/or its computation time is very high. In this variant, there is no control parameters being calculated in every time interval, instead a lookup table for a grid of system scenarios is pre-computed using simulation software (Coffey, 2012). The table contains the values of optimal control parameters for each scenario which are found after following an optimization process. When the real system is found to be in a particular status –represented by a cell of the grid– the specific parameters are then employed to control the

system without running any additional simulation (Figure 1-9). To apply the concept of lookup tables the optimization problem is simplified by using problem decomposition and conditions parameterization (Coffey, 2012).

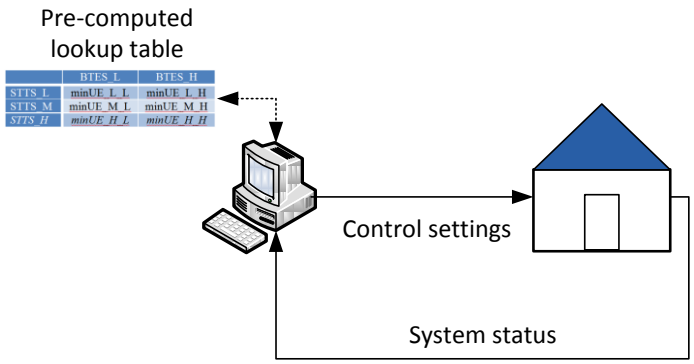

Figure 1-9: Offline MPC

1.4.2 MPC research and applications

Using Model Predictive Control for buildings is already proposed by Kelly (1988), but the intensive computation power required for the calculations limited its development. There are some early works by Braun (1990) focusing on controlling cooling systems and building thermal mass, and Camacho et al. (1994) for controlling solar collector fields.

With increasing and less expensive computing power, there have been more research works in this field: a predictive optimal controller for thermal storage (Henze, Dodier & Krarti, 1997), validation and test for a passive solar building (Kummert, 2001), a review of MPC potential and challenges (Coffey, Morofsky & Haghighat, 2006), MPC for controlling a geothermally heated bridge (Xie & Whiteley, 2007), a comparison between MPC and PID control for a single solar system (Ferhatbegovic, Zucker & Palensky, 2011), MPC and weather forecasts for controlling a building temperature (Oldewurtel et al., 2012), Predictive control for buildings with thermal storage (Ma et al., 2012).

It is also worth mentioning the ongoing European interdisciplinary project OptiControl (www.opticontrol.ethz.ch) presented as the "Use of weather and occupancy forecasts for optimal building climate control." Simulation results indicate a theoretical energy saving potential of 1% to 15% for non-predictive algorithms and up to 41% for predictive control algorithms depending

on the location, building case, and other parameters (Gyalistras, 2010). The companion website www.bactool.ethz.ch allows online access to the *Building Automation and Control Tool* (BACTool) for graphical evaluation of different control algorithms.

Improving MPC results is clearly dependant on accurate forecasts. Florita & Henze (2009) compare and evaluate different weather forecast models for MPC applications, especially those based on Moving Average (MA) and Neural Networks (NN). They found that for MPC applications, MA models, in spite of their simplicity, are often better than complex NN models at predicting outside temperature. For solar irradiation forecasts, Perez et al. (2007) evaluate a model to produce finer forecasts using information from simple sky cover predictions, Cao & Lin (2008) define and compare the accuracy of a proposed type of Neural Network, called Diagonal Recurrent Wavelet Neural Network (DRWNN). In 2010, Perez et al. present a validation, against ground measurements, of the algorithms employed by the US Solar Anywhere system (solaranywhere.com). IEA, task 46, "Solar Resource Assessment and Forecasting", also points in this direction. In another kind of forecasting, Mahdavi et al. (2008) explore the usage patterns and profiles of office building occupants to facilitate the operation control.

No comprehensive research for applying Model Predictive Control strategies for SDH was found; articles refer to particular or local control problems. In an IBPSA workshop about MPC, Candanedo (2011) presents models for individual house heat loads and solar gains at the community scale, and he also summarizes some results of the "effect of imperfect solar gains forecasts on predictive control". Some other works more related to general district heating can be found, for example, application of predictive control for district heating to keep a low district supply temperature (Palsson, Madsen & Søgaard, 1993); Dobos et al. (2009) uses the Matlab toolbox for applying MPC in different local problems of a heating district. Sandou (2009) states that the Particle Swarm Optimization (PSO) algorithm for predictive control gathers better results than classical control rules for heating districts.

1.4.3 Software

To solve an optimization problem using MPC, two main software processes are needed: simulation and optimization. For building applications, simulation software such as TRNSYS (Klein et al., 2012), EnergyPlus, or ESP-r, are widely employed for system modelling and simulation. For optimization, the program GenOpt (Wetter, 2001) easily integrates with

simulation software through input and output text-files. Matlab also provides an MPC toolbox but it requires the system to be defined in terms of the transfer function or a state-space model (www.mathworks.com/products/mpc/). The optimization program evaluates the simulation's output and applies special algorithms to find the control parameters values that minimize a defined *cost function*, which should corresponds to the best point of system operation.

CHAPTER 2 CASE STUDY: DRAKE LANDING SOLAR COMMUNITY (DLSC)

2.1 Description

The SDH plant at Drake Landing Solar Community provides solar space heating for 52 homes. The community is located in the town of Okotoks (Alberta, Canada) at 50° latitude North and 1000 meters above sea level. It is the first district with solar seasonal storage in North America and the first in the world to reach a 90% solar fraction.

The community was designed in 2003 by a team led by Natural Resources Canada (NRCan) following an initiative to apply the concept of solar energy and seasonal storage for sustainable communities. The project's success is testimony to the commitment of NRCan and its multiple partners, including the municipality and private companies, such as Sterling Homes and ATCO Gas.

Construction started in 2005, after some delays and unexpected expenses it was set in operation two years later. Distributed sensors monitor the system and performance reports are generated monthly and yearly. After three years of operation, solar fraction was already 80%. At the end of year 5 (July 2012), solar fraction reached 97% (Sibbitt, 2012), surpassing the design values.

In 2011, the community was awarded with the prestigious Energy Globe Award in the Fire (Energy) category and the overall World Energy Globe Award. Countries like South Korea are also considering similar communities based on the learning from this experience (Patterson, 2012); the same article indicates that "The [DLSC] project's partners are now looking at taking the technology to the next level by developing a large-scale solar community with between 200 to 1,000 homes".

2.2 Components

The excellent energy performance observed in this plant is mainly the result of a careful design; components characteristics were defined to maximize solar energy collection and storage, and to minimize heating load. On one side, these considerations apply for the centralized solar plant equipments; on the other, they translate in better homes' insulation and very efficient air handler units. As objectives are not only related to energy performance but also to sustainable

development principles, material and supplies were chosen according to special criteria, such as certified lumber source, local manufacturing, and recycled sources.

The main components of the plant and circuits (fluid loops) that connect them are depicted in Figure 2-1. Their characteristics are extracted from (McClenahan et al., 2006), (Wong et al., 2007) and Drake Landing's website (http://www.dlsc.ca). Heat exchangers, pumps, boilers and short-term storage tanks are installed in a building called the Energy Centre. BTES storage is underneath an adjacent park.

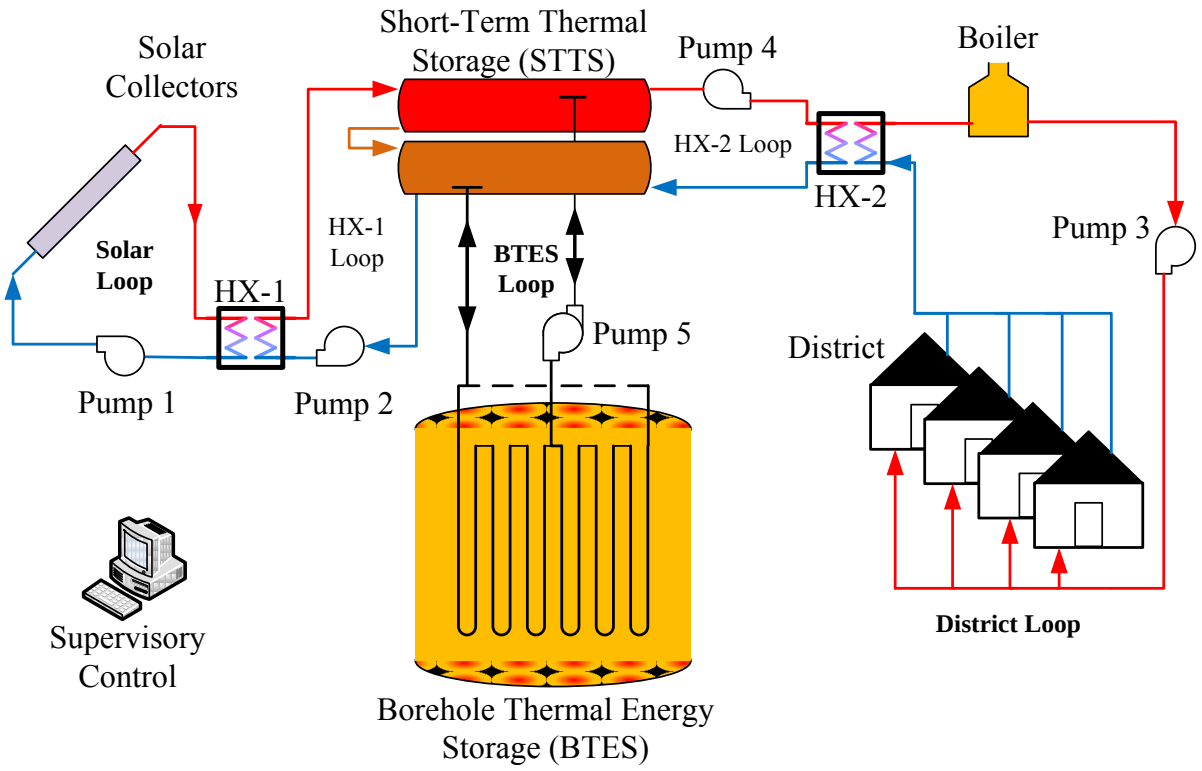

Figure 2-1: Drake Landing Main Components

Solar collectors: There are 798 flat-plate collectors oriented towards the south and tilted 45° above the horizontal. Each one measures 2.45 m x 1.18 m; the whole array covers an area of 2293 m^2. Mounted in the garages' roofs, they are grouped in 4 blocks following the community's layout of four rows of houses (Figure 2-2). The heat carrier fluid circulating through them is a mix of glycol and water.

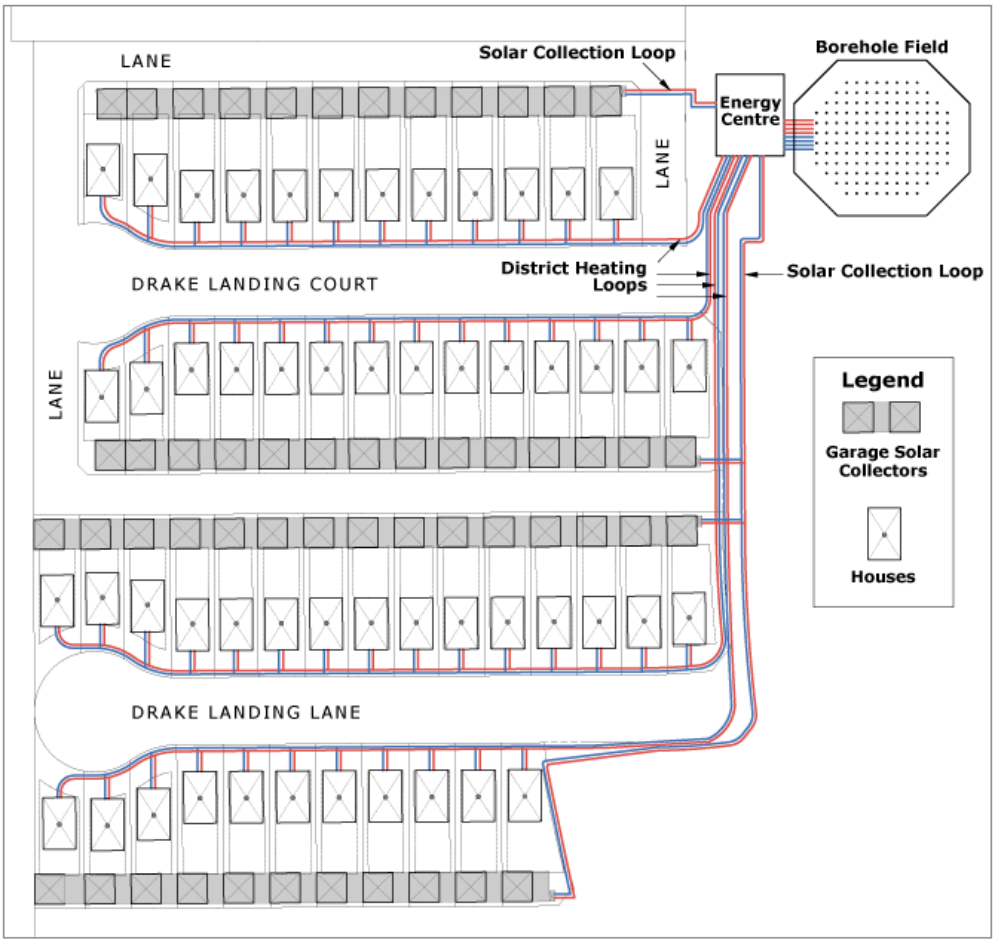

Figure 2-2: Drake Landing layout (Source: http://www.dlsc.ca, retrieved May 15, 2013)

Heat Exchanger 1 (HX-1): it allows heat transfer from solar collectors to the Short-Term Thermal Storage (STTS). When collectors are hot enough, heated glycol circulates through HX-1 transferring heat to water in the *HX-1 loop*. Cold glycol *returns* from HX-1 to the collectors' inlet to reinitiate the sun's energy transfer cycle.

Pumps 1 and 2: They are variable speed pumps. Pump 1 circulates the glycol in the *solar loop*. At the same time, Pump 2 circulates water in the *HX-1 loop*. For backup purposes, both pumps are duplicated.

Short-Term Thermal Storage (STTS): it consists of two 120 m^3 tanks, totalizing 240 m^3. The first tank (hot tank) receives hot water directly from HX-1. The bottom outlet of the hot tank is connected to the top inlet of the second tank (cold tank). Closing the loop, cold tank returns cold

water to HX-1. For improved stratification, each tank has an internal division by means of a special baffle.

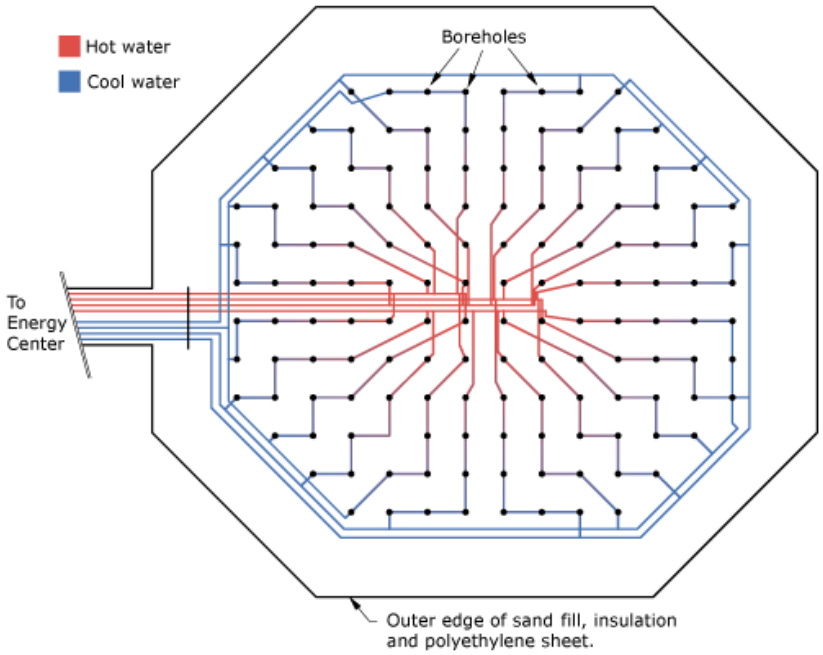

Figure 2-3: BTES distribution (Source: http://www.dlsc.ca, retrieved March 22, 2013)

Borehole Thermal Energy Storage (BTES): It is composed of 144 boreholes of 15 cm diameter and 35 m deep, separated 2.25 m from center-to-center. Each borehole contains a single U-tube. These pipes are serially connected in strings of 6 from the center to the edge for better radial stratification. Four circuits made up of non-adjacent strings increase reliability of water supply and return (Figure 2-3). The total earth volume is 35 000 m^3, and the equivalent water thermal capacity is 15 800 m^3.

Pump 5: It is the pump for BTES charge and discharge operations. The pump is actually unidirectional, with the flow direction dependant on the position of the *BTES loop* valves determined by the control platform. Two constant speed pumps in standby-backup configuration were initially installed for this operation, but a variable speed pump was retrofitted in 2012.

Heat Exchanger 2 (HX-2): Transfers heat from STTS' hot tank to the *district loop* when heat demand exists. The HX-2's outlet in the small *HX-2 loop* is the return path for cold water to STTS's cold tank.

Pumps 3 and 4: They are synchronized for simultaneous operation whenever there is heat demand by the district. Pump 4 is the only pump with no backup.

(Back-up) Boiler: Operates only when the temperature of hot water, coming from STTS to the *district loop*, is below a value called the District Loop Set-Point (DLSP, presented in section 2.3.1.2). There are currently three boilers, 2 of high capacity in standby-backup configuration and one of smaller capacity. In the last year, the small one is mainly employed because BTES has reached a high level of charge.

District: It consists of four 11 to 15 house blocks with orientation East-West (Figure 2-2). They are especially insulated to comply with the NRCan's R-2000 Standard for energy efficiency. A customized air handler unit, with high efficiency and significant drop in water temperature, is installed in each home to facilitate the district operation at relatively low temperatures.

District loop: It is a direct return system in parallel configuration. There is a circuit of buried plastic pipes for the supply and return in each one of the rows. In this configuration, the hot water temperature is practically the same for all homes.

Supervisory Control: It is based on specialized building management software which allows defining rules, actions and alarms for the system. Output depends mainly on temperature, flow and pressure sensors. It activates valves, controls pumps speeds, and ignites boiler. More details follow in the next section.

2.3 Operation and Control (STD)

The information here is mainly based on Wong et al. (2007) –for the general concepts– and the internal document by Enermodal (2011) for the details. According to Wong, the objectives of the DLSC control system are

- To maximize solar fraction
- To operate the district loop at the lowest possible temperature and still ensure occupant comfort
- To respond appropriately to changing weather conditions

As it has been stated before, control strategies have to deal with conflicting goals, for instance, working at high temperatures easily guarantees occupant comfort but it results in drawbacks,

such as the increase in thermal losses through the system and the reduction of solar collector efficiency.

It is important to mention that control rules and parameters, defined during the design phase, have been changing through time due to control system improvements or physical upgrades, e.g., the replacement of the constant speed BTES pump –with a variable speed pump– implied extending the pump control beyond the original on/off switch.

2.3.1 General concepts

2.3.1.1 Operation modes

To provide the district with the maximum possible of solar thermal energy under different seasonal weather conditions, two modes of operation, *winter* and *summer* are defined. There is a fixed *winter mode* between September 1st and April 30th, but a "temporary" *summer mode* from May to August. During these months, *summer mode* can be switched back and forth to winter mode depending on the number of cumulative degree hours (DH) below or above 17 °C: if the number of degree hours below the reference reaches 5, *winter mode* is imposed; s*ummer mode* is set again when the *DH-above* condition is 15 or more. As a control measure, the *cooling DH* counter is reset (to 0) when the number of heating DH is higher than 15; in an analog way, *heating DH* counter is reset when *cooling* DH is more than 20. This mechanism is especially useful during the shoulder months when days are still warm but nights are cold.

District and BTES loops operate differently in each mode: district loop is only active in *winter mode*, BTES loop is active during both operation modes but the control strategy parameters are different. Solar loop is not affected by the operation mode; it works always in the same way and the control parameters are not changed.

2.3.1.2 District Loop Set Point (DLSP)

This is another important concept in the system control strategy. It defines the set-point of the minimum water temperature that must be supplied to the district depending on the external air temperature. If the temperature of hot water coming from STTS does not reach DLSP, then the boiler is set in operation. Figure 2-4 shows how DLSP is between 37°C and 55°C depending on three air temperature ranges delimited by -40°C and -2.5°C.

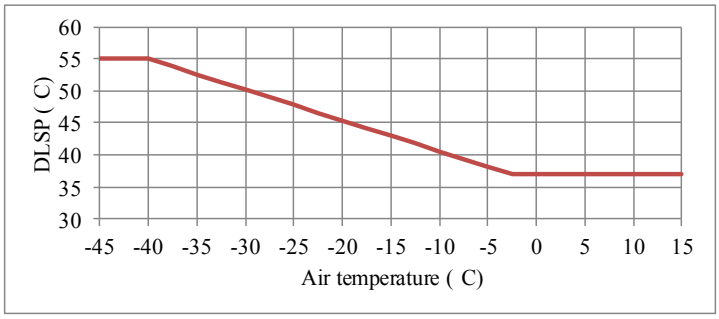

Figure 2-4: DLSP vs. Air Temperature

2.3.1.3 STTS percentage of charge (STTS % charge)

Finally, it is worth highlighting the central role the STTS has. As it is involved in all the heat transfers through the heating district, the control system looks to keep an adequate STTS stratification to maximize thermal energy transfers: control rules for the three main loops always take in consideration STTS' internal temperatures or parameters that indicate its status.

The main parameter to measure STTS status is *STTS % charge*; it is calculated from DLSP and from the temperatures of two nodes in each of the STTS tanks. Each node temperature is only taken into account for the total % of charge if it is higher than a certain limit called *Minimum Usable Temperature*, which depends on DLSP. In other words, the philosophy of the defined *STTS % charge* is to assess "how warm" the STTS is when compared to the DLSP.

STTS % charge is obtained from the following formulas:

$$dT\ Base = 0.5*DLSP - 10\ (\text{in } °C) \quad (2.1)$$

$$Minimum\ Usable\ Temperature = (DLSP + 4) - dT\ Base\ (\text{in } °C)$$

For each node's temperature, Ti (i=1,..,4):

If (Ti - Minimum Usable Temperature) > 0,

Then Usable dTi = Ti - Minimum Usable Temperature

Else Usable dTi = 0

% Charge Ti =100 (Usable dTi) / dT Base;*

$$STTS\ \%Charge = \sum \%\ Charge\ Ti;\ i=1,..,4$$

2.3.2 Solar collector loop control

From the existing options for solar collector control, the DLSC Design Team selected the alternative of pumps speed modulation because it provides increased solar collector efficiency and offers the possibility of electricity savings compared to other methods using constant speed. In normal operation mode, Pump 1 and Pump 2 speeds are controlled to keep a 15°C difference between the HX-1's input and output in the collectors side. The process stops whenever the average collector temperature is very close to the cold tank's outlet.

Other operating modes are also needed for the loop:

HX-1 bypass: This operation mode is applied in the mornings when the collectors start getting warmer and the fluid temperature in collectors and pipes needs to be stabilized. Only Pump 1 starts working in an on-off cycle, and glycol is diverted away from going to HX-1. Normal operation resumes once the temperature of returning glycol is higher than the cold tank temperature.

Fluid cooler bypass: This mode is enabled if temperature in STTS is too high to accept more energy. In that situation, glycol temperature in HX-1's return outlet is too high and glycol must be diverted to the fluid coolers.

2.3.3 District loop control

The special air handler unit installed in each house contributes to the *district loop* efficiency. It has a two position valve (on/off) that allows full water flow when opened. The internal fan-coil, for water to air heat exchange, is designed to provide up to 25 °C drop in water temperature. This is very important because the colder return water allows achieving a better STTS stratification.

To guarantee that the last house in each row is able to receive an adequate flow rate, the district loop has a constant pressure condition (75 kPa). For doing so, Pump 3 has its speed adjusted to compensate the pressure losses dues to heat demands when the valve in the air handler units is on. If heat is not demanded, hot water keeps flowing at the minimum rate to ensure heat availability at all times.

In the short *HX-2 loop* (including STTS and HX-2), Pump 4 speed is continuously modified so that hot water temperature on the HX-2's district side is close to the required DLSP temperature. Pump 4 operates only if Pump 3 is working and the STTS' hot tank temperature is higher than the district loop return. If the supplied hot water temperature is 6°C above the scheduled DLSP Pump 4 stops operating.

Three boilers complement the operation of the loop. One or more are activated when the temperature of the hot water coming from the STTS, through HX-2, is below the DLSP.

2.3.4 BTES loop control

The control strategy for the BTES loop, as described by Enermodal (2011), is called hereafter the Standard strategy (STD). In *winter mode*, its main objective is to reduce boiler gas consumption by trying to maintain "enough thermal energy" in the STTS, so, the District Set-Point (DLSP) is more easily reached and operation of the boiler is not needed. The BTES is discharged into the STTS when the heat load is too high regarding the STTS charge level, and/or when there is insufficient collected solar energy transferred to the STTS. To maximize the temperature difference between the BTES' inlet and outlet the flow rate is set to a relatively low value (3.7 l/s). As a consequence, heat transfer rate from BTES to STTS is usually short of capacity for sharp increases in the heating load.

In *summer mode*, the controller's goal is to store as much solar energy as possible in the BTES. Whenever conditions are met, the STTS charges the BTES with the collected solar energy building in more energy reserve. In doing so, STTS also makes room for collecting next day solar thermal energy.

Although the objectives are different for each operation mode, decision rules for BTES charge and discharge are similar for both of them; differences are only found in the trigger values that determine when to start charging or discharging. During *winter mode* the whole system is actively working due to the district heating demands; that operating mode is further described because it is most relevant for this research's purposes.

2.3.4.1 Winter mode operation

The decision for starting BTES charge or discharge depends on the STTS state of charge (*STTS % Charge*) relative to the estimated amount of charge required (*STTS % Charge required*) for meeting the envisioned near-future heating demand. If there is a *STTS % Charge* deficit the BTES discharges into the STTS. On the contrary, important STTS surplus are stored in the BTES.

STTS % Charge required is set by a schedule (Figure 2-5) which is defined in terms of the time of day and the DLSP value. For example, if the DLSP temperature is 40°C (which correspond to an ambient temperature of -10°C), the *STTS % Charge required* will be 25 % at 6 AM but 92% at 8 PM (red bars).

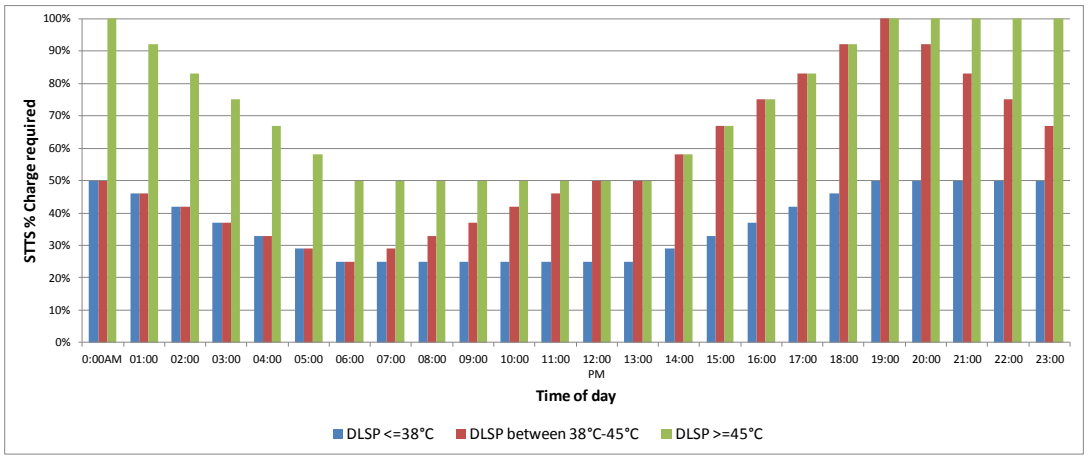

Figure 2-5: STTS % Charge required schedule

Figure 2-6 shows the general flow diagram for the processes; two factors, *Winter Charge Factor* and *Winter Discharge Factor*, define the relation between the aforementioned *% Charge* parameters:

> If *STTS % Charge* is less than *Winter Discharge Factor* times *STTS % Charge Required*, then the BTES loop's pump and valves are enabled for discharge.
>
> Otherwise, if *STTS % Charge* is greater than *Winter Charge Factor* times *STTS % Charge Required*, the BTES is charged from the STTS.

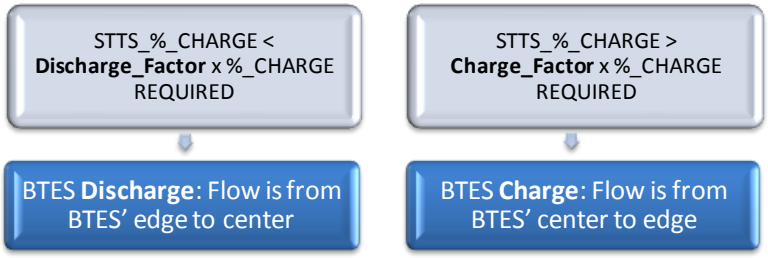

Figure 2-6: Standard Control Strategy (STD)

To be more accurate, additive factors –not shown– are also taken into account for fine tuning the relationship between *% Charge* amounts. Moreover, if the rule condition that enabled the operation is no longer true, the operation is not stopped immediately, the charge or discharge can continue until a threshold (or tolerance) is reached. This is helpful to avoid switching off the process-in-execution during temporary situations that may change the ratio between the *% Charge* variables. An absolute condition for stopping the processes-in-execution is when BTES input and output temperatures cause a change in the direction of the net heat transfer rate, e.g. BTES discharge is actually removing energy from the STTS.

2.4 Summary

This concludes the general description of the case study and more importantly the control details for each of the three main loops of the system. Some control aspects were especially highlighted as they are directly involved when applying Model Predictive Control (MPC) methods.

The control strategy described above will be used as a reference in the following chapters, and it will be referred to as the STD (standard) control strategy. That strategy was established by the DLSC Design Team and refined over time using engineering judgement. The concept of "charge required" (see section 2.3.4.1) shows that the STD control strategy does, in fact, include a simple predictive element; it works by assuming that the temperature changes are smooth and that more or less charge is required depending on the time of day. However, STD control has no rules regarding the current solar irradiation or its estimated amount in the near-future.

CHAPTER 3 METHODOLOGY

The main steps followed during this study are presented together with the concepts that help to explain the elements found in each phase. The discussed general steps are model calibration, inception and design of control strategies, implementation, and evaluation of control strategies.

3.1 Model calibration

According to Rossiter (2003), "philosophically MPC reflects human behaviour whereby we select control actions which we think will lead to the best *predicted* outcome (or output) over some limited horizon. To make this selection we use an internal *model* of the process in question. We constantly update our decisions as new observations become available." In that line of thought, a *practical approach* (see section 3.2.1) was followed to implement MPC while keeping its two characteristic elements, a system model and observed disturbances.

3.1.1 Model

Traditional MPC research includes mathematical models expressed either in terms of state-space matrixes or transfer functions; in both cases, they can be optimally *solved* using a broad range of advanced algorithms to find the optimal control settings. They are the settings applied to the system to obtain the desired response under the predicted external conditions (disturbances). In this study, the system representation is a TRNSYS model that is not solved but rather *executed;* multiple *executions* are needed to find the optimal control parameters that minimize a given cost function that represents the system's output. Working with a TRNSYS model was an advantage given the existing in-house TRNSYS expertise and the software's modular approach. No other model or software was considered for simulating DLSC.

Accuracy is the most critical requirement for models employed in MPC implementations: the better the model represents the physical system and its response to disturbances, the more reliable will be the results. There is some terminology regularly applied to the process of achieving desired model accuracy: calibration, validation, verification, tuning, etc. In general, calibration of component parameters is considered as being part of a validation process where the simulation outputs are compared with actual operation data. In the context of this dissertation, a full validation with the meaning of demonstrating that the parameters and equations of all model

components are accurate was not performed. Calibration and tuning are preferred as expressions and they are employed with the meaning of finding the parameters that make the simulation results close to the real system's outputs. The calibration was limited to the last two years. It would have been impossible to have a unique *calibrated* model for the whole five years of operation because the real system and the control strategies have been changing during the operation time.

An additional characteristic regarding simulation models is the computation time, especially when optimization requires a large number of successive runs over a long period. If the computational time is excessive, off-line studies to develop and tune the controller could become impractical (e.g. months or years of CPU time). Implementation in a real-time (on-line) MPC application would also be impossible if the time required to obtain control signals for a horizon period is longer than that period. Computation time depends on multiple factors, such as system complexity, period to be simulated, and the time *granularity* –the size of the simulated time interval, or time-step, used to compute the interaction among the system components. There is often a trade-off between simulation speed and the accuracy reached by using shorter time-steps.

In Chapter 4, the TRNSYS model for the Drake Landing Solar Community (DLSC) is described in detail along with the steps taken for *increasing its accuracy* and reducing simulation time without compromising results accuracy.

3.1.2 Disturbances and predictions

The disturbances to the real system are mainly weather variables: solar irradiation, wind speed and direction, air temperature, humidity, etc. They affect the amounts of collected solar energy, the level of component losses and the system heating load. The latter, is also dependant on *human* disturbances, such as daily/weekly usage profiles and occupant comfort –which is influenced in a subjective way by weather conditions.

In the case of the simulation model, only solar irradiation, air temperature and heating load are considered as disturbances because these are the inputs that have the strongest impact on the simulation execution.

The predictions employed in the simulation model are all taken from measured data; it can be said that they are *perfect* predictions not subject to uncertainty because the disturbances just

behave as predicted. In situations of actual forecasts, uncertainty has to be taken into account when applying a method and evaluating the results (e.g. Robust MPC).

3.2 Inception and design of control strategies

3.2.1 Online or offline MPC?

Figure 3-1 is shown to remind the differences between online and offline MPC (lookup tables). The former has a frequent feedback from the real system and can find optimal control settings using that information and updated forecasts. In the offline case, the best control settings for a grid of scenarios is pre-computed and then applied depending on the system status.

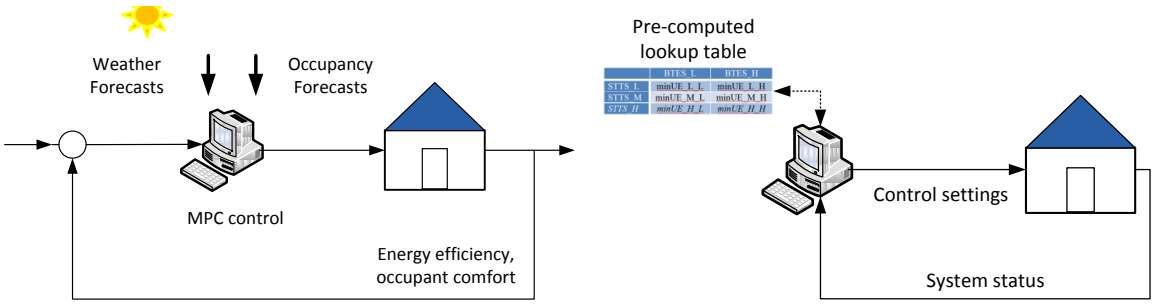

Figure 3-1: Online (left) and Offline MPC (right)

Having a software model simulating the system is not enough to implement online MPC, an optimum trajectory (or cost function to be minimized) must be defined, and an optimization process is needed to find the best control values. The control settings are then applied to the real system and its output and status are fed back to update the simulation model for the next iteration.

Before implementing new MPC control strategies in the real system, they must be developed and tuned using simulation. This can be performed using two models of the system: one model plays the role of the real plant, and another model is used internally by the controller to calculate optimal control signals. The two models can be the same or the internal model can be simplified.

In this study, the MPC's internal model is a detailed TRNSYS simulation. That choice has the inconvenience that it is not currently possible to "reset" the state of the model to reflect measured values. So the feedback process, where measured outputs are used before calculating the optimal

control signals for the next periods, cannot be performed in a direct manner. The method selected to work around this issue was twofold:

- Employ pre-computed lookup tables (offline MPC) for certain local control problems.
- Apply online MPC methods (without the actual system's feedback) over 1-year period.

3.2.2 Introduction of control strategies

From the beginning it was clear that the current control strategy (STD) has powerful and well-thought features; the new control strategies were not to be designed to completely replace STD, rather the emphasis was put on specific control elements that are susceptible of bringing additional energy savings.

The basic modes and rules of operation described in section 2.3 were retained. Table 3.1 shows an overview of the proposed strategies along with a brief description of the current implementation and the proposed modifications.

Table 3.1 : Summary of modified control elements

Element	**Current**	**Proposed modification**
Winter BTES charge	Comparison between *STTS % Charge* and *% Charge required.*	Parameter *Winter BTES Charge Factor* set to a very high value, so Winter BTES charge almost never occurs.
Winter BTES discharge	Comparison between *STTS % Charge* and *% Charge required.*	Keep the current control but *force* BTES discharge based on high forecast load (function of temperature) or low solar irradiation.
Solar loop (control of pumps 1 and 2)	Pumps speed is modulated to keep a fixed Temperature delta (*Delta_T*) between collector's inlet and outlet.	Four different values for *Delta_T* depending on STTS status and system operating mode.
BTES loop (pump control for discharge only)	On/off for the original constant speed pump. Manual/historical settings for the variable speed pump.	Pump speed proportional to STTS status. Two different conditions depending whether forecast load is normal/moderated or very high.

The first two control elements were chosen because it was considered that the winter-mode BTES operation could be improved if the control parameters were adjusted, and weather forecasts and load estimations were taken into account. The last two elements were selected because it was

suggested by NRCan that they offered an interesting possibility of reducing electricity consumption. The district loop control and summer-mode BTES operation were not considered in order to limit the scope of this study, but they could also be optimized in a global approach. Changing the district loop control parameters (e.g. supply temperature) would have implications on the occupants comfort and would require to carefully assess these with a detailed house model, which was not used in this study.

3.2.3 Rationale behind the selected approach

As explained before, the objective was not to replace the existing control strategy with an MPC controller, but rather to modify the existing rule-based controller to take into account the information provided by a detailed model and a forecast of future system behaviour. The reasons for selecting specific control elements and the basic idea behind of each proposed control strategy are described in the following sub-sections. Detailed implementation and results of these alternative control strategies are presented in Chapters 5 and 6.

3.2.3.1 Winter BTES charge

This control element is included in the set of modifications because it was observed in simulation results and the actual measured data that sometimes the BTES was *unwisely* charged –thus discharging the STTS– just hours before a critical weather condition appeared: sharp temperature changes and/or scarce solar irradiation. The ideal system response would have been leaving the STTS accumulate more thermal energy instead of transferring it to the BTES. The proposed solution is logical: allowing BTES charge only when a very high ratio (*Winter BTES Charge Factor*) between the current STTS charge and the required charge exists. An indirect advantage of this approach is the decrease in the pump operation with the resulting electricity savings.

3.2.3.2 (Forced) Winter BTES discharge

In this case, the motivation was similar to the BTES charge process: to keep more thermal energy in the STTS to better cope with difficult weather conditions. The proposed solution could not be limited to modifying the *Winter BTES Discharge Factor*. Frequent BTES discharges –into the STTS– could be useless or counterproductive under mild weather conditions, because they would use more electricity for pumping and they could lead to the STTS being unnecessarily warm,

therefore lowering the solar collector efficiency. The selected approach is to force the BTES discharge whenever weather forecasts announce extreme conditions that could significantly lessen the collected thermal energy and/or sharply increase the heating load. This decision is then based on the *predicted* imbalance between the heat added to the STTS (solar energy collected) and the heat removed from the STTS (heating load).

3.2.3.3 Solar loop

The *Temperature difference* parameter (*Delta T*), set in the loop control rules, plays an important role in the amount of collected solar energy: low values translate into more solar energy being collected, because the solar collector operates at a lower average temperature. But lower Delta T values also result in higher flow rates, hence more electricity being consumed. The main reason behind including this loop in the proposed control was to achieve electricity savings without compromising the solar performance. As collected solar energy also depends on the STTS stratification, it was decided to define four *Delta_T* values that would be selected taking into account the STTS level of charge.

3.2.3.4 BTES loop pump control

This last element required a different control strategy due to the change of the existing BTES pump for a variable speed pump; achieving some level of electricity savings was also in the list of priorities. For the new control strategy, the speed of the BTES pump in discharge mode (i.e. when transferring heat from the BTES to the STTS) was varied depending on the STTS level of charge and the forecast load. Lower pump speeds will charge the STTS slowly, with lower electricity consumption, and will induce a better thermal stratification in the STTS. On the other hand, if the forecast load is high and the current energy stored in the STTS is insufficient to meet that load, the STTS must be charged quickly to avoid using gas boilers –in that case the BTES pump must operate at a higher speed.

3.2.4 STTS Absolute Charge Level (STTS ACL)

The discussion above shows that many control decisions are based on the STTS level of charge. The current parameter *STTS % Charge* is defined in a relative way, depending on the desired

district loop temperature (DLSP) –which changes all the time (see section 2.3.1.3 and Equations 2.1).

Early tests showed that with the proposed control strategies, it was more efficient to assess the STTS state of charge in an absolute manner. The parameter *STTS Absolute Charge Level (STTS ACL)* was defined for that purpose. It is based on the same formulas as the *STTS % Charge* but the terms *Minimum Usable Temperature* and *dT Base* are always calculated with the minimum DLSP (37 °C) –equivalent to an air temperature of -2.5°C or higher. *STTS Absolute Charge Level* is more helpful to evaluate and to compare different control strategies because it is independent of air temperature variations. Table 3.2 lists the values of these parameters for three possible combinations of STTS temperatures. Note that ACL has always the same value independently of the DLSP setting.

Table 3.2: STTS Relative and Absolute Charge Level

STTS % Charge Level (relative)	**STTS Absolute Charge Level (STTS ACL)**
100% if DLSP=37°C, or other values based on particular DLSP	1.0 (100%)
200% if DLSP=37°C or, 100% if DLSP=48°C, or other values based on particular DLSP	2.0 (200%)
310% if DLSP=37°C, or 100% if DLSP=55°C, or other values based on particular DLSP	3.1 (310%)

3.2.5 Disturbances forecast

Only two of the four proposed control elements are based on predictions of disturbances. The other two are not because they depend on tuning their parameters to find optimized values for them. The list is summarized in Table 3.3.

Table 3.3 : Control and disturbances

Control Element	**Predicted disturbance**
Winter BTES charge	
Winter BTES discharge	Solar irradiation and heating load
Solar loop (pumps control)	
BTES loop (pump control)	Heating load

It can be noticed that the *heating load* is listed while the *air temperature* is not. In this study, they are in fact equivalent because measured values at DLSC have shown that there is a very good correlation between the heating load and the ambient temperature averaged over a certain number of hours. A linear regression with 6-hour average is used in the original model (see Equation 4.1).

In a real implementation, both the ambient temperature and human occupancy impacts (e.g. heating thermostat settings) would need to be anticipated. Although this work does not address this issue, the adopted formulation would make it easier to include both aspects in one estimated disturbance.

3.3 Implementation

The main elements for the implementation were the initial TRNSYS model and the 5-year monitored data. In the same way TRNSYS model needed calibration, the measured data had to be processed to eliminate inconsistencies (section 4.3.1).

Once the calibrated simulation model with the measured data was ready, it was used to test different control strategies and to optimize system operation based on a *desired* output. It has been told that the desired system's output is equivalent to minimizing a given *cost function*. The name does not necessarily imply that actual monetary costs have to be considered in the function. For all the optimization experiences carried out in the scope of this research, cost function is always related, but not limited, to energy consumption.

As it has been suggested, the optimization process means running multiple simulations and comparing their results to find the combination of control parameters producing the desired output. For each proposed control strategy, the cost function and associated optimization conditions are described in detail in the corresponding chapter. Table 0.1 can also be consulted to quickly identify the naming and the control parameters in each case.

3.3.1 Software

For carrying out the simulation and the optimization processes, the two main software tools TRNSYS and GenOpt were selected. They are briefly described in the next sections.

3.3.1.1 TRNSYS

TRNSYS (a TRaNsient SYStems Simulation program) was designed as a generic simulation tool for transient systems, but it is most often used to analyze buildings and energy systems in the built environment. It belongs to the type of software known as Building energy Performance Simulation (BPS) tools. In a TRNSYS model the various pieces of equipment, or system components, are represented by encapsulated models known as "types". These units can represent physical components (solar collectors, pipes, tanks, etc.) or perform some accessory functions, such as reading files, displaying and integrating outputs, making intermediate calculations, etc. Each type's outputs depend on their configuration parameters, inputs coming from other types and internal logic representing either a physical phenomena or an intended utility for the type. TRNSYS' modular architecture allows to add new models, or types, to model new equipment or to add other functionalities. Examples of TRNSYS projects, showing how components are arranged in the visual interface (called the Simulation Studio) are shown in Chapter 4.

TRNSYS models are run to simulate the operation of a system during a specific number of hours. Type outputs are computed every certain period of time (timestep) depending on simulated phenomena and required level of accuracy. For each simulation timestep, multiple iterations may be needed before reaching convergence between the calculated inputs and outputs.

3.3.1.2 GenOpt

GenOpt is a specialized optimization tool that can be integrated with any software using text files for configuration and output results. GenOpt has built-in algorithms for dealing with different cases of parameters optimization; the default one is a hybrid implementation that consists of two parts: Generalized Pattern Search (GPS) method and Particle Swarm Optimization (PSO) (Wetter, 2011). This hybrid algorithm can be applied to problems dealing with discontinuous cost functions and continuous and discrete variables, as is the case for this research.

GenOpt tests different values for the parameters to be optimized and searches for those that minimize the cost function. Figure 3-2 is a screenshot of GenOpt execution, for each new simulation the values of control parameters are modified according to some initial set of possibilities (all lines except the red one); the cost function value (red line) smoothly decreases as the GenOpt algorithms get more accurate values for the parameters. Depending on the selected

algorithm and on the stage where GenOpt is in the solution process, it can launch several instances of TRNSYS in parallel to benefit from multi-core processors.

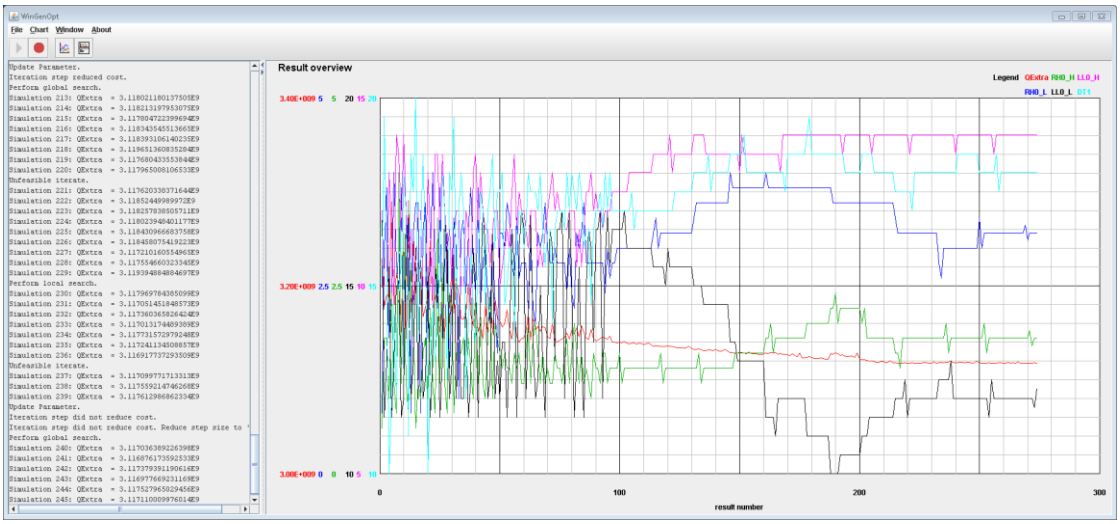

Figure 3-2: Running optimizations in GenOpt

3.3.1.3 Integration

Figure 3-3 represents the integration of TRNSYS and GenOpt. A special TRNSYS model, used as a template by GenOpt, has placeholders (keywords) for the parameters that are to be optimized; from there GenOpt generates a valid TRNSYS model by replacing the placeholders with values chosen from a pre-configured range defined for each parameter. The TRNSYS simulation is then run and, when it finishes, GenOpt evaluates the cost function from the simulation's output. Based on the configured optimization algorithm, GenOpt selects new values for the parameters and repeats the process until the minimum value for the cost function is found.

The most important tasks before starting an optimization process are the following:

- Selecting simulation parameters and their possible range of values.
- Defining the cost function. It can be anything that can be obtained from the simulation outputs.

Preparing the simulation template to include placeholders for the parameters and making available the required outputs for calculating the *cost function*.

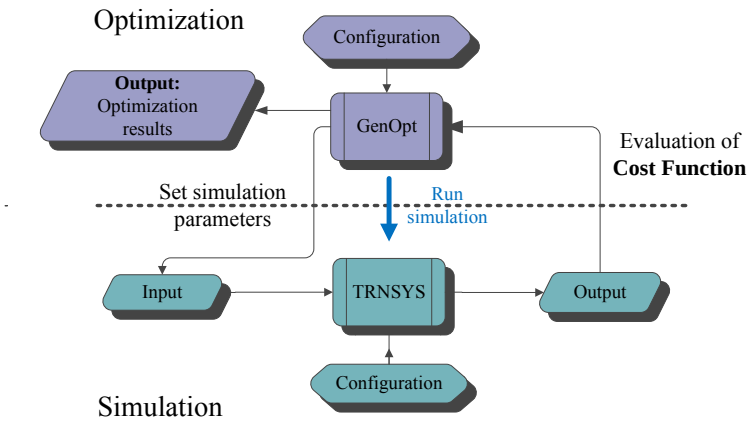

Figure 3-3: TRNSYS - GenOpt integration

3.3.2 MPC implementation details

In Chapter 5 only the control strategies for better managing the STTS level of charge (STD+) and for *forcing* the BTES discharge (FRC) are implemented and tested in the simulation model. For the former, optimal values are found for the simulation period, in the latter, the implementation employs the concept of lookup table. In Chapter 6, all four proposed control strategies are implemented; their optimal parameters are found by following two different mechanisms related to online MPC: CTBO and CLO. As explained before, they are not actual online MPC implementations because of the existing limitations for an actual integration between simulation and the real system. Moreover, there is no frequent feedback on how the real system reacts to the proposed control settings.

The intervals for applying optimized control settings (and then having system feedback) and the optimization horizon are much longer than traditional MPC applications; the interval of application is defined as 1-year period while common values are in the range of minutes or hours. Besides the practical limitations, the long interval was also chosen due to the system's 1-year cycle and the interest for analyzing the impact of control settings on the following years' behaviour. Regarding the *horizon length*, it is usually defined in terms of hours or days; horizon length is much longer for CTBO and CLO: one and six years respectively.

This approach could be considered as an option for deploying MPC control in the real system using a defined *time-interval*. In this situation, a calibrated or validated model could be prepared

and evaluated every *time-interval* (it could be one year or even shorter, depending on the availability of an updated accurate model). The control parameters for one *time-interval* would be then optimized based on seasonal forecasts and the expected system performance (either function of energy and/or cost savings) over a longer time period (horizon) consisting of multiple *time-intervals*. The resulting optimal control settings would be only applied for the first *time-interval*, and at the end of it, when the real systems' output is available the process is repeated but the horizon moves forward. The process, illustrated in Figure 3-4 for the two first iterations, can be continuously repeated after each *time-interval*.

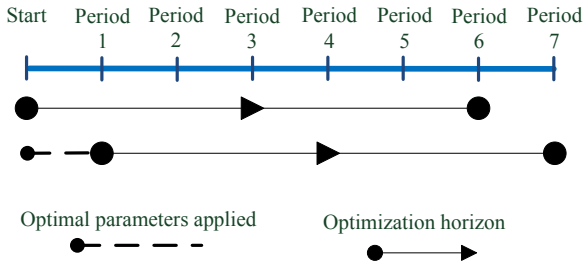

Figure 3-4: Receding horizon

3.4 Control strategies assessment

Several performance indicators can be used to assess different control strategies. Yearly energy performance indicators naturally come to mind: *Solar Energy delivered to District Loop*, *Solar fraction, Energy extracted from BTES,* are for example the selected performance indicators in the Drake Landing reports (Sibbitt et al., 2012).

Although the electricity consumed by pumps and accessories is reported, it is not currently included in the most prominent performance indicators. Electricity use does have a significant impact on operating costs and on CO_2 emissions, so a new global performance indicator was used to include it: the Weighted Solar Fraction.

3.4.1.1 Weighted Solar Fraction (WSF) definition

The Solar Fraction (SF) does not represent the impact of electricity consumption nor the actual gas consumption, Q_Boiler which depends of boiler's efficiency. Solar fraction (SF) is by definition:

$$SF = \frac{Solar\_Energy\_to\_District}{Total\_Energy\_to\_District} = \frac{Q\_Solar_{toDistrict}}{Q\_Solar_{toDistrict} + Q\_Boiler_{toDistrict}} \quad (3.1)$$

In other words, SF is a measure using as reference the district load demand (*Total_Energy_to_District*). With the demand being the 100% of what is supplied to the district, SF is calculated with $Q\_Boiler_{toDistrict}$ instead of the higher value of Q_Boiler.

To take into account all the different energy sources needed for system operation, the reference is shifted from thermal energy demand (*Total_Energy_to_District*) to primary energy consumption (*Total_Energy_System_Operation*, the total energy invested for operating the system). This is consolidated in the new parameter named Weighted Solar Fraction (WSF):

$$WSF = \frac{Q\_Solar_{toDistrict}}{Total\_Energy\_System\_Operation} = \frac{Q\_Solar_{toDistrict}}{Q\_Solar_{toDistrict} + Q\_Boiler + 3P_{pumps}} \quad (3.2)$$

For WSF calculation, gas consumption by the boiler (Q_Boiler) replaces thermal energy provided by the boiler. Moreover, pumps electricity (P_{pumps}) is multiplied by a factor of three – representing the typical fossil-fuel plants performance. The value of three is also a reasonable approximation of the respective weights of the two forms of energy if monetary costs or CO_2 emissions are of interests. Actual energy costs for DLSC show an annual electricity-gas ratio between 3 and 4 (NRCan, 2012c). The ratio of three in WSF was always used during this research to be consistent and to facilitate the comparisons, but it could be changed in a particular case or application.

Table 3.4 allows comparing the two measures for three different cases. WSF is always lower than SF but there is not a direct equivalence between them; sometimes SF increases but WSF not.

Table 3.4: SF vs. WSF

Item	**Case 1**	**Case 2**	**Case 3**
Solar Energy to District (GJ)	2 044	2 046	2 048
$Q\_Boiler_{toDistrict}$ (GJ)	53	51	49
Total Energy to District (GJ)	2 097	2 097	2 097
Q_Boiler (GJ)	59	57	54
Pumps electricity (GJ)	124	118	123
SF (%)	*97.5*	*97.6*	*97.7*
WSF (%)	*82.6*	*83.3*	*82.9*

3.5 Summary

In this chapter the four main steps of the methodology were presented along with the supporting concepts. Explanations were provided for the decisions that were taken when designing and implementing alternatives to four elements of the standard control strategy. Existing concepts were modified or adapted from their original definition to serve the purpose of this research: CLO/CTBO implemented on *offline* mode, STTS *Absolute* Charge Level, *Weighted* Solar Fraction.

CHAPTER 4 SIMULATION MODEL

The first step required to implement the methodology described in the previous chapter is to obtain a TRNSYS model of the Drake Landing Solar Community (DLSC) suitable for comparing MPC strategies. The DLSC model was provided by one of the Design Team members, Thermal Energy System Specialists (TESS). This model dated from 2009 and it had not been updated to reflect changes in the system and/or control rules since then, but it was complete enough to be used with some modifications. Figure 4-1 shows the different steps followed to adapt the model to the research's requirements.

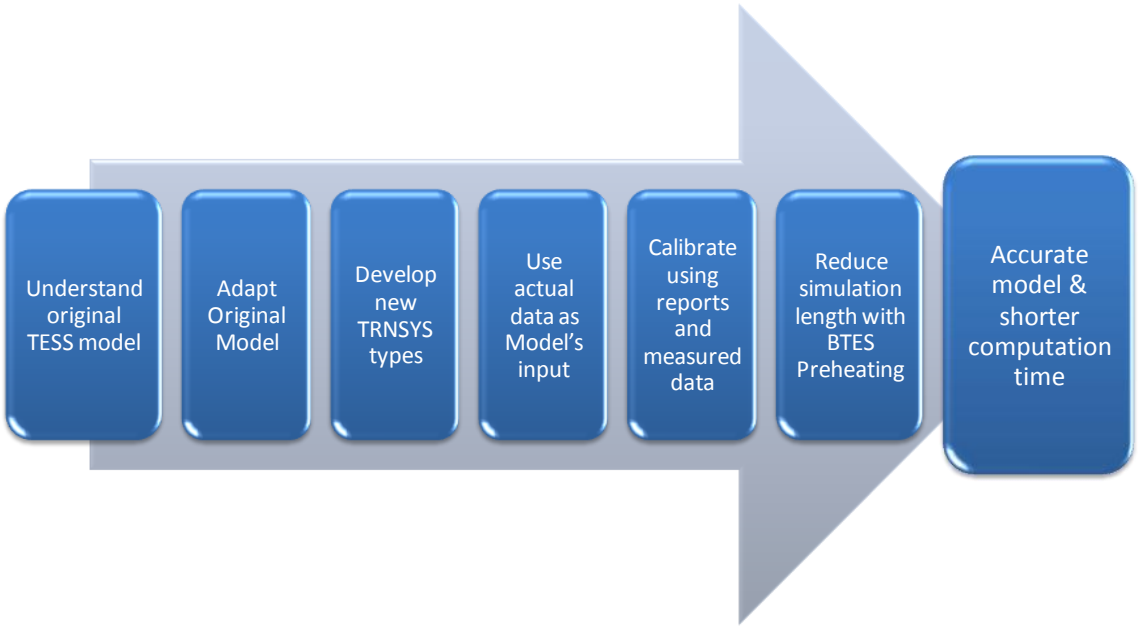

Figure 4-1: TRNSYS model calibration process

The modification and calibration process consisted of several steps with the objective of finding a model which:

- Behaves very closely to the physical system for the last two years of operation, and,
- has short computation time to speed up the optimization of control strategies parameters (optimization is a very demanding process because it needs to execute a large number of simulations)

Before undertaking the calibration process, the initial task was the understanding of the existing TRNSYS model, to identify the system loops and their components along with the model's inputs and outputs. The existing model review is described in section 4.1. The two following steps, adapting the model to reflect the current control strategy and developing new TRNSYS components, are presented in section 4.2. Section 4.3 (Model calibration) describes how actual monitored data (provided by NRCan) were used to obtain a calibrated model. Finally, section 4.4 (Improving computational speed) introduces the concept of BTES pre-heating used in the last task for shortening simulation time.

4.1 Existing TRNSYS Model

In the following description of the DLSC TRNSYS model, system loops and model's main inputs and outputs are identified. Particular emphasis is placed on components affected or involved during the model calibration process.

4.1.1 Solar loop

Figure 4-2 shows the TRNSYS components (types) representing the solar loop. Thick solid lines represent fluid flowing between the components. Light-green lines bring information about weather conditions (temperature and solar radiation). Solid blue lines indicate output samples needed for taking control decisions. Dashed blue lines are control signals.

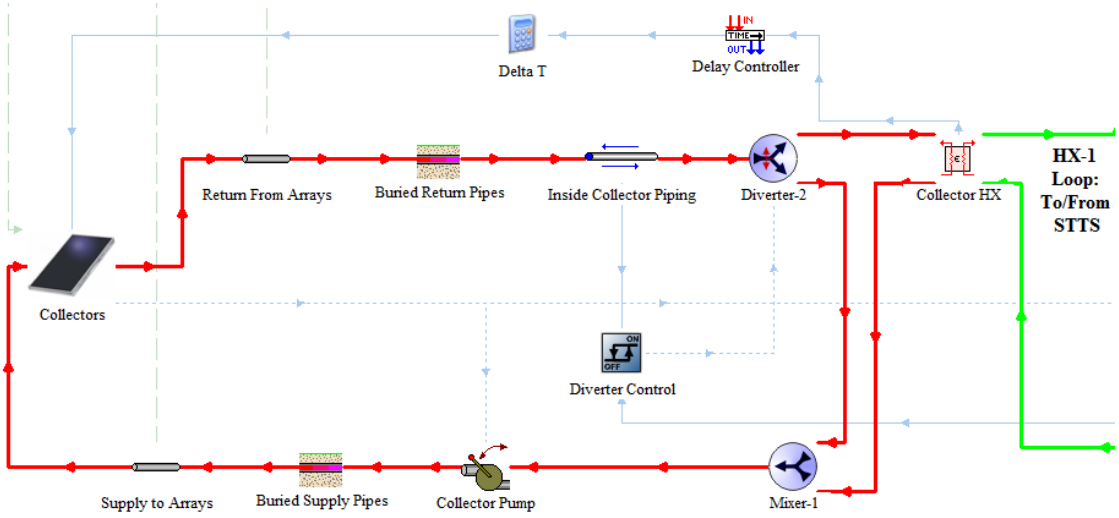

Figure 4-2: Solar Loop

Pipes surrounded by air and buried pipes are represented by the appropriate models. *Mixer, Diverter*, and *Diverter Control* allow switching between normal and bypass modes. The *Solar Collectors'* desired output temperature is set by a formula (Calculator icon) named *Delta T*; it is the *HX-1's* output temperature (solar loop side) plus the desired temperature rise (15°C in the current control strategy). The *Collectors* type models the energy performance of solar collectors but also includes the control logic for the *Collector pump* speed in order to maintain the desired temperature rise. The *Delay Controller* prevents convergence issues by using the HX-1 outlet temperature from the previous time step.

Last, but not least, the *Heat Exchanger* type links this loop with the complementary HX-1 loop which involves the STTS.

4.1.2 District loop

As it can be seen in Figure 4-3, there are some new types in this model section: *Auxiliary Boiler*, *HX-2* (Heat Exchanger 2) and *Imposed Heating Loads*. As in the real system, the *Boiler* here is only enabled when the temperature of hot water coming from STTS through *HX-2* is below the district loop set-point (DLSP). *HX-2* is a type that combines the functionality of bypass and pump speed control (Pump 4) for keeping its output at the required set-point (DLSP).

Detailed DLSC models included the four branches of homes with their pipes and individual homes heat load (Thermal Energy Systems Specialists-TESS, 2007). The selected model is simpler and employs the *Imposed Heating Loads* type to replace all the houses with an estimated load (linear regression based on the ambient 6-hour moving average of the temperature). The different piping loops are aggregate within a single one.

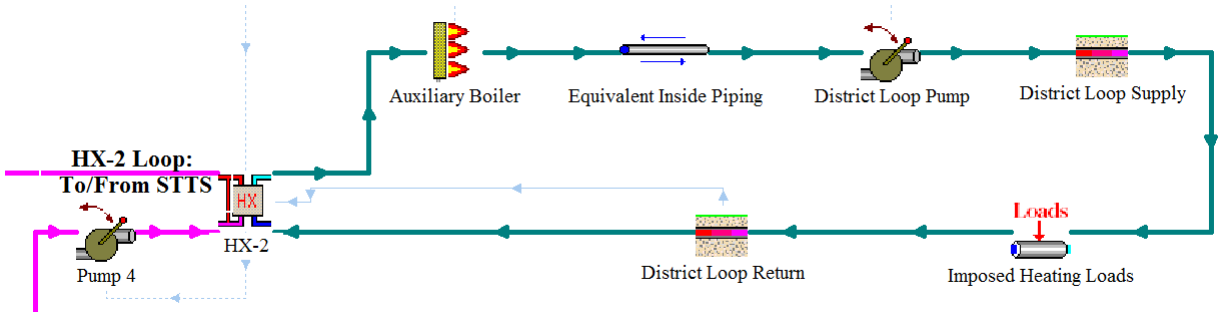

Figure 4-3: District Loop

4.1.3 BTES loop

The main type in the loop is labeled *Borefield* (type 557); it represents the borefield seasonal storage (BTES) with the Duct Storage Model (DST). Type 557 can simulate charge or discharge depending on a switch that indicates its operation mode and reverses the fluid direction (center to periphery or opposite). In Figure 4-4, the olive green line represents the *BTES discharge circuit*, and the red-brown line is the *BTES charge circuit*. Both circuits flow in opposite directions and are connected to the borefield loop through a *Mixer* and a *Diverter*. This model representation is not exactly as the piping network in the real DLSC system, but both configurations are equivalent if piping lengths within the energy center are neglected.

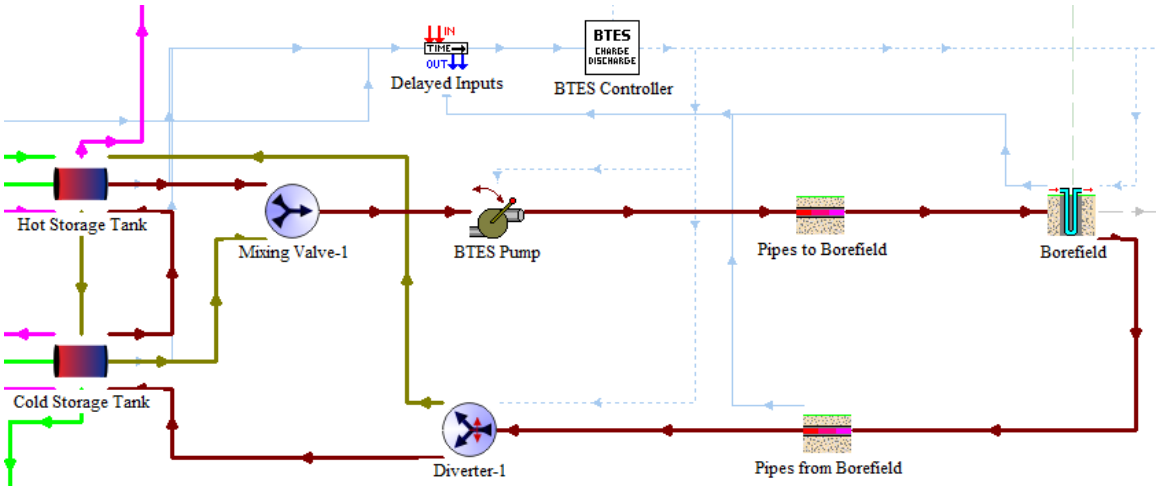

Figure 4-4: BTES Loop

At any time, the operation mode of *Borefield* is determined by *BTES Controller* using the logic presented in section 2.3.4 (BTES loop control) and the delayed outputs of the two tanks (nodes temperatures) that constitute the STTS.

4.1.4 Model Inputs

The CWEC file (Canadian Weather for Energy Calculations) for Calgary (Alberta, Canada) was used as input for weather conditions, including solar irradiation. The CWEC file contains a full year of weather variables made of typical months selected over a 30 years period; it is read sequentially and rewound if the simulation lasts for more than one year (which is the usual

situation). The *District Loop Set Point* (DLSP) is read in a lookup table as a function of the ambient temperature.

To determine if the simulation enables *summer* or *winter* operation mode, another file was included in the original model. This *degree-hour* file depends on the CWEC file being used, it means that the number of *degree heating or cooling hours* –that mark the temporary winter conditions or the return to summer mode (as explained in section 2.3.1) –is pre-computed using the CWEC temperature data. As the CWEC file, this one is read sequentially and rewound if needed.

Another important input is the district load. It has been indicated in section 4.1.2 that a simple regression on dry bulb ambient temperature (see Equation 4.1 below) is used to calculate the space heating load. There is no file directly connected to this input but it obviously depends on weather information (provided by the CWEC file).

$$Q\_HeatLoad = 1000000.*MAX(0,(-0.803*T\_Amb\_Rolling+9.31))/24 \quad [kJ/hr] \qquad (4.1)$$

where, T_Amb_Rolling is the air temperature moving average over the last 6-hour period.

All the inputs, excepting DLSP, were replaced, in a further phase, by the actual data obtained from the physical system's monitored variables.

4.1.5 Model Outputs

During the simulation execution, more than 50 variables are integrated and recorded monthly, most of them are heat transfers (including thermal losses) but there are also variables regarding pumps electricity consumption. For analysis and reporting purposes, those variables are consolidated in a smaller set of items closely related to those found in DLSC's official reports (See Table 4.1).

Table 4.1: Model's output items

Item	Notes
Total Incident Solar Energy	Total tilted radiation over the whole area of collectors array
NET Total Solar Energy Collected	Including solar loop thermal losses
Total Solar Energy Delivered to STTS	
Total Energy Delivered to BTES	

Item	Notes
Total Energy Extracted from BTES	
Total Solar Energy Delivered to District Loop	
Natural Gas Energy Used by Boiler	
Boiler Thermal Energy Delivered to District Loop	After the Boiler's efficiency is taken into account
Total Energy Delivered to District Loop	Includes Solar energy and effective boiler's delivered energy
Net Average Solar Collector Efficiency	Using NET Total Solar Energy Collected
Solar Fraction	*= Total Solar Energy Delivered to District Loop / Total Energy Delivered to District Loop*
Electrical energy used by Pumps	

4.2 Model changes and new TRNSYS components

After the model was understood, the following changes were made to prepare the model for calibration against measured data and to update the control rules:

- The DLSP input file was changed to reflect the current range from 37°C to 55°C (the previous range was from 38°C to 65°C).
- A new BTES controller type was developed to represent the actual control strategy described in (Enermodal, 2011). This component is described below.
- The CWEC file was replaced with monitored data. The pre-computed *degree-hour* file (to switch between summer and winter modes) was replaced by a new TRNSYS type (see section 4.2.2 Degree-hour counter).

4.2.1 BTES controller

The main skeleton of this new type's logic is the existing BTES controller but modified to include all the rules from the current control strategy. The parameters and inputs are different from the original type, but the outputs are still the same. Table 4.2 displays the type's parameters grouped in a few categories. Inputs and outputs are summarized in Table 4.3.

Table 4.2: BTES controller's configuration parameters

Configuration parameters	**Notes**
Winter and summer charge Factors	They are the multiplicative *factors* for the relationship between *STTS % Charge* and *STTS % charge required*. When *STTS % Charge* is higher than *factor* times *STTS % charge required,* it indicates the BTES charge process must start.
Winter discharge Factor	If *STTS % Charge* is lower than *factor* times *STTS % charge required,* it indicates the BTES discharge process must start. Summer discharge factor is always set to 1 but this mode is rarely used.
Winter and summer discharge Level	The relationship between *STTS % Charge* and *STTS % charge required* is complemented with this additive *Level* for fine tuning purposes. Levels for *charge* process are set to constants; they are not *type's* parameters.
Winter and summer charge Hysteresis	Once the charge process is initiated it does not stop if the multiplicative-additive rule is no longer valid. It has a tolerance value defined by this 'hysteresis'.
Winter and summer discharge Hysteresis	Same concept is applied for discharge.
Start Charge BTES temperature delta	It defines the temperature difference that must exist between the BTES input and output in order to start the charge process.
Start Discharge BTES temperature delta	Same concept is applied for discharge.
Keep Charging BTES temperature delta	Similar to the previous rule but applied to allow the process to continue given the BTES temperature delta is respected.
Keep Discharging BTES temp. delta	Same concept is applied for discharge.

Table 4.3: BTES controller's inputs and outputs

Inputs	**Outputs**
Winter mode	BTES circulation switch
Summer mode	STTS % charge
DLSP	STTS required % charge
3 Hot tank temperatures: top, middle, bottom	BTES pump signal
3 Cold tank temperatures: top, middle, bottom	BTES charge signal
Temperatures from pipes going to BTES	BTES discharge signal
BTES out temperature	

4.2.2 Degree-hour counter

It counts the number of cooling and heating degree hours (DH). When the range of dates indicates it is *summer* mode, operation can be changed to *winter* or switch back to *summer* based on the DH rules found in Enermodal (2011). The parameters are explained in Table 4.4.

Table 4.4: Degree-Hour Counter's inputs and outputs

Configuration parameter	Notes
Degree_hours_base	17 °C for DLSC
CLGreset_HTGvalue	When the number of heating DH reaches this amount, the counter for cooling DH is reset. For DLSC it is 15.
HTGreset_CLGvalue	When the number of cooling DH reaches this amount, the counter for heating DH is reset. For DLSC it is 20.
Max_Cooling_DHR	The threshold value for cooling DH that indicates switching the operation mode to *summer*. For DLSC it is 15.
Max_Heating_DHR	The threshold value for heating DH that indicates switching the operation mode to *winter*. For DLSC it is 5.

The type's only input is dry-bulb temperature which is provided by weather or text files. Besides the outputs for the number of degree-hours, there are two Boolean outputs that directly indicate the operation mode to apply:

Is_Max_CLG_DHR: Set when the simulation should switch to summer mode.

Is_Max_HTG_DHR: Set when the simulation should switch to winter mode.

4.3 Model calibration

Using the changes to the original model and the new types described in previous sub-section, the next objective was to have a calibrated long-run model for the last two years of DLSC operation. (The model could not be tuned for the whole five years due to the changes in operating conditions and control system through the years.)

To achieve that objective, the measured data needed to be processed before being used as model's input. Additionally, some BTES control parameters had to be tuned to achieve a close

agreement for the simulation's *Solar energy sent to District Loop* and the actual value found in the official DLSC reports. Calibration and further simulations adopted a time-step of 10 minutes to synchronize simulation with the same interval used for monitored data.

4.3.1 Using measured data

The Drake Landing Solar Community (DLSC) is monitored by a set of sensors measuring temperature, radiation, pressure and flow meters. Control signals, such as BTES charge or discharge, or boiler ignition are also recorded. The monitoring system records the measures every 10 minutes, and then the values are stored in CSV files. Each file contains between a month and a year of data. The measured data started to be collected on July 1st 2007, and this study uses data recorded until June 2012, the end of the 5th year of operation.

4.3.1.1 Processing of monitored variables

The total number of monitored variables has been changing because more information and control signals have become available with system updates, for instance, the addition of new small capacity boiler and the signal that indicates when it is active.

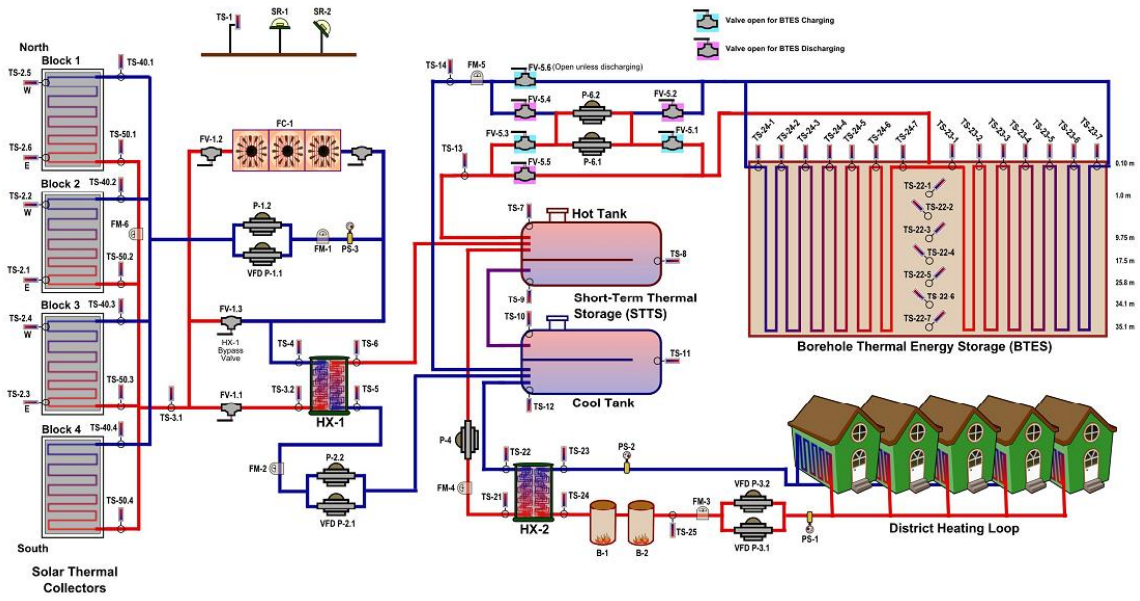

Figure 4-5: Monitored variables (Source: Sibbitt et al., 2012)

Figure 4-5 shows the position of sensors and actuators; they cover all the important points to deliver information about the system status. TS stands for temperature sensors, FM for flow meters, SR for solar radiation sensors (pyranometers), PS for pressure sensors, FV for flow valve, P-x.y's make reference to the pumps. Some extra columns, not indicated in the figure, are: GM-1, the gas meter; EPM-1, the electric power meter; BBE-x, the control signals for the 3 boilers, B-1, B-2 and B-3 (the schematic is not updated to include the new boiler).

Using measured data as model input was not straightforward, there were several data inconsistencies: missing or zero records, duplicated rows, wrong high values due to defective sensors, Day-light Saving Time (DST) disregard. Before being able to use the data as input to the model, they were processed for detecting and fixing those inconsistencies. The process of data conversion/fixing was done using mainly Matlab.

4.3.2 Calibration details

Two text files containing 5-year variables were generated after data processing; they were used as inputs for the TRNSYS model. One contained weather information: dry-bulb temperature, the three solar radiation components and the sun's azimuth. The other included only the heating load. The CWEC (weather) file and the heating load formula were replaced in the model by the actual measured weather and heating load using the generated files.

Using the measured data files as inputs of the model was not enough to have a calibrated model, the *BTES controller* parameters needed to be adjusted because the control strategy document (Enermodal, 2011) indicated that some values have changed (and probably will change) over time. More challenging was the fact of running a simulation for five years with the same control parameters when in the real system these parameters have been changing. For these reasons the model was calibrated only for the last 2 years of operation. Multiple simulations were run to find the best BTES controller parameters leading to that objective.

This tuned model with modified inputs matches closely (less than 2 % difference) the amount of *Solar energy sent to District Loop* for years 4 and 5 in the real system. The gas consumption was also found to match the measured value.

To be able to consider electricity consumption in the optimization processes, parameters of the solar, district and BTES loop pumps, which together represent 80% of electricity usage, were

also adapted. Regression curves and electricity consumption reported by NRCan (Natural Resources Canada-NRCan, 2012a) allowed to closely match (within 5% difference) electricity consumption.

The resulting model out of this process is called the *reference long-run* model because it runs from year 1 (July 2007) until year 5 (June 2012); DLSC operating years start on July 1st and end on next year's June 30. Table 4.5 summarizes the variables considered for model calibration and compares the values from official reports and those obtained after running the calibrated model.

Table 4.5: Reports vs. Calibrated model

	Year 4 (July 2010-June 2011)		**Year 5 (July 2011-June 2012)**	
Energy parameter (GJ)	**Report**	**Model**	**Report**	**Model**
Solar energy delivered to District	2 456	2 489	2 048	2 028
Gas consumption	436	429	76	76
Electricity consumption	145	142	130	123
Heating load	2 859	2 875	2 120	2 097

4.4 Improving computational speed

To achieve shorter computation time a *reference short-run* model was needed. The concept behind it was to start the simulation at a later time than the *long-run* model but still be able to have the same output for years 4 and 5. The "pre-heating period" feature of Type 577 was used for that purpose. When simulation starts and the *pre-heating* parameters are configured, the type acts as if there were already some level of stored heat in the ground so there is no need to run the simulation from year 1. Since the interest is in the results for years 4 and 5, the objective was to find a pre-heating strategy that would account for the first three years of operation.

4.4.1 BTES preheating

Figure 4-6 depicts the three periods involved in BTES preheating implementation:

- *Skipped period*. As the *short-run* simulation starts on January 2010, the period from July 2007 to January 2010 is not *simulated* (that period is indicated by the dashed line).

- The 6-months transition period is included to let the BTES and other simulation components reach long-run model's status. This is needed because BTES preheating does not provide a perfect match for BTES temperature distribution when the simulation starts, especially in the case of a stratified system. BTES conditions, though, are close enough to be set on track after a few months of simulation run. The period of 6 months was found to be long enough to deliver the desired accuracy, and it allowed starting the simulation at the beginning of an operation year (July) while using the preheating feature for an integer number of years (as required by the pre-heating parameter).
- Simulation results are only analysed for year 4 and 5 (*observed period*).

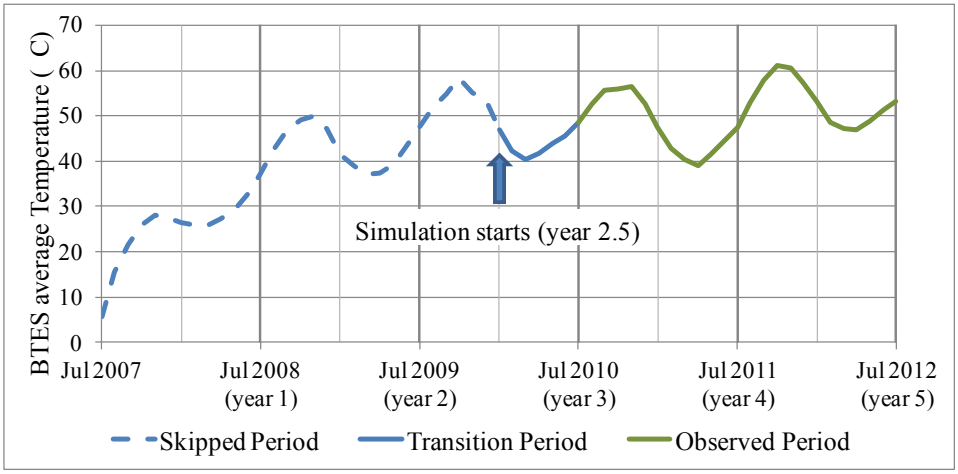

Figure 4-6: BTES pre-heating

Type 557 has seven parameters related with the pre-heating feature, 3 for the air temperature distribution through the year and 4 for ground temperatures distribution. Due to BTES top insulation, air temperature parameters proved to have minimal impact in preheating configuration. The parameters listed in Table 4.6 are only those related to ground temperature distribution in the whole volume.

Table 4.6: BTES pre-heating parameters

Parameter	Value	Notes
Minimum preheat temperature (°C)	37.5	It is assumed that the ground temperature distribution follows a yearly sinusoidal shape defined by these two parameters.
Maximum preheat temperature (°C)	47.0	

Parameter	Value	Notes
Preheat phase delay (days)	182	It indicates the sin function's phase needed to make its minimum coincide with the day of minimum BTES temperature.
Number of preheating years	1	It is used to define and calculate the extent and distribution of radial heat conduction.

The value for *Preheat phase delay* is derived from year 4 data. For the other three parameters, values were found by applying root-mean-square-error (RMSE) to the difference of BTES temperatures for long-run and short-run models and running an optimization process to reduce it. The Type 557's outputs representing ground temperatures that were taken into account for calculating the RMSE are *Average storage temperature* and *Average near-the-boreholes temperature(s)*. Exact meaning of these variables and more details of the process can be found in Appendix 1.

Figure 4-7 shows how *Average storage temperature* starts at a different value for each simulation model but it gradually converges before reaching the first 6 months (4380 hours) –corresponding to the transition period. For the observed period of two years (hours 4380 to 21900) the two simulation curves are virtually indistinguishable. The other *near-the-boreholes* temperatures exhibit a similar response but they are not displayed in the Figure.

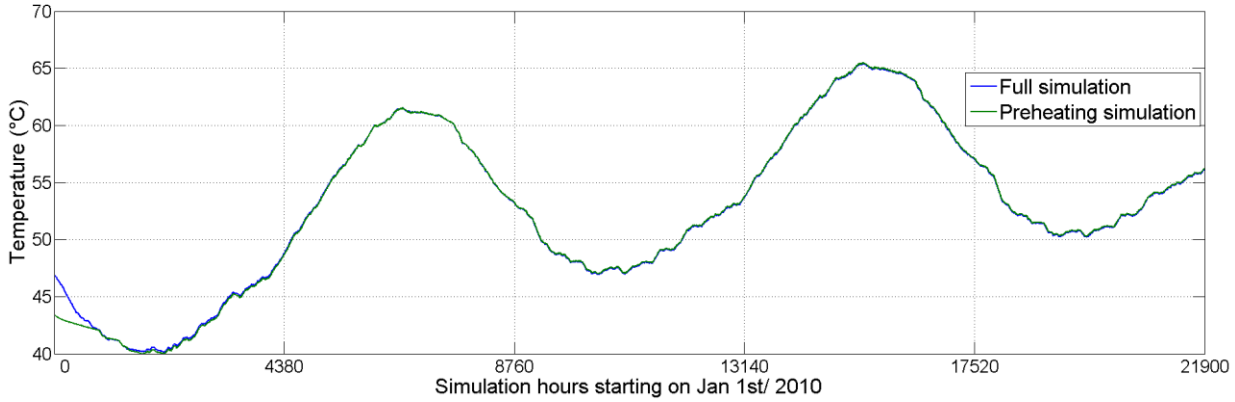

Figure 4-7: BTES average temperature for short- and long- run models

4.5 Summary

This chapter presented the modifications applied to an existing TRNSYS model to meet the requirements of outputs accuracy and short computation time. The main four activities were developing new types, processing actual data, calibrating the model and improving the execution time (BTES preheating).

A calibrated model was obtained; it matches the measured energy performance at DLSC within 2% for the parameters *Solar energy sent to District Loop* and *Gas consumption*, and 5% for electricity consumption.

A procedure was established to use Type 557 preheating feature and shorten the required simulation length. The BTES is pre-conditioned by a (not simulated) preheating and a 6-month (simulated) transition period. The simulation length to obtain realistic values for years 4 and 5 is reduced from 5 years to 2.5 years, thereby saving 50% of the computational time.

CHAPTER 5 CONTROL STRATEGIES FOR BTES OPERATION

This chapter explains the implementation details of alternatives for BTES control. As explained in the methodology, the developed control strategy builds on the expert knowledge included in the current DLSC control strategy, referred to as STD (which is described in section 2.3).

Four alternative strategies will be discussed: Standard improved (STD+), Force BTES discharge coupled with STD strategy, Force BTES discharge with STD+ and Continuous Time Block Optimization (CTBO). All the strategies were tested, optimized and evaluated using the *short-run* model.

Results are discussed at the end of the chapter. Strategies parameters are summarized but emphasis is put in comparing strategies in the short and long term behaviour.

5.1 Standard improved (STD+)

This strategy is not based on Model Predictive Control (MPC); it is basically the same standard strategy-STD (described in Chapter 2) with the difference that the parameters *Winter Charge Factor* and *Winter Discharge Factor* were optimized to obtain increased energy performance for years 4 and 5. Thus, the *cost function* to minimize was defined as the addition of gas consumption and 3 times electricity consumption (the factor of three is to account for usual energy efficiency in fossil fuel power plants, as discussed in the methodology).

5.1.1 Optimization results

Optimized parameters (STD+) are compared with original parameters (STD) in Table 5.1. The sharp increase in parameter *Winter Charge Factor* shows that the BTES should be charged only in cases where the STTS has a very high *% Charge*, i.e., BTES charge should be practically avoided during the winter mode if the objective is to increase solar fraction.

Table 5.1: Strategies comparison

Case	Winter Charge Factor	Winter Discharge Factor	Solar Fraction (%) - years 4 and 5	Collectors efficiency (%) - years 4 and 5
STD	3.5 – 5.0	1.0	90.9	31.0
STD+	9.0	2.1	91.4	30.2

The other parameter, *Winter Discharge Factor*, is more than doubled in value for STD+. What it means is that the BTES discharge process should be started before the STTS had discharged beyond the minimum acceptable to fulfil the expected district load (*% Charge required*). It is important to highlight that the change in the factors has the indirect effect of reducing collectors' efficiency as seen in the last column of the Table.

The STD+ parameters' net effect is to maintain a higher STTS level of charge compared to the STD strategy: a charge reserve is imposed for difficult weather conditions. A consequence due to fewer charge/discharge cycles is the reduction of BTES pump electricity consumption.

5.2 Force BTES discharge coupled with STD (FRC)

5.2.1 Description

This control strategy is actually an *add-on* to the STD strategy; it means that STD is working all the time except for some intervals when the FRC strategy takes over to force the BTES discharge in anticipation of difficult weather conditions.

The mechanism is derived from manual trials that proved that, in the case of important heat load increases, starting the BTES discharge some time ahead of the moment determined by STD provided the STTS with higher level of charge. FRC will overwrite STD's output when forecast weather for the near future indicates:

- Very low air temperatures, leading to an increase of the district heating load, or,
- Low solar irradiation, meaning a reduction of collected thermal energy sent to the STTS.

To determine how low these values can go before forcing the discharge, representative threshold levels are established for them. Using the thresholds, FRC strategy can be summarized as:

IF (District Load > Maximum District Load Threshold)

OR (Usable Solar Energy < Minimum Usable Solar Energy Threshold)

THEN Force BTES discharge

Usable Solar Energy is a fraction (20% in this study) of the total incident solar energy on the collectors over the next 24-hour period. That fraction represents the reduction due to the average

collector performance (30%) and approximated heat losses. *District Load* could be estimated using forecast temperatures.

This rule is evaluated every hour over the 24-hour forecast horizon. The value was chosen after that manual tests with longer periods did not indicate a clear advantage in the STTS level of charge for days of extreme weather. Shorter periods were considered in the first automatic tests; the implementation was complicated because extra rules were needed to deal with night periods when no sun energy is available.

The controller has a built-in check to avoid the special situation whereby *forcing* the BTES discharge could provoke the reverse of heat transfer flow and mistakenly remove thermal energy from the STTS.

The thresholds used in the rules above are the most important parameters. They are set according to different scenarios corresponding to given sets of operating conditions, as explained in the next section.

5.2.2 Operating scenarios for the FRC strategy

The implementation of FRC is based on the Model Predictive Control (MPC) concept of pre-computing lookup tables for a grid of possible scenarios. It has been pointed out that to implement this MPC method, the problem has to be *decomposed* into simpler problems, and the varying conditions should be parameterized to reduce the range of values to consider. The first requirement is considered by limiting the problem to *winter mode* BTES discharge only. Charge process is much less important for increasing energy performance. External weather conditions are *parameterized* using terms that convey more information: District Load and Usable Solar Energy (both over 24 hours).

An additional *parameterization* is done to define the grid of scenarios in terms of STTS status and BTES status. Using *STTS Absolute Charge Level (STTS ACL)*, defined in section 3.2.4, three STTS charge-related scenarios are defined:

STTS_L (low) corresponds to STTS ACL < 1

STTS_M (medium) corresponds to, 1 <= STTS ACL < 2

STTS_H (high) corresponds to STTS ACL >= 2

Regarding BTES status, two scenarios are derived in an approximate way: January-June (BTES_L) and July-December (BTES_H). For the scenario BTES_L, BTES temperatures are usually low and for BTES_H they are normally high. This pattern is confirmed in Figure 5-1, where the BTES average temperature follows the described annual pattern.

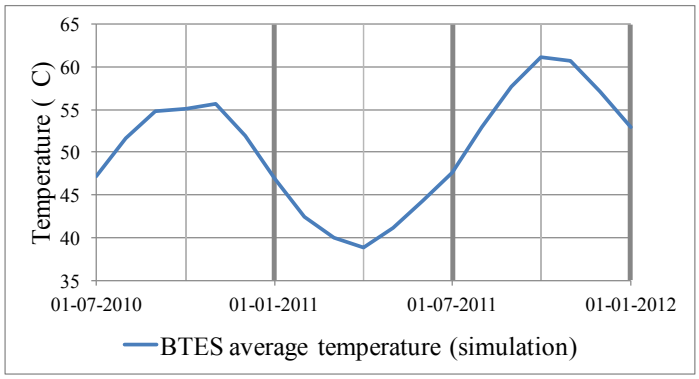

Figure 5-1: BTES temperatures

In Table 5.2, FRC strategy looks at the STTS row and the BTES column to locate the particular thresholds *Minimum Usable Solar Energy (minUE)* and *Maximum District Load (maxL)*, and then to decide –based on comparing future weather conditions to the thresholds– whether BTES is to be discharged or not.

Table 5.2: FRC strategy scenarios/lookup table

STTS charge/BTES case	BTES_L (Jan-Jun)	BTES_H (Jul-Dec)
STTS_L	minUE_L_L, maxL_L_L	minUE_L_H, maxL_L_H
STTS_M	minUE_M_L, maxL_M_L	minUE_M_H, maxL_M_H
STTS_H	*minUE_H_L, maxL_H_L*	*minUE_H_H, maxL_H_H*

Initial optimization tests included the 12 parameters (two per each scenario). Even so, it was found that parameters for STTS_H scenarios were not relevant because in those cases the STTS had enough charge and there was no need for forcing the BTES discharge. The number of FRC parameters was thus reduced to eight which helped to decrease optimization time.

5.3 FRC+: Force BTES discharge with STD+

It is the same FRC strategy with the only difference being that BTES *Winter Charge* and *Discharge* Factors are also included in the optimization process. In other words, STD+'s output is

overwritten by FRC strategy's output to discharge the BTES when conditions apply. In this way, their best characteristics are combined, energy reserve provided by STD+ and FRC's anticipated BTES discharge.

5.3.1 Cost function and optimization cases

When long-term storage is considered for optimization, the period over which the cost function is evaluated can change the results. Optimizing control parameters for a short period of time could affect the system performance in the long-term. E.g. if the BTES is deeply discharged to reduce the gas consumption during a short period, it would surely cause an increase in gas consumption later on. This constraint implies that the *cost function* optimization period has to cover at least one entire heating season, and possibly several years. To assess the long-term impact of FRC+, the cost function is calculated over a three-year period –equivalent to years 4, 5 and 6 of DLSC operation. FRC+ strategy is only applied for the first two years and in year 6 (July 2012 to July 2013) the control is switched back to the standard control strategy. As the actual year six data were not available, two options were tried: year 6 is warm as year 5, or it is cold as year 4 ("warm" and "cold" translate into heating loads respectively lower and higher than average).

Cost function definition is the addition of gas and *weighted* electricity consumption for the 3-year period. Two *weight* factors (W) were evaluated:

- W=3, to take into account the average performance of fossil-fuel plants. This is also close to DLSC average electricity to gas cost ratio for 2008-2010 (NRCan, 2012c)
- W=8, to account for a possible (but extreme) cost ratio between electricity and gas in Alberta.

Four optimization cases (Table 5.3) result from combining the two options for year 6 and the two weight factors for electricity.

Table 5.3: Test cases

	Electricity weight = 3	**Electricity weight = 8**
Year 6 is *Warm*	3E_W	8E_W
Year 6 is *Cold*	3E_C	8E_C

5.4 Continuous Time Block Optimization (CTBO)

CTBO-based control searches for a 24-hour period (block), the best BTES control values for each hour: charge (1), discharge (-1), or idle (0), depending on the disturbances affecting the system. All the optimized settings for the period are applied to the system and not only those found for the first hour as it would be the case for Closed-Loop Optimization (CLO). CTBO is thus close to the ideal optimal control settings and it is employed as the best-case when comparing strategies for short periods of time.

CTBO cannot be applied for long periods of time if the time interval is 1 hour because it would require very high computational power. Every hour added to the *time-block* would become an additional parameter to be optimized. In this particular application, only one optimization cycle was executed; it means that only 24 parameters had to be found. Even if GenOpt does not evaluate the 2.8E+11 combinations (3^{24}), each additional parameter increases the number of simulation runs and thus the computation time.

Figure 5-2 depicts how CTBO is implemented. In a 4-day period, CTBO is employed for the first 24 hours, and then STD is applied for the remaining three days. The 1-day limitation is also due to the fact that in the period used for short-term results (see section 5.5.2), the first day is critical for taking the BTES control decisions.

The cost function is the same as described for the FRC+ strategy but it is calculated over the 4-day period only.

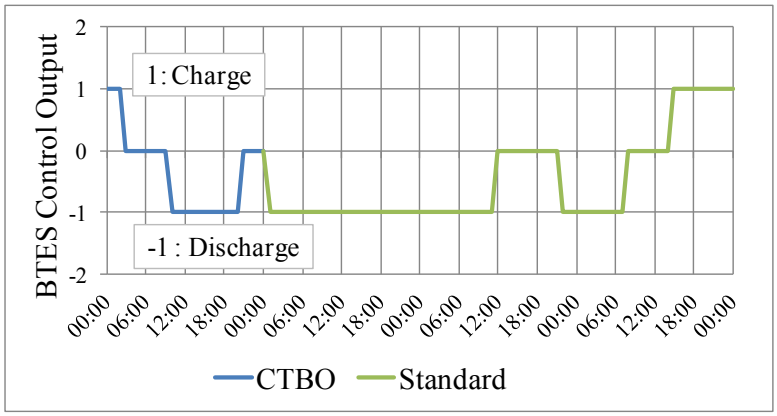

Figure 5-2: CTBO implementation

5.5 Results discussion

The results are analyzed from multiple perspectives. The first one looks at optimal values found for strategy parameters and thresholds. The second aspect is the dynamic behaviour; it examines the system's response over a short period. Finally, three-year results are compared in terms of overall energy savings and BTES average temperature.

The four optimization cases from Table 5.3 (3E_W, 3E_C, 8E_W, 8E_C), which come from combining two weights for electricity and two types of year 6's conditions, were only executed for the best performing FRC+ strategy.

5.5.1 Optimal parameters and thresholds

Initial optimization tests showed that the optimal value for the parameter *Winter BTES Charge* was always found to be the maximum value set at 9, which results in avoiding BTES charge in *winter* mode. For that reason and to limit the number of parameters to optimize, it was not included in subsequent optimizations.

Besides STD+, where *Winter BTES Discharge* factor was approximately twice the STD's value, the FRC+ values were actually lower than those of the STD strategy; its values fluctuated between 0.5 and 0.75. The feature of *forcing* BTES discharge appears to be more important than this factor for reducing energy usage. It can also be concluded that BTES discharge is more affected by the "force BTES discharge" rules implemented in FRC/FRC+ than by the basic comparison rules implemented in the STD strategy.

5.5.1.1 FRC/FRC+ thresholds

Figure 5-3 presents the threshold *Minimum Usable Solar Energy* –the low limit for available solar radiation before imposing BTES discharge– for the four optimization cases.

Using results from the 3E_W case as an example, it can be seen that if the STTS charge level is low (STTS_L) and the BTES charge level is low (BTES_L), BTES discharge will be forced if the usable solar energy anticipated for the next day is 1 GJ or less. If the BTES has a higher charge level (BTES_H), the BTES discharge will be forced if the anticipated daily usable solar energy is 1.5 GJ or less – i.e. more often. On the other hand, if the STTS charge level is higher (STTS_M), the usable solar energy threshold is zero, i.e. BTES discharge will never be forced.

The threshold values for other cases follows the same general trend: BTES discharge will be forced mostly if the STTS charge level is low, and even more often if the BTES charge level is high. If the STTS charge level is medium (STTS_M), BTES discharge is very rarely forced.

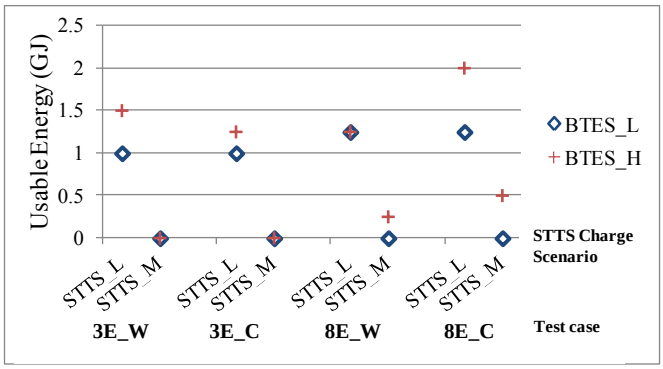

Figure 5-3: Minimum Usable Solar Energy threshold (MinUE)

Figure 5-4 represents the *Maximum District Load* thresholds for the lookup table cells using two columns for each of the four optimization cases. As it has been stated, thresholds for the situations of high STTS level of charge (STTS_H) were not included in optimizations because it was found that there was no need to *force* BTES discharge in these scenarios.

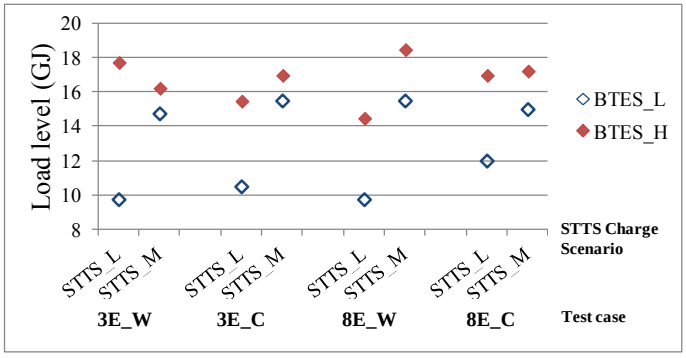

Figure 5-4: Maximum District Load threshold (MaxLoad)

As an example, we will look at the values obtained for the first case (3E_W, which corresponds to a weight factor of 3 for electricity and to a warm year 6). If the STTS charge level is low (STTS_L) and the BTES charge level is high (BTES_H), BTES discharge should be forced if the anticipated load for the next day is around 18 GJ or more. If the STTS charge level is higher (STTS_M), discharged should be forced if the anticipated daily load is 16 GJ or more, i.e. more

often. This may seem counterintuitive at first, but it must be remembered that the "force" rules act to override the standard control strategy, which is still applied. A higher threshold value for the (STTS_L, BTES_H) case than for the (STTS_M, BTES_H) does not necessarily mean that BTES discharge will be used less often – the standard control strategy will, in fact, use that mode. The higher load threshold in this case means that it will only be necessary to override the standard control strategy in exceptional cases (anticipated load higher than 18 GJ).

In all the four optimization cases, the threshold named *Max Load* –the maximum load before control forces BTES discharge– has the minimum value for the scenario where STTS and BTES have the lowest charge ([STTS_L, BTES_L]. As discussed in the example above, some of these results may seem counterintuitive, but they can be interpreted as showing that the standard control strategy must be overridden more when charge levels in the STTS and BTES are low.

These optimized thresholds define a range of possible values for them; actual values would depend on changing weather conditions and costs relationship between gas and electricity.

5.5.2 Dynamic/Short-term behaviour

The 4-day period from February 4th - 7th / 2011 was selected to analyze the control strategies for short-term results. This period is characterized by days having low temperatures (high District Load) and/or low Usable Solar Energy (Figure 5-5, top).

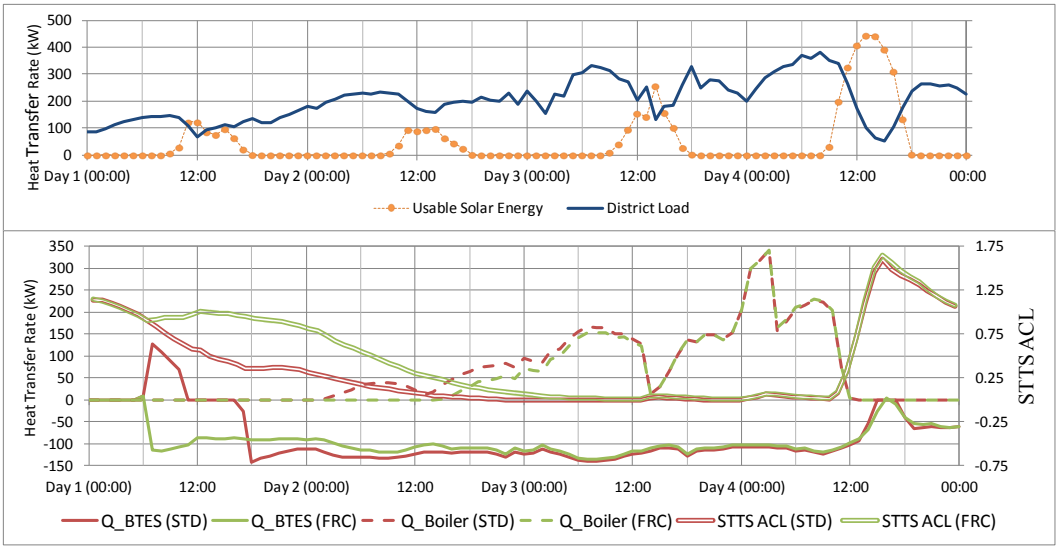

Figure 5-5: Controller comparison for cold winter days

The same Figure (lower part) also represents the STTS Absolute Charge Level (STTS ACL, doubled line), boiler gas consumption (Q_Boiler, dashed line) and BTES heat transfer rate (Q_BTES, solid line). Negative values for the latter indicate that thermal energy is being extracted –i.e. the case when BTES discharges.

It can be seen that on day 1, the FRC strategy (green lines) anticipates low solar radiation and high heating load for day 2, and makes the decision to force BTES discharge. Contrast that to STD strategy (red lines) which, *unaware* of future weather conditions, starts charging the BTES on Day 1. FRC overriding of STD action provokes a rise on STTS ACL and delays using the boiler on Day 2 for almost 12 hours. However, the selected period is extremely unfavourable, and FRC cannot avoid gas consumption on days 3 and 4 due to the high district load, low *Usable Solar Energy*, and limited BTES thermal energy.

The next Figure 5-6 compares STD (red), FRC+ (green) and CTBO (blue) strategies. One problem for carrying out a detailed short-term comparison is that the days of interest are not at the beginning of the simulation and the cumulative impact of different control decision can lead to a very different STTS state of charge at the beginning of the period of interest. To compare the control strategies on the given period, the solution adopted was to start applying them at the beginning of this 4-day period (i.e. February 4th/2011).

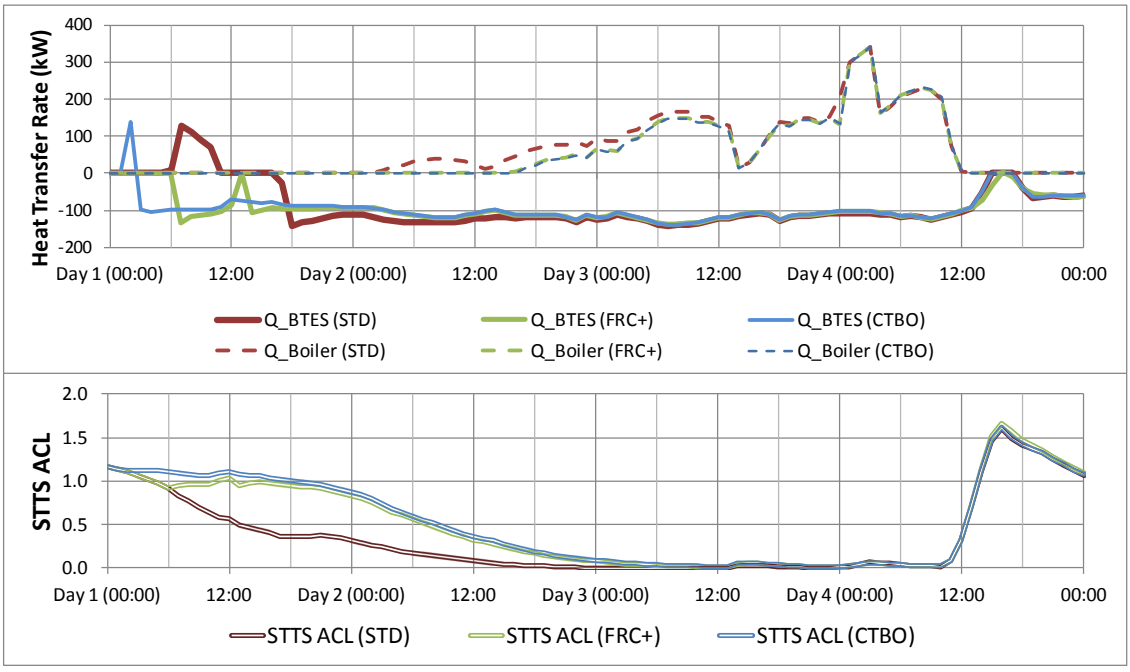

Figure 5-6: STD, FRC+ and CTBO

Note how the STD's STTS ACL (bottom graph) decreases early, starting on day 1, in turn causing boiler to start earlier in day 2 –than in the case for CTBO and FRC+. STTS ACL values diverge depending on BTES being charged or discharged. When BTES discharge is not enough to allow STTS fully supplying the district load, STTS ACL values gradually converge to zero; only during the last day –warm and sunny– their values rise again altogether.

Even if CTBO and FRC+ differ in the time BTES discharge begins, the net effect on Q_Boiler is almost identical; so FRC+ is not far from the ideal control strategy when considering this short period only. To confirm that FRC+ behaves almost as efficiently as CTBO, the data shown in Table 5.4 summarizes energy transfers: the difference between CTBO and FRC+ is effectively very small for both Q_BTES and Q_Boiler.

An additional observation from this table is the confirmation that early BTES discharge reduced FRC+ and CTBO gas consumption.

Table 5.4: Energy transfer (MWh) for the 4-day period

	STD	**FRC+**	**CTBO**
Q_Boiler	6.50	5.49	5.43
Q_BTES	-8.25	-9.12	-9.14

5.5.3 Long-term analysis

The long-term effects are assessed over a three-year period representing DLSC's years four to six. As it has been indicated, years 4 and 5 were run with one of the tested strategies, and the fictitious year 6 (warm or cold) with the STD strategy –the idea of applying the STD control strategy for the 3rd year of this period is to assess the long-term impact of control decisions made by the new control strategies during years 1 and 2. The reference case employs STD strategy for the 3-year period. Two aspects are evaluated: Average energy savings, and BTES temperatures.

Average energy savings per year represented in Figure 5-7 are relative to the reference case. In percentage terms, the best FRC+ strategies are close to 4% energy savings; this includes electricity consumption normalized by a weight factor of 3. It can be noticed that FRC suits better the objective of reducing gas consumption (blue) at the expense of not having electricity

reduction but a slight increase. On the other hand, STD+ is superior for reducing electricity usage (green). When combining the two of them in FRC+, the best energy performance is obtained.

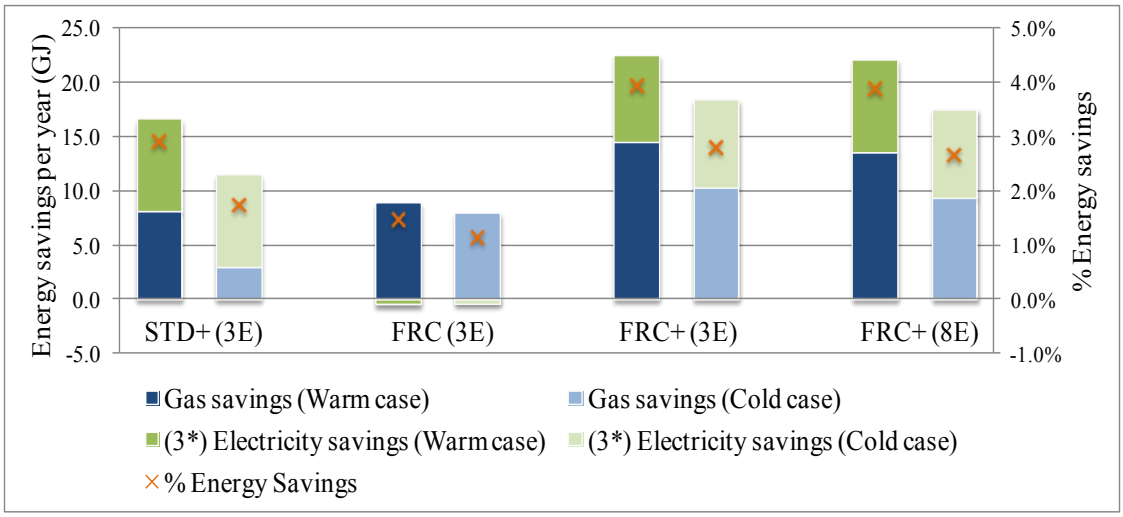

Figure 5-7: Average energy savings

Whereas FRC+ total energy savings for the two different electricity weights (3E and 8E cases) are similar, it can be noticed, though, that in the 8E cases gas savings are slightly less important than electricity –the opposite being true for 3E. In other words, more gas is used if the pumps work less time charging and discharging the BTES. This is the natural result for 8E cases because of the higher electricity influence in the cost function.

Figure 5-8 depicts the impact of control strategies on the BTES average temperature. Blue line and diamonds indicate the warm and cold cases under STD strategy. Green line and crosses do the same for FRC+.

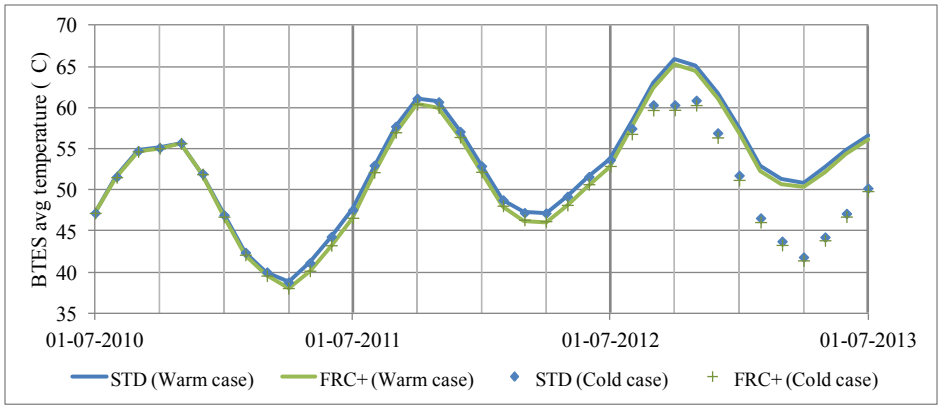

Figure 5-8: BTES average temperature

BTES temperature levels are slightly lower for FRC+ cases because they have more recourse to energy stored in the BTES –by forcing its discharge. Starting from year 6 (July 2012), the difference between the *warm* (lines) and *cold* (markers) cases is more important than the difference between equivalent STD and FRC+ cases. This shows that the year's weather has much more influence in the BTES temperature than the control strategy employed in previous years.

5.6 Summary

The control strategies presented in this chapter mainly attempt to maintain in the STTS a level of charge that is enough to meet the predicted heating load taking the predicted solar input into account. The analysis of dynamic behaviour for a short period of time was complemented with the comparison to a CTBO control strategy, which can be considered as the optimal strategy for the period. On the long-term analysis, CTBO –with 1-hour timesteps– cannot be used due to the high computation time it would require; FRC+ which combines improvements to the standard strategy (STD) and the *forcing BTES discharge* feature is the one with the larger energy savings (close to 4%).

CHAPTER 6 MPC FOR INTEGRATED CONTROL STRATEGIES

This chapter presents the process and the outcome of testing and optimizing the four control alternatives together using two MPC schemas. In the first part, the solar and the BTES loop control are presented in detail. Next sections describe how the two MPC mechanisms, CTBO and CLO, were applied using incremental 1-year periods. Finally, results are presented and reviewed.

6.1 Control strategy for collector loop

In the reference control strategy (Enermodal, 2011), the principal parameter for controlling this loop is the temperature difference between the collector outlet and inlet. The pump speed is modulated to keep the temperature difference (ΔT) as close as possible to a fixed value of 15 C for all weather conditions and STTS/BTES status. It is worth to bring again the fact that if ΔT were above 15°C, less solar energy would be collected, because the collectors would operate at a higher average temperature. The usability of that energy might be higher (higher temperature) and the induced stratification in the STTS could also be improved, but the main positive impact of a higher ΔT would be reduced electricity consumption. A ΔT value below 15°C would result in more solar energy being collected at the cost of higher pump electricity consumption.

The proposed control strategy is based on the idea that ΔT may depend on certain system conditions (STTS status, BTES status) and/or weather forecasts. Nevertheless, only STTS status –by means of the parameter STTS Absolute Charge Level (STTS ACL) – was chosen due to the inverse but clear relation between the collected solar energy and the STTS charge level: More solar energy can be gathered when STTS is low in charge, and vice versa. If this control were to be implemented in the real system, it would be more intuitive and easier to tune-up by system operators than other rules depending on forecasts. So, even though a detailed model was used to develop this control strategy, it is not an MPC strategy. It is included in this dissertation because it is part of the overall effort to develop a practical implementation of MPC for solar communities.

As a reminder, FRC/FRC+ strategies have three scenarios defined in terms of STTS Absolute Charge Level: STTS_L, STTS_M and STTS_H (for low, medium and high values). For solar collector loop control, the same three scenarios were kept but one more was added to consider the

system working in summer mode. In that operation mode, STTS is mainly discharging into the BTES and the operation rules differ from the winter mode.

For each scenario, ΔT is the representative parameter. During the optimization process, the four parameters, identified as ΔT_L (low), ΔT_M (medium), ΔT_H (high) and ΔT_S (summer), are evaluated to find their optimal values.

6.2 Control strategy for BTES loop

Adopting a new control strategy for the BTES pump is needed because of the replacement of the constant speed pump –that was operated in a simple on/off fashion– by a variable speed type. According to discussions with NRCan, the new variable speed pump is currently being managed, more manually than automatically, with settings defined and adjusted to keep an appropriate flow rate and reduced electricity consumption. These settings take into account weather forecasts, current system conditions, historic records and personnel expertise regarding BTES pump operation.

For the proposed control strategy, only BTES discharge was considered. To limit the scope, it was assumed that during BTES charge the pump should operate at maximum flow rate. The control approach was to define flow rate that is adjusted linearly as an inverse function of STTS charge level. Maximum flow rate should be applied when STTS charge is lower than a certain STTS Absolute Charge Level (STTS ACL) limit (ACLmin) so the heat transfer rate could be more significant. On the other hand, minimum flow rate should be set for STTS ACL values higher than a superior limit (ACLmax) because less energy is needed but at a higher temperature.

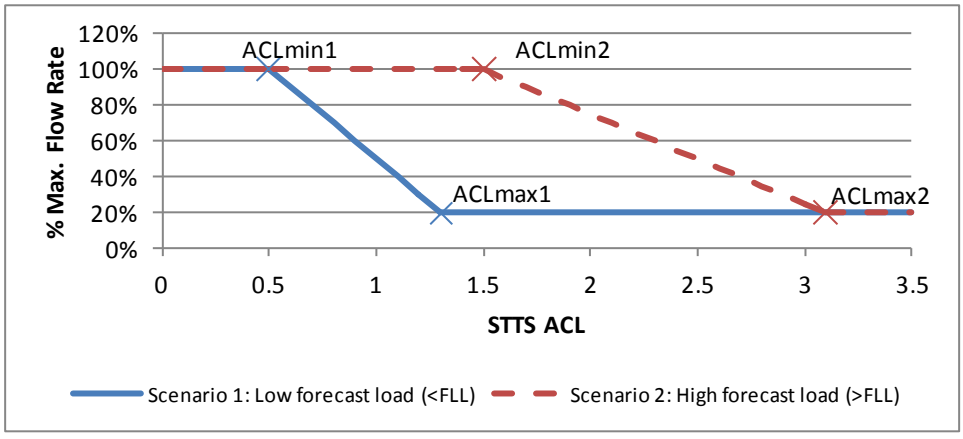

Figure 6-1: Flow rate vs. STTS ACL

The predictive aspect of this strategy resides in the estimated future district load. The two scenarios in Figure 6-1 illustrate the concept: when forecast district load over a 24-hour period is lower than a certain amount (*scenario 1*), ACLmax and ACLmin are rather small because there is no need for fast discharge; on the other hand, *scenario 2* is more sensitive to high load, so it must start increasing the flow rate even if STTS absolute level of charge (STTS ACL) is not too low. To differentiate between the two scenarios another limit called *Future Load Limit* (FLL) was defined; it indicates whether the predicted load is low or high. Depending on the optimization process, some of the five limits (parameters) introduced for this strategy are evaluated for finding their best values while others are just set to constant values.

6.3 Optimization and MPC

Three optimization cases are presented in the following sub-sections. The first one analyzes the individual effect of new pump control strategies over a period including years four and five. The second (CTBO) and third (CLO) cases combine the two pump strategies (collectors and BTES) and FRC+ to perform incremental optimizations (year to year) in a different way.

6.3.1 Proof of concept

These optimization processes are intended to assess the impact on energy performance of pump control strategies and validate their relevance. Besides energy considerations, the idea was also to identify control parameters having less impact in the cost function so they could be set to constant values and be removed from future optimizations.

To assess the two new pump control strategies separately, optimizations were run by enabling the new control in one loop while the other loop was working with the original control strategy. The *cost function* was used as always, as the sum of the gas and 3 times the electricity consumption.

Table 6.1 compiles the results. *Delta T* (solar loop) control exhibited reduced solar energy collection and increased gas consumption –and thus lowered the Solar Fraction (SF) when compared to the others; however, its overall energy performance (Weighted Solar Fraction, WSF) is improved due to the reduction in electricity usage. On the other hand, *BTES pump* strategy had an interesting behaviour: It is not as effective as STD for collecting solar energy nor does it have a large reduction in electricity consumption as *Delta T* but it provided the district with the maximum amount of solar energy of the three cases –which means higher SF and minimized gas

consumption. This shows that, even though the main objective of controlling the BTES pump speed was saving electricity, there is also a positive impact on the STTS thermal performance.

Table 6.1: Summary of pump control strategies

Control strategy / Item	Year 4			Year 5		
	STD (ref)*	**ΔT**	**BTES pump**	**STD (ref)***	**ΔT**	**BTES pump**
Net collected solar energy (GJ)	3 976	3 662	3 870	4 152	3 890	4096
Solar Energy to District (GJ)	2 547	2 539	2580	2 044	2 036	2 048
Gas (GJ)	364	373	328	59	67	54
Electricity (GJ)	142	*119*	137	124	*98*	120
SF (%)	88.6	88.3	89.7	97.5	97.1	97.7
WSF (%)	76.3	77.6	77.8	82.6	84.9	83.2

*Reference case and values are slightly modified compared to Chapter 5 because pump parameters were modified to better reflect actual operating conditions that define a minimum and a maximum flow rate.

6.3.2 CTBO and CLO introduction

The main aspect of Continuous Time Block Optimization (CTBO) is that all the optimized control values for a given period (time-block) are applied to the system and not only to the first interval; in this way, any discrepancies between forecast disturbances and their actual values are neglected for the other intervals in the block which affects the accuracy of the *optimal* solution. The lack of accuracy can also be seen as a consequence of taking into account the system output feed-back only when the process is repeated for the next time-block instead of doing so for each interval. Even with these shortcomings, CTBO has the advantage of shorter computation time.

In contrast, classic MPC implementations, e.g. Closed Loop Optimization (CLO), only apply the values found for the first interval of the period (horizon), and then repeat a new optimization process for the successive intervals. CLO gets a finer system feed-back which leads to a better response to changing external conditions but the trade-off is increasing processing time.

To run CTBO and CLO optimizations over longer periods than before, weather input files were structured to duplicate the five years of measured DLSC weather. As the short-run model is used, the valid simulation period starts on DLSC's year 4. For that year and the next, actual weather data were fed to the simulation. For the following years, the data are *recycled* as shown in Table 6.2.

Table 6.2: Weather data for simulations

Simulation year	*4*	*5*	6	7	8	9	10	11	12	13	14
Weather year	*4*	*5*	1	2	3	4	5	1	2	3	4

Weather conditions exhibit a very different behaviour for every year. It is illustrated in Figure 6-2 with the aid of percentage values for solar radiation and heating load –which are referred to the exceptional year 2 (7 and 12 in simulation). It can be noticed that year 4 had very low solar radiation and year 5 had minimum heating load.

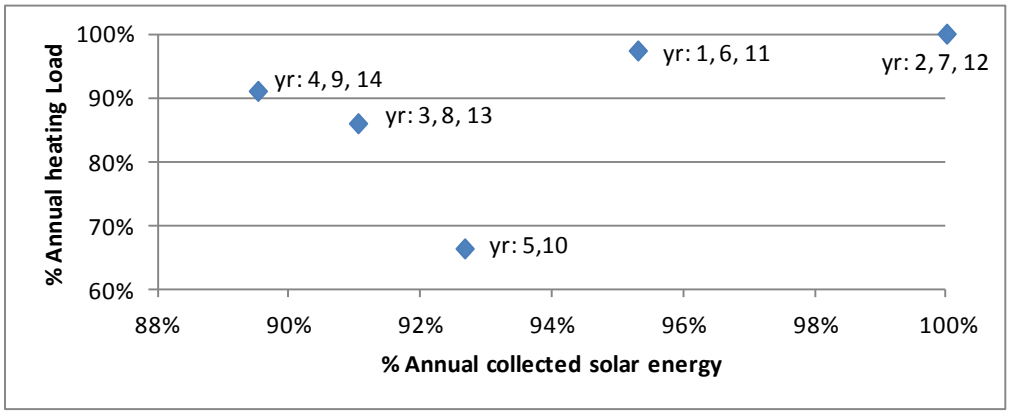

Figure 6-2: % Heating load vs. % Collected solar energy

6.3.3 Incremental Continuous Time Block Optimization (CTBO)

Figure 6-3 represents the particular CTBO implementation details.

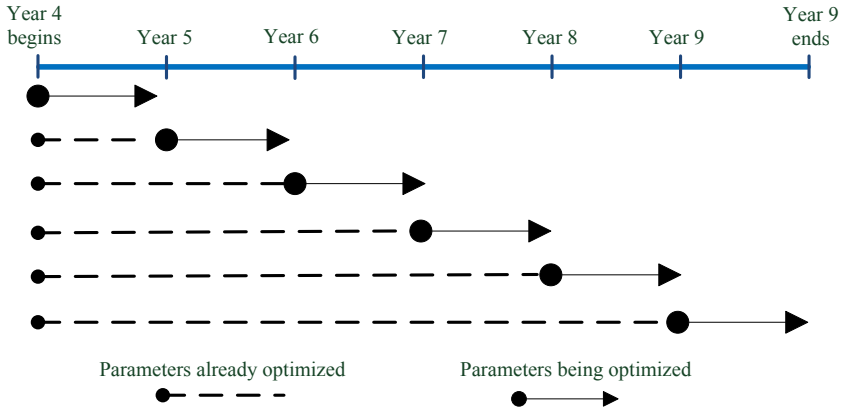

Figure 6-3: Incremental CTBO optimization

Six optimization processes were run, one for each of six consecutive years (4 to 9). Besides the transition period (due to pre-heating configuration) it can be considered that simulations always start at year 4; stop time, though, moves one year ahead with each iteration (receding horizon).

Cost function, which includes again gas and three times electricity consumption, is evaluated and minimized only for the period being optimized; the resulting optimal parameters are aggregated year to year and are progressively employed to control the system.

Pump control strategies and FRC+ were all simultaneously applied for controlling the system simulations. If all the control parameters were optimized, they would amount to 21 (12 from FRC+, 4 for Delta T and 5 for BTES pump) and would cause an increase in the number of simulation runs beyond practical possibilities. Thus, it was needed to reduce the amount of optimizable parameters; the ones not included in optimization were set to constant values identified in exploratory studies. In total, 11 optimizable parameters were retained:

For FRC+, four thresholds (minUE and MaxLoad) for the two lowest STTS charge level (STTS_L) scenarios were kept; *Max Load* for STTS_M was also included but the same value was shared by BTES_L and BTES_H scenarios.

For BTES pump control, only the maximum STTS ACL for low future load (ACLmax1) and the minimum STTS ACL for high future load (ACLmin2) were optimized.

All the 4 *Delta T* values for solar pump control: ΔT_L, ΔT_M, ΔT_H and ΔT_S.

Even with the reduction of optimizable parameters, the last process, for year 9, took more than 2 days to be completed.

6.3.4 Incremental Closed-Loop Optimization (CLO)

In this case, the cost function (gas + 3*electricity) was evaluated over a six year period but optimal parameters were applied only for the first year of each period. The mechanism can be seen in Figure 6-4: six optimization processes were executed using the resulting parameters from previous years.

It has been stated that CLO demands more computer power than CTBO. To partially compensate that, the number of parameters was reduced again: *Max Load* for STTS_M scenarios and the

minimum ACL for low future load (ACLmax1) were set to constant values. Even if only nine parameters were left for optimization, the last process took more than three days to be completed.

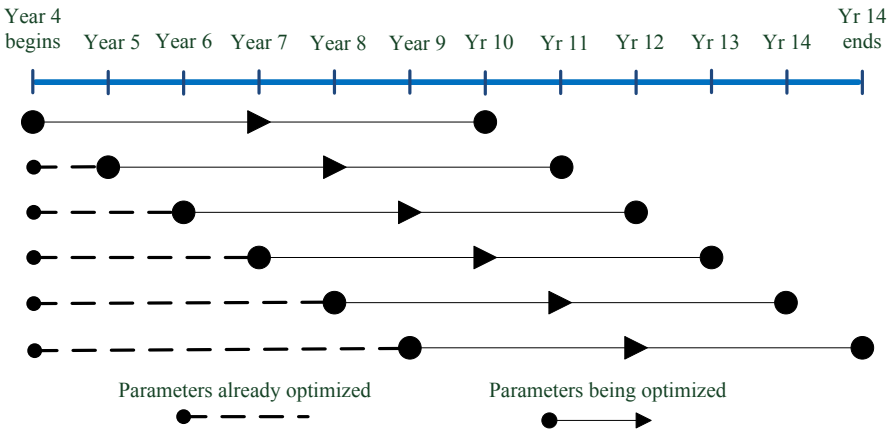

Figure 6-4: Incremental CLO optimization over 6 years

6.4 Results discussion

Results from CTBO and CLO cases are compared to two *references*: the model using STD strategy and the model with FRC+ (and optimized values from Chapter 5). Once more, results are analyzed from multiple perspectives, namely: optimized parameters, pump dynamic behaviour, solar fraction, BTES behaviour, and energy savings.

To establish a comparison period of 11 years (Year 4 to 14), CTBO and CLO simulations with optimal parameters were run for that period. As CTBO's optimal parameters were calculated only for the first six years, they were carefully repeated for the remaining years to match similar weather conditions. In the CLO case, parameters found for the last optimization (years 9 to 14) are applied for that same period in the simulation.

To better understand how the control strategies results are affected by each year's weather, the following Table 6.3 lists the mnemonic keys employed in the next Figures.

Table 6.3: Measured weather features

Years	**Radiation**	**Load**	**Mnemonic**
4,9,14	Very Low	Medium	LR,ML
5,10	Medium	*Very* Low	MR,xLL
6,11	High	High	HR,HL

Years	Radiation	Load	Mnemonic
7,12	*Very* High	High	xHR,HL
8,13	Medium	Medium	MR,ML

Year 4 is the only one having 2 *clones* because it was considered that two full 5-year cycles starting on year five were more suitable/enlightening for comparison purposes: Actual year 4 is interesting for assessing changes in the system operation but it is still part of the initial warming-up process of the DLSC system –it is only in year 5 and after that the system can be deemed to have reached a steady-periodic state.

6.4.1 Optimized parameters

A summary of results and optimized parameters for the two cases is listed in Appendix 2. The following paragraphs review the most interesting findings for the optimized parameters (Table A2.4 for CTBO and Table A2.6 for CLO).

The low impact of BTES pump control strategy is especially confirmed in the CLO case, the parameter *MinACL2* has almost the same value (1.0) for all the years being optimized.

Regarding solar loop parameters, it is worth to mention that in all the cases, ΔT values are higher than the fixed value of 15°C used in current control strategy; this indicates that some control tuning to STD could be possible. For low and medium STTS charge conditions they (ΔT_L, ΔT_M) have in general lower values (average: 18.5 and 22.0) which translates into less solar energy being collected and less electricity consumption when compared to STD. The effect is more pronounced for high STTS charge and summer-mode operation (ΔT_H and ΔT_S) with values being even higher (average: 23.9 and 22.2). From another perspective, the CTBO solar loop parameters are most of the time greater than CLO's. As CTBO only looks at current year's weather, it is more *aggressive* in reducing electricity consumption when searching for the optimized parameters.

In the case of thresholds, Minimum Usable Solar Energy (MinUE) for the lowest STTS charge scenario becomes more relevant (values being three or more) than it was thought when the analysis was performed for the results of the Chapter 5 (values were less than 1.5). This outcome could be associated with the active role played by the solar loop control and the limitations it imposes to collecting solar energy.

On the other hand, Maximum Load (MaxLoad) threshold values for the [STTS_L, BTES_L] scenario are generally smaller for CTBO (10 most of the cases) than CLO (close to 12). It means that CTBO is more sensitive to the heating load levels when they increase beyond the threshold: *forced* BTES discharge occurs more frequently for CTBO than CLO causing less gas consumption for the former. The caveat is that the BTES is left with less thermal energy for following years as it will be confirmed in section 6.4.4 (BTES behaviour).

For scenarios where BTES displays superior charge levels, differences in threshold values between the two MPC methods were less significant. The reason could be that forcing BTES discharge is less needed for those charge levels.

6.4.2 Pumps dynamic behaviour

Figure 6-5 is a mosaic of three graphs; first graph (top) represents the weather conditions for the same 4-day period (in year 4) that was used in Chapter 5. The following two graphs compare the pumps' flow rate and the STTS ACL for the STD (in the middle) and the CLO case (bottom graph) where the four proposed strategies are integrated.

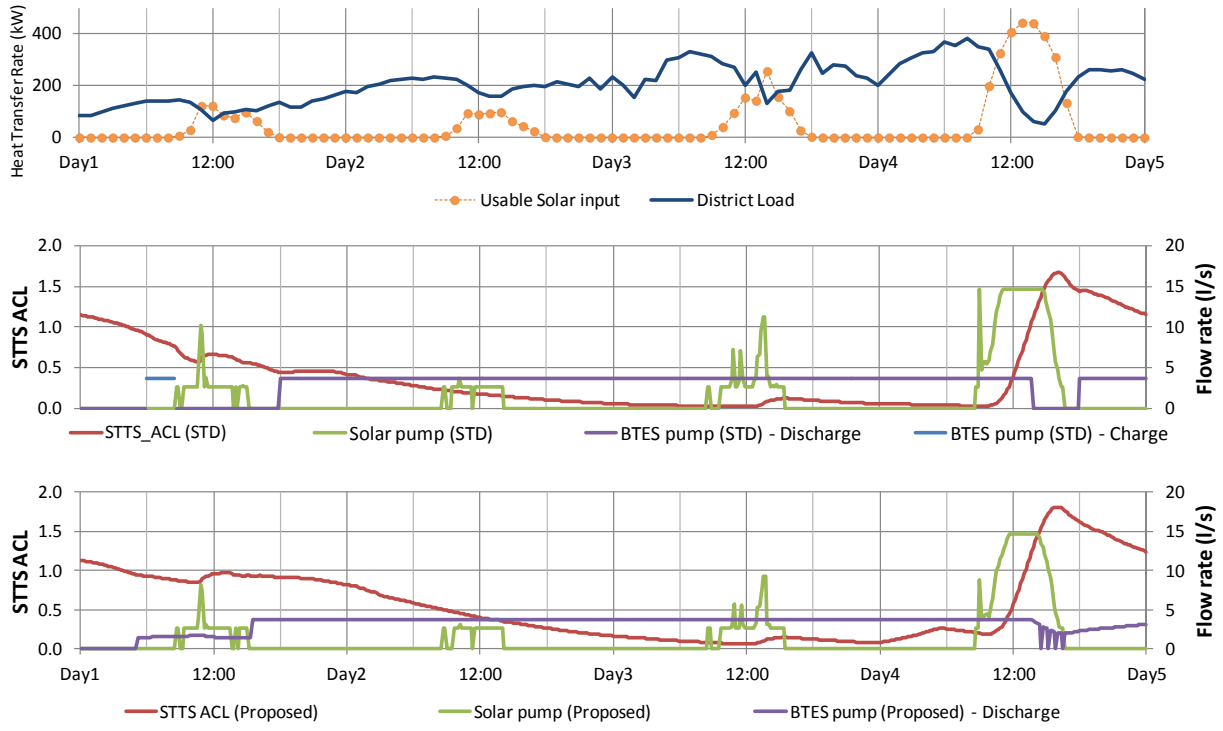

Figure 6-5: External conditions and pumps flow rate for STD and CLO cases

The solar loop pump (green lines) operates at a reduced speed for the CLO case and for less time than the STD case. This is especially noticeable in the curves' peaks. As the ΔT values for CLO are higher (> 17°C) than in the STD case (15°C), the pump runs at a lower speed to guarantee a larger temperature drop. Speed changes due to the STTS ACL influence cannot be visualized in the Figure because the ΔT_L and ΔT_M values are almost equal.

In the case of the BTES pump (purple and blue lines), the STD case features an implementation at constant speed and because there is no *awareness* of future external conditions there is a small period of a few hours where the BTES is charged. The CLO case discharges the BTES almost all the time but not always at the same speed. The influence of degrading STTS ACL levels and increasing heating load make the control to change the pump speed to maximum during the afternoon of the day 1. The maximum speed is kept for most of the period until the day 4, when relatively mild weather changes the control behaviour so the BTES discharge is not interrupted but the flow rate is reduced.

6.4.3 Weighted Solar Fraction

The graphic presented in Figure 6-6 depicts the Weighted Solar Fraction (WSF) values for each of the four cases over an 11-year period.

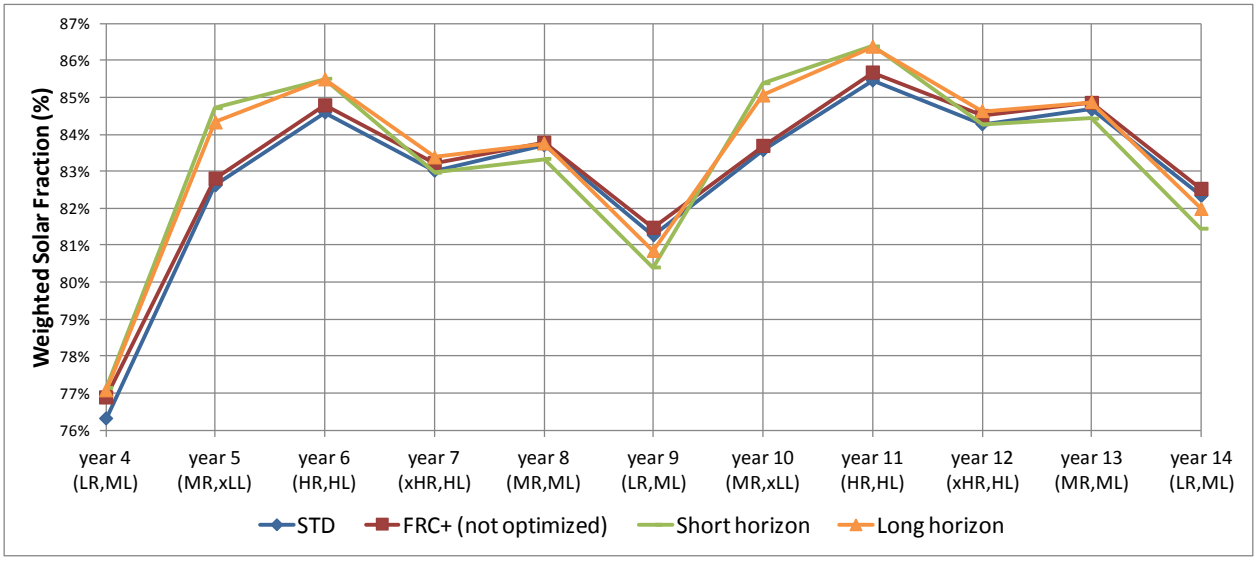

Figure 6-6: Weighted Solar Fraction

The differences among the cases are relatively small but allow drawing certain conclusions. STD and FRC+ are very close in value and they are more conservative than CTBO and CLO; for instance, in years 5 and 10 (very low load) the two former have a relatively low WSF but they are less affected by low solar radiation conditions in year 9 (and 14). CTBO and CLO benefit of mild weather conditions but underperform in harsher weather.

CLO is more moderated than CTBO; its values for warm years (5 and 10) are lower than the CTBO case but, for the other years CLO clearly outperforms and behaves even better under higher load conditions. The concept behind CLO –to include future years in optimization but only applying immediate year's results– could prove to be very useful for changing climate conditions and uncertainties in energy prices for the coming years.

For simplification purposes, the Figure above does not include annual Solar Fraction (SF), instead a summary showing how SF and WSF values differ is presented in Table 6.4. While WSF grows for each improvement applied to the control strategies, SF declines almost all the time. This confirms that if solar fraction were to be employed as a measure of the system energy performance it would be less representative of the energy costs incurred during the system operation.

Table 6.4: SF vs. WSF over the 11-year period

Case	SF	WSF
STD	96.2%	83.0%
FRC+	96.4%	83.2%
CTBO	95.0%	83.4%
CLO	95.4%	83.5%

6.4.4 BTES behaviour

This section consists of three parts: Analysis of delivered and extracted BTES energy, BTES average temperatures comparison, and evaluation of thermal losses.

Figure 6-7 shows the average delivered and extracted BTES energy for the four cases. Even if the particular values for every case are different, the general trend is the same for all of them. What is noteworthy is the BTES response for rather opposite years 5 and 9 (and their clones, 10 and 14):

- Year 5(10), being a warm case, has the lowest demand for BTES thermal energy and at the same time it delivers to the BTES the highest amount of energy.
- Year 9(14) has average values for energy delivered to BTES but, due to limited solar radiation and high load, it demands the highest amount of thermal energy from BTES.

In year 6 (and 11) BTES receives the least amount of thermal energy. It seems that the significant amount stored during the previous year (5 or 10) limits the BTES capacity to absorb collected solar energy.

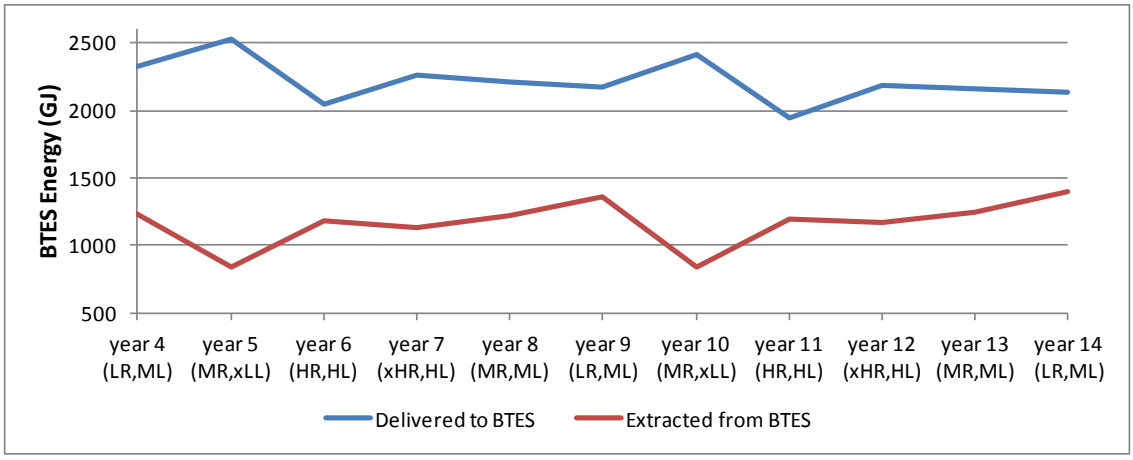

Figure 6-7: BTES average thermal energy

The BTES Volume average temperature at the end of each year is displayed in Figure 6-8. It is clear that the STD case is the one having the highest values; it could be a positive feature of this control strategy when the system is under difficult weather, but, it should not be forgotten that the electricity consumption and the BTES heat losses go up in that case. FRC+ case is closer to the STD curve than the other cases are, the gap between these two lines is especially noticeable: It is small for years 8, 9 and 10 (and clones) which have reduced load but it widens for years 6 and 7 (11 and 12) under high load conditions. This behaviour matches the fact that FRC+ strategy (forcibly) discharges BTES more deeply when load demand rises.

Still in the same Figure 6-8, CTBO and CLO, which optimize indirectly electricity consumption of the solar pump, have always lower BTES temperature than the other two cases because less solar radiation is being collected and stored in the BTES. CLO, as expected, has higher values for

BTES temperature, but the gap is smaller for the difficult year 9; it can be in part explained by the low solar radiation for that year and the limits for solar pump electricity consumption.

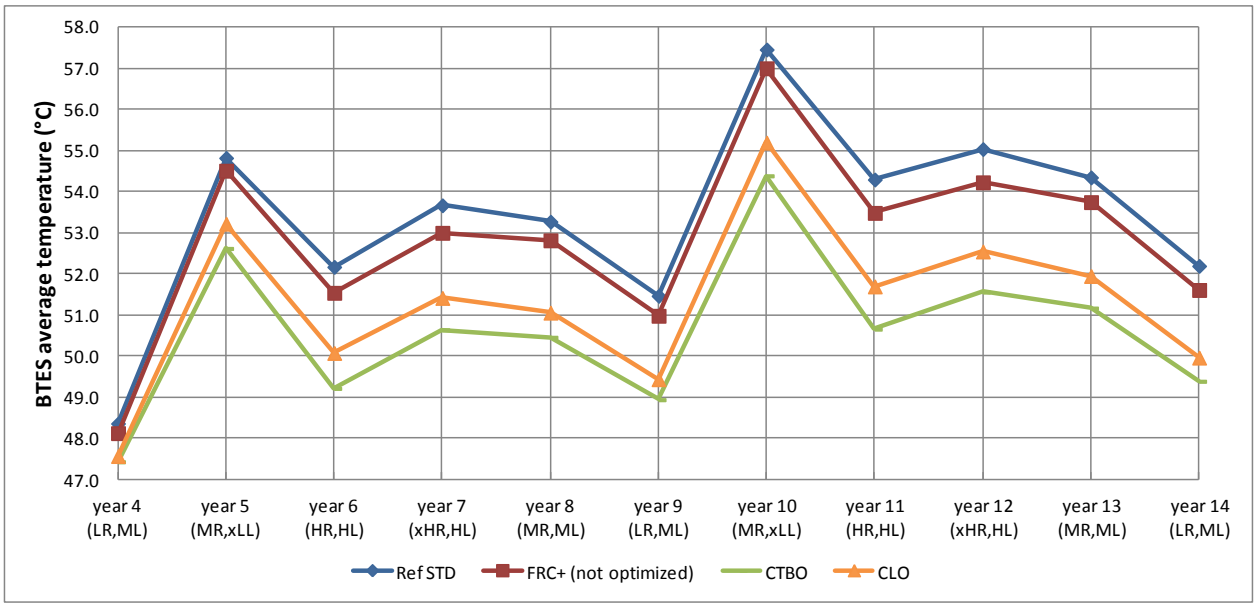

Figure 6-8: BTES Volume average temperature

As it is depicted in Figure 6-9, BTES losses behave almost in the same way as BTES temperatures do (when analyzing the 5-year cycle).

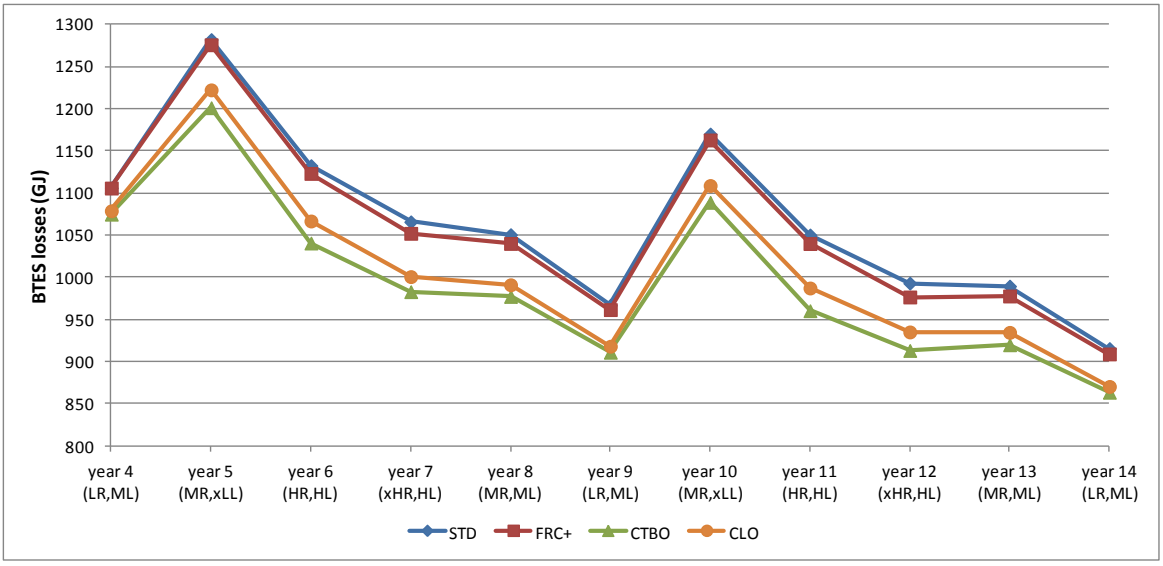

Figure 6-9: BTES losses over the 11-year period

It is interesting to notice how losses draw the same pattern for the two cycles but in a minor scale for the second one –even if BTES temperatures are higher for the second cycle. It confirms that the BTES storage gradually warms a larger volume of the surrounding earth.

6.4.5 Energy savings

Weighted Solar Fraction gives a good indication of primary energy consumption by defining a relationship among all the different energy sources involved. Nevertheless, to compare the different cases from an economics and environmental point of view, energy savings can provide a better measure. Figure 6-10 presents the average energy consumption over the 11-year period and the percentage of primary energy savings relative to the STD reference case in two different situations. Energy consumption amounts include the weight factor of three for electricity.

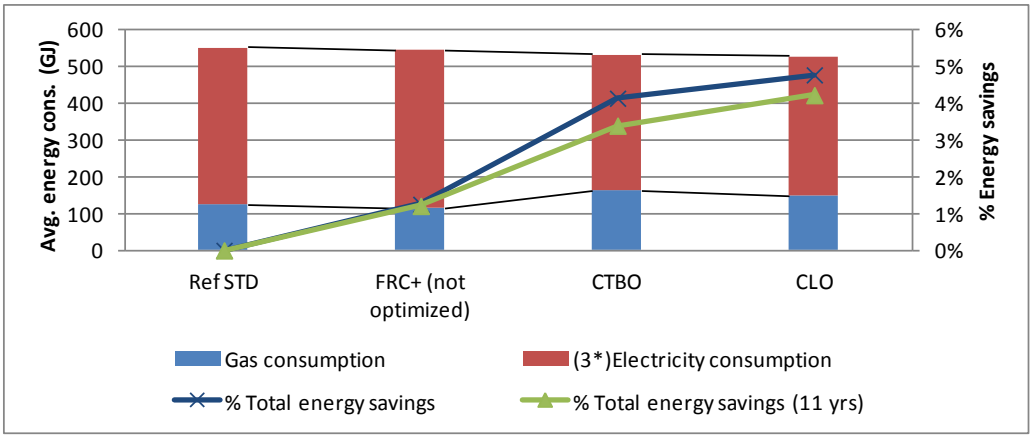

Figure 6-10: Average energy consumption and % of total energy savings

FRC+ is just slightly better than STD, with a small decline in gas and electricity usage. As it has been repeated, CTBO and CLO demand less electricity consumption at the expense of an increase in the amount of gas and a reduction in the solar energy being collected and stored. Even so, the CLO overall energy consumption is reduced by 5% (23 GJ/year), as it was implicit in WSF results.

6.5 MPC strategies for operation: Review

Results from Chapter 5 showed that FRC+ has primary energy savings below of 4% over the defined three year period. When FRC+ parameters found in that case are applied over an 11-year

period (with different weather conditions) the savings drop to 1%. With the changes introduced in the current chapter, especially those regarding the solar loop control and the MPC optimization mechanisms, primary energy savings in the CLO case are close to 5% for 10 years average; when the difficult year 14 (LR, ML – i.e. low radiation and medium load) is taken into account in an 11-year average the value is just above 4%.

CLO has a limited increase in primary energy savings (less than 1%) in respect to CTBO. But it should be remembered that the results were obtained using *perfect* forecasts; in a real environment the divergence between CTBO and CLO could be higher. Considering the system seasonal behaviour and the impact on control settings of the solar energy stored in the BTES, it seems less risky to apply the CLO approach because of the regular system feed-back.

Regarding an actual deployment of proposed *solar loop control*, the temperature difference between collectors' inlet and outlet (Delta T) could be adjusted depending on STTS charge status and on energy prices.

CONCLUSION

The calibrated TRNSYS model featuring shorter computation time is accurate enough to test and analyze the impact of the proposed control strategies. Even if only *perfect* forecasts were employed, the applied MPC methods illustrate the possibility of including not only weather forecasts but also energy costs forecasts.

When analyzing the system dynamic behaviour, it was found that the most significant energy savings are possible during short periods of extreme weather. In long-term analysis, the Weighted Solar Fraction (WSF) was shown to be a useful measure to account for the fact that electricity costs more than natural gas, or to consider the primary energy relationship.

The impact of control strategies is influenced by the trade-offs between collected solar energy and STTS charge level, BTES temperatures and BTES losses, electricity vs. gas consumption. The latter is mainly manifested in the amount of collected and stored solar energy, and in a less proportion in the amount of thermal energy extracted from the BTES.

Long-term improvements of energy performance (and/or operating costs) are possible but relatively small. The predictive strategy FRC+ delivered a maximum of 3.9 % on primary energy savings using pre-computed lookup tables. FRC+, solar and BTES loops control yield 5% on the same primary energy savings when applying the CLO mechanism –with year-to-year optimization.

Discussion

The overall energy and cost savings are modest, in the order of a few percent. But these savings were achieved without any hardware changes, just by modifying control algorithms –so the cost to implement the new control strategies could be low. The modest performance increases are a testimony to the very high level of expert knowledge that is already included in the standard control strategy. That control strategy was developed by members of the Design Team having a very good knowledge of the system and its operation, and it was further refined during the first years of operation. The application of MPC-based strategies would have the added advantage of expressing mathematically the compromise to be reached between the Solar Fraction, based only on the solar energy delivered to the district loop, and the operating costs (or CO_2 emissions for

example). It would also provide a framework to adapt this compromise to varying energy prices or related conditions.

Contributions

The main contributions of this work are:

- Obtaining a calibrated TRNSYS model of DLSC adapted to MPC studies. The model includes new TRNSYS components: the *BTES controller* which implements the standard control strategy (dated on 2011), and the *Degree-hours counter* which helps to identify heating or cooling trends from air temperatures.
- Introduction of a methodology for applying Model Predictive Control that can be employed when there are limits to the traditional implementation. The method uses predictions based on a system model to tune existing rules and to define new rules for the supervisory control strategy, and to dynamically adjust the set-point of local pump speed controllers.
- Definition of new concepts for control implementation and evaluation: STTS absolute charge level (STTS ACL) and Weighted Solar Fraction (WSF).
- Inception and evaluation of four control alternatives for different parts of the current control strategy: winter-mode BTES charge enable, winter-mode BTES discharge enable, solar loop and BTES loop.

Recommendations for practical implementation

The results of this work could be partially or fully implemented in the real DLSC supervisory controller –which is based on specialized software for facilities management and control. The main limitation could be the software's inability to read weather forecasts.

Since most of the alternative control strategies use elements already present on the existing rules or derived from them, they can be explained to the engineers managing the system and their behaviour can be followed and understood. Before implementing those rules in a definitive way, the MPC-based rules and parameters can be separately or simultaneously applied within a period of a few days or weeks to assess their impact on the real system.

Recommendations for future work

The proposed MPC methodology could be employed to test new control strategies for other parts of the current control, for example, the BTES charge when in summer operation mode.

FRC+ strategy could be refined to include more scenarios for the lookup tables and assess if this could lead to increased energy performance. These additional scenarios would consist of finer levels when STTS charge is low. Additionally, they could include a more accurate way to determine the levels of BTES charge status used to define the grid of scenarios.

If computation power is available, Closed-Loop Optimization (CLO) should always be considered. The interval for applying optimal control settings should be reduced as much as possible (e.g. one month) but the horizon should not be less than two years –to include the impact of control settings in the next year. In that context, actual forecasts and the feedback of the real system would be regularly updated. The most important requirement to achieve this implementation is a simplified way to calibrate the DLSC model at the end of each interval.

The next step in assessing the potential of MPC for solar communities would be to explore the possibility of applying the MPC methodology and proposed control strategies during the design phase of solar communities. Designers aiming to reduce the size of the system components could assess the impact of MPC control in achieving that target. As mentioned above, the very ambitious solar fraction target at DLSC and the large amount of expert knowledge included in the current control strategy resulted in relatively modest performance improvements. It would be interesting to evaluate the benefits of MPC when designing new solar communities with lower solar fraction targets; that would present more latitude in selecting configurations, components and control strategies in an integrated approach.

Our work also showed that the lack of possibility to impose a given (non-uniform) initial state for most existing TRNSYS components requires workarounds that can be very complex to implement and costly in terms of computing time. To make TRNSYS really suitable to be deployed for *online* MPC applications, a mechanism should be implemented to set the current state of TRNSYS components based on feedback from a real system.

REFERENCES

Bauer, D., Marx, R., Nußbicker-Lux, J., Ochs, F., Heidemann, W., & Müller-Steinhagen, H. (2010). *German central solar heating plants with seasonal heat storage*. Solar energy, 84(4), 612-623.

Bernier, M. A., Pinel, P., Labib, R., & Paillot, R. (2004). *A multiple load aggregation algorithm for annual hourly simulations of GCHP systems*. HVAC&R Research, 10(4), 471-487.

Bernier, M., Kummert, M., & Bertagnolio, S. (2007). *Development and application of test cases for comparing vertical ground heat exchangers models*. In Proceedings of the 10th International IBPSA Conference, Beijing, China.

Brædstrup SolPark. (2012). *Brochure*. Retrieved April 30, 2013, from http://www.e-pages.dk/nordad/1810/

Braun, J., (1990). *Reducing energy costs and peak electrical demand through optimal control of building thermal storage*. ASHRAE Transactions, 96 (2), 264-273.

Camacho, E. F., Berenguel, M., & Bordons, C. (1994). *Adaptive generalized predictive control of a distributed collector field*. Control Systems Technology, IEEE Transactions on, 2(4), 462-467.

Candanedo, J.A., Bucking S., Allard A., & Athienitis A. (2011). *Model-Based Predictive Control Applications for Solar Homes and Communities.* Presentation at Model Predictive Control in Buildings Workshop, Montreal. Retrieved March 9, 2013, from: http://www.ibpsa.us/pub/mpc2011/presentations/Fri06_Candanedo.pdf

Cao, J., & Lin, X. (2008). *Study of hourly and daily solar irradiation forecast using diagonal recurrent wavelet neural networks*. Energy Conversion and Management, 49(6), 1396-1406.

Carslaw, H.S., & Jaeger, J.C. (1959). Conduction of heat in solids, Oxford.

Chapuis, S. (2009). *Stockage thermique saisonnier dans un champ de puits géothermiques verticaux en boucle fermée* (Doctoral dissertation, École Polytechnique de Montréal, Montréal).

Chung, M., Park, J. U., & Yoon, H. K. (1998). *Simulation of a central solar heating system with seasonal storage in Korea*. Solar energy, 64(4), 163-178.

Clarke, J.A. & Cockroft, J. & Conner, S., Hand, J., Kelly, N.J., Moore, R., O'Brien, T. & Strachan, P.A. (2002). *Simulation-assisted control in building energy management systems.* Energy and Buildings, 34 (9), 933-940.

Coffey, B., Morofsky, E., & Haghighat, F. (2006). *Model-based control of responsive building systems: a summary of its potential and challenges*. Proceedings of eSim 2006 Building Performance Simulation Conference, Toronto, 2006, (pp. 157-164).

Coffey, B. (2012). *Using Building Simulation and Optimization to Calculate Lookup Tables for Control*. ((Doctoral dissertation, University of California, Berkeley: Center for the Built Environment).

Dalenbäck, J. O. (2009). *Large-Scale Solar Heating and Cooling Systems in Europe*. In Proceedings of ISES World Congress 2007 (Vol. I–Vol. V) (pp. 799-803). Springer Berlin Heidelberg.

Dalkia. (2010). *Montréal, Québec, Canada, District Energy System.* Retrieved March 9, 2013, from http://www.dalkia.ca/link/dl?site=canada-energie.en&objectId=15186&src=kit_veolia

De Ridder F., Diehl M., Mulder G., Desmedt J., Van Bael J. (2011). *An optimal control algorithm for borehole thermal energy storage systems.* Energy and Buildings, 43 (10), 2918-2925.

District Heating. (n.d.). In *Wikipedia*. Retrieved March 9, 2013, from http://en.wikipedia.org/wiki/District_heating

Dobos, L., Jäschke, J., Abonyi, J., & Skogestad, S. (2009). *Dynamic model and control of heat exchanger networks for district heating*. Hungarian Journal of Industrial Chemistry, 37(1), 37-49.

Dounis, A. I., & Caraiscos, C. (2009). *Advanced control systems engineering for energy and comfort management in a building environment-A review*. Renewable and Sustainable Energy Reviews, 13 (6-7), 1246-1261.

Enermodal Engineering Ltd. (2011). *Okotoks sequence of Control V5*. Internal NRCan document.

Eskilson, P. (1987). *Thermal analysis of heat extraction boreholes*. Department of Mathematical Physics, University of Lund.

Ferhatbegovic, T., Zucker, G., Palensky, P. (2011). *Model based predictive control for a solar-thermal system.* IEEE AFRICON, 2011, (pp. 1-6).

Fisch, M. N., Guigas, M., & Dalenbäck, J. O. (1998). *A review of large-scale solar heating systems in Europe*. Solar energy, 63(6), 355-366.

Florita, A. R., & Henze, G. P. (2009). *Comparison of short-term weather forecasting models for model predictive control*. HVAC&R Research, 15(5), 835-853.

Gyalistras, D. (2010). *Final report: Use of weather and occupancy forecasts for optimal building climate control (OptiControl)*. ETH Zürich, Switzerland.

Hadorn, J.-C., & Chuard, D. (1988). *Guide du stockage saisonnier de chaleur*. Société suisse des ingénieurs et des architects, Zürich, Swiss.

Heier, J., Bales, C., Sotnikov, A., & Ponomarova, G. (2011). *Evaluation of a high temperature solar thermal seasonal borehole storage*. In ISES Solar World Congress 2011.

Heller, A. (2000). *15 Years of R&D in central solar heating in Denmark*. Solar energy, 69(6), 437-447.

Hellström, G. (1989). *Duct Ground Heat Storage Model,Manual for Computer Code*. Department of Mathematical Physics, University of Lund, Sweden.

Henze, G. P., Dodier, R. H., Krarti, M. (1997). *Development of a Predictive Optimal Controller for Thermal Energy Storage Systems*. HVAC&R Research, 3 (3), 233-264.

Henze, G. P., Felsmann, C., & Knabe, G. (2004). *Evaluation of optimal control for active and passive building thermal storage*. International Journal of Thermal Sciences, 43(2), 173-183.

Ingersoll, L. R., Adler, F. T., Plass, H. J., & Ingersoll, A. C. (1950). *Theory of earth heat exchangers for the heat pump*. ASHVE Trans, 56, 167-188.

Jalali, A. A., & Nadimi, V. (2006). *A survey on robust model predictive control from 1999-2006*. Computational Intelligence for Modelling, Control and Automation, 2006 and International Conference on Intelligent Agents, Web Technologies and Internet Commerce, International Conference on, 207-207).

Kelly, G. (1988). *Control system simulation in North America*. Energy and Buildings, 10 (3), 193-202.

Klein, S. A., Beckman, W. A., Mitchell, J. W., Duffie, J. A., Duffie, N. A., Freeman, T. L., Mitchell, J. C., et al. (2012). *TRNSYS 17 – A TRaNsient SYstem Simulation program, User manual*. Madison, WI: University of Wisconsin -Madison, USA.

Kummert, M. (2001). *Contribution to the application of modern control to solar buildings - Simulation-based approach and experimental validation*. (Doctoral dissertation, Fondation Universitaire Luxembourgeoise, Belgique).

Lundh, M., & Dalenbäck, J. O. (2008). *Swedish solar heated residential area with seasonal storage in rock: Initial evaluation*. Renewable energy, 33(4), 703-711.

Ma, Y., Kelman, A., Daly, A., & Borrelli, F. (2012). *Predictive control for energy efficient buildings with thermal storage: Modeling, stimulation, and experiments*. Control Systems, IEEE, 32(1), 44-64.

Maciejowski, J. M. *Predictive Control with Constraints*. 2002. Harlow, England: Pearson Education

Mahdavi, A., Mohammadi, A., Kabir, E., & Lambeva, L. (2008). *Occupants' operation of lighting and shading systems in office buildings*. Journal of building performance simulation, 1(1), 57-65.

McDowell, T. P., & Thornton, J. W. (2008). *Simulation and model calibration of a large-scale solar seasonal storage system*. In 3rd National conference of IBPSA, USA, Berkeley (California), USA.

Natural Resources Canada (NRCan). (2012). *DLSC pump power consumption v2*. Internal document.

Natural Resources Canada (NRCan). (2012). *Energy Use Data Handbook Tables*. Retrieved April 27, 2013, from http://oee.nrcan.gc.ca/corporate/statistics/neud/dpa/handbook_totalsectors_ca.cfm

Natural Resources Canada (NRCan). (2012). *Utility Cost Summary.xls*. Internal document.

Nielsen, J. E. (2012). *IEA-SHC Task 45: Large Solar Heating/Cooling Systems, Seasonal Storage, Heat Pumps*. Energy Procedia, 30, 849-855.

Nussbicker-Lux, J., & Drück, H. (2012). *Solare Nahwärmeversorgung in Crailsheim mit 7500 m² Kollektorfläche*. Symposium Thermische Solarenergie 2012. Kloster Banz.

Oldewurtel, F. , Parisio, A. , Jones, C.N. , Gyalistras, D. , Gwerder, M. , Stauch, V. , Lehmann, B. , Morari, M. (2012). *Use of model predictive control and weather forecasts for energy efficient building climate control.* Energy and Buildings, 45, 15-27.

Palsson, O. P., Madsen, H., & Søgaard, H. T. (1993). *Application of predictive control in district heating systems*. Proceedings of the Institution of Mechanical Engineers, Part A: Journal of Power and Energy, 207(3), 157-163.

Patterson, D. (2012, April 25). *Korean researchers learn from Drake Landing*. Okotoks Western Wheel. Retrieved from http://www.westernwheel.com/article/20120425/WHE0801/304259996/-1/whe/korean-researchers-learn-from-drake-landing

Pavlov, G. K., & Olesen, B. W. (2011). *Seasonal ground solar thermal energy storage-review of systems and applications*. In Proceedings of ISES Solar World Congress, Kassel (DE), ISSN (pp. 1583-1078).

Perez, R., Moore, K., Wilcox, S., Renné, D., & Zelenka, A. (2007). *Forecasting solar radiation – Preliminary evaluation of an approach based upon the national forecast database*. *Solar energy*, *81*(6), 809-812.

Perez, R., Kivalov, S., Schlemmer, J., Hemker, K., Renné, D., & Hoff, T. E. (2010). *Validation of short and medium term operational solar radiation forecasts in the US*. Solar Energy, 84(12), 2161-2172.

Petersen, S., & Svendsen, S. (2010). *Method and simulation program informed decisions in the early stages of building design*. Energy and Buildings, 42(7), 1113-1119.

PlanEnergi. (2010). *Solar Heating and Seasonal Heat Storage*. Retrieved March 9, 2013, from http://www.planenergi.eu/solar-heating-and-seasonal-heat-storage.html

Rossiter, J. A. (2003). *Model-based predictive control: a practical approach* (Vol. 4). CRC press.

Roth, K. (2009). *Seasonal Energy Storage*. ASHRAE journal, (January), 41-43.

Saarinen, L. (2008). *Modelling and control of a district heating system* (Doctoral dissertation, Uppsala University, Sweden).

Sandou, G., & Sorin O. (2009). *Particle swarm optimization based nmpc: An application to district heating networks*. Nonlinear Model Predictive Control (2009): 551-559.

Schmidt, T., Mangold, D., & Müller-Steinhagen, H. (2004). *Central solar heating plants with seasonal storage in Germany*. Solar energy, 76(1), 165-174.

Schmidt, T., Miedaner, O. (2012). *Solar district heating guidelines-Storage*. Retrieved March 9, 2013 from http://www.solar-district-heating.eu/Portals/0/Factsheets/SDH-WP3-D31-D32_August2012.pdf

Schubert, M., Trier, D. (2012). *Solar district heating guidelines-Control Strategies*. Retrieved March 9, 2013 from http://www.solar-district-heating.eu/Portals/0/Factsheets/SDH-WP3-D31-D32_August2012.pdf

Sibbitt, B., McClenahan, D., Djebbar, R., Thornton, J., Wong, B., Carriere, J., & Kokko, J. (2012). *The Performance of a High Solar Fraction Seasonal Storage District Heating System–Five Years of Operation*. Energy Procedia, 30, 856-865.

Smart Net-zero Energy Building Research Network (SNEBRN). (2013). Consulted March 9, 2013, from http://www.solarbuildings.ca/index.php/en/themes

Solar District Heating organization (SDH). (2013). *Ranking List of European Large Scale Solar Heating Plants*. Retrieved March 9, 2013, from http://www.solar-district-heating.eu/SDH/LargeScaleSolarHeatingPlants.aspx

Tamasauskas, J., Poirier, M., Zmeureanu, R., & Sunyé, R. (2012). *Modeling and optimization of a solar assisted heat pump using ice slurry as a latent storage material*. Solar Energy, 86(11), 3316-3325.

Thermal Energy Systems Specialists (TESS). (2007). *Drake Landing Solar Community, Okotoks, Alberta, Canada*. Retrieved November 19, 2012 from http://www.tess-inc.com/site-com/assets/filedownloads/Okotoks%20Project%20Summary%20-%20New.pdf

Turpin, F.B. *District Heating.* 1996. London, Heywood Books.

Wetter, M. (2001). *GenOpt®,Generic Optimization Program*. Seventh International IBPSA Conference. 601-608.

Wetter, M. (2011). *GenOpt®,Generic Optimization Program, User Manual Version 3.1.0*. Retrieved May 30, 2013, from http://simulationresearch.lbl.gov/GO/download/manual-3-1-0.pdf

Wong, W.P., McClung J.L., Kokko, J.P., & Snijders, A.L. (2007). *First Large-Scale Solar Seasonal Borehole Thermal Energy Storage in Canada.* Ecostock 2006 Conference Proceedings.

Verstraete, A. (2013). *Étude d'une communauté solaire avec stockage thermique saisonnier par puits géothermiques* (Doctoral dissertation, École Polytechnique de Montréal).

Verstraete, A., Bernier, M. (2013). *Étude d'une communauté solaire utilisant un réseau de distribution à un seul tuyau*. XIe Colloque Inter-universitaire Franco-Québécois, Reims, France, 289-294

Xie, F., & Whiteley, J. R. (2007). *Model Predictive Control of a Geothermally Heated Bridge Deck*. In American Control Conference, 2007. ACC'07 (pp. 2214-2219). IEEE.

Yang, H., Cui, P., & Fang, Z. (2010). *Vertical-borehole ground-coupled heat pumps: A review of models and systems*. Applied Energy, 87(1), 16-27.

APPENDIX 1 BTES PRE-HEATING PARAMETERS OPTIMIZATION

The process started with a general review of the Type 557 source code to have a basic idea of the software implementation of the Duct Ground Heat Storage (DST) model and the impact of pre-heating parameters in the storage temperature. After identifying the most relevant pre-heating parameters, they were optimized to find their best values so the pre-heating simulation produced the same results as the long-run simulation. A complete description of the source code can be found in Hellström (1989) and Chapuis (2009).

Preheating parameters

The BTES Preheating parameters can be classified in two groups:

- Those affecting only the storage's top layer, related with air temperature
- Those affecting the whole storage volume, related with storage's earth temperature

After inspecting the source code it was validated that air temperature parameters could be ignored, the documentation confirms that "the variation of the boundary conditions at the ground surface during the year can be neglected, except for very shallow ground heat stores" (Hellström, 1989).

The storage's earth temperature parameters are the following: Maximum preheat temperature (TCMAX), Minimum preheat temperature (TCMIN), Preheat phase delay (TCPH) and Number of preheating years (IPRE). When IPRE is set to a value different from zero, the Initial storage's temperature (TST0) is calculated from TCMAX, TCMIN and TCPH. At simulation start time, TST0 is the value given to the storage's output; it is also used to set the initial value for most of the arrays' cells representing the sub-regions.

For calculating TST0, it is assumed that it follows an annual sinusoidal behaviour, according to the equation:

$$TST0=TCM+TCA*Sin(ACK*(TT+TCPH)) \qquad (A1.1)$$

where, TCM is the mean between TCMAX and the TCMIN. TCA is the amplitude of the Sin function, TCA=TCMAX-TCM. TT is the initial simulation time in seconds, it is set to zero. TCPH is the parameter *Preheat phase delay* expressed in seconds. ACK is the normalized argument for the Sine function, so 1 year is a full sinusoidal cycle:

*ACK = 2*PI/(8760 hours*3600 seconds/hours)* *(A1.2)*

Preheat phase delay can be confusing; it represents 270 minus the *Day of minimum storage temperature day* (N), i.e., the initial storage temperature is calculated for an angle being N/360 degrees before the minimum value of the Sine function (which is at 270 degrees, approximately the day 270).

In the following example, the *Day of minimum storage temperature* (N) is 60, TCMAX is 50, and TCMIN is 40. The supplementary variables take the values:

Preheat phase delay = 270 – N = 210

TCM = (TCMAX +TCMIN)/2 = 45

TCA = TCMAX – TCM = 5

*Initial storage temperature (TSTO) = TCM + TCA*Sin(210°) = 45 + 5*(-0.5) = 42.5*

Figure A1.1 shows the point on the Sine function corresponding to the time 0 of the simulation. It can be seen how the minimum value is found 60 days (degrees) after simulation start time.

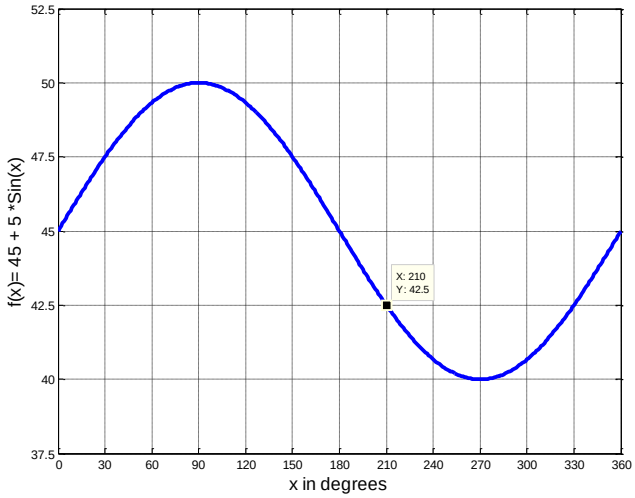

Figure A1-1: Example of *Day of minimum storage temperature (N)*

These findings could lead to think that by setting TCMAX=TCMIN=*Intended initial storage temperature* is enough to define the pre-heating parameters –so that the *Number of preheating*

years (IPRE) is not important. However, it was found that IPRE and TCMIN are also used in other equations that set the temperature for certain storage's sub-regions.

IPRE, TCMAX and TCMIN were the only parameters to be considered when finding the optimum settings for preheating. *Preheat phase delay* (TCPH) was not included because it was found in preliminary optimizations that its impact was low if the value was properly selected. It was set to 182 because in the year 4 the minimum *BTES average temperature* occurs on day 88 (270 – 88 = 182).

Pre-heating parameters calibration

The idea is to compare selected outputs between a long-run simulation and one running with the pre-heating settings. As this process is on the domain of the optimization, GenOpt was employed with the objective of finding the optimal pre-heating settings that minimize the root-mean-square-error (RMSE) of selected simulation outputs. These outputs are mainly BTES temperatures but there is also the *STTS % of charge*. Even if the latter is not directly related to the BTES, it is included to assess the behaviour of other simulation components when executing the short-run simulation with preheating parameters.

Type 557 provides an output for the storage average temperature and temperature outputs for each radial region (six for the DLSC case) close to the boreholes (*temperature-near-the-boreholes*). The default type 557's *proforma* was modified to include all the 6 regions' temperatures because in the original TRNSYS distribution only the one for the central region is available. TRNSYS Visual Studio –the TRNSYS graphic user interface that facilitates the configuration and interconnection of types– needs the *proformas* to let know the user the inputs, outputs and parameters that are available for each type.

In total, the compared outputs are eight: The average BTES temperature, the six *temperature-near-the-boreholes* and the *STTS % of charge*. A reference file was prepared with the outputs of the long-term simulation for years 4 and 5. The optimization process is commanded by GenOpt and supported by TRNSYS and Matlab, the latter runs TRNSYS and calculates the RMSE. At the end of each TRNSYS simulation the resulting outputs and the long-run reference data are loaded in Matlab, then, it calculates and writes the RMSE to a file that is read by GenOpt. According to an optimization algorithm, GenOpt repeats the process for a new set of pre-heating parameters until the minimum RMSE is found.

The range of possible values for the preheating parameters was based on the maximum and minimum value of BTES *average temperature*. The maximum is approximately 57°C and the minimum 40°C.

APPENDIX 2 SUMMARY OF RESULTS AND OPTIMAL PARAMETERS

Table A2.1: Results for reference case*

Item/Year	4	5	6	7	8	9	10	11	12	13	14
Total Incident Solar Energy (GJ)	12480	12919	13286	13941	12692	12498	12922	13265	13946	12699	12505
NET Total Solar Energy Collected (incl. Solar loop losses) (GJ)	3976	4152	4258	4534	3978	3835	4036	4164	4468	3925	3798
Total Solar Energy Delivered to STTS (GJ)	3954	4132	4234	4509	3954	3811	4016	4139	4443	3901	3774
Energy Delivered to BTES (GJ)	2359	2565	2030	2258	2217	2181	2419	1916	2159	2150	2133
Energy Extracted from BTES (GJ)	1215	798	1096	1079	1196	1350	800	1103	1111	1212	1379
Solar Energy Delivered to District Loop (GJ)	2547	2043	3005	3034	2629	2692	2060	3025	3074	2656	2723
Total Gas Energy Used (GJ)	364	59	77	137	95	204	39	51	94	68	170
Boiler Thermal Energy Delivered to the District Loop (GJ)	328	53	69	124	86	184	35	46	85	61	153
Total Energy Delivered to District Loop (GJ)	2875	2097	3074	3157	2715	2876	2096	3070	3159	2717	2876
Electrical energy used by Pumps (GJ)	142	124	157	161	139	139	122	155	160	138	138
Gas + 3*Electricity (GJ)	791	430	547	620	512	620	405	515	574	481	584
Solar Fraction (%)	88.6	97.5	97.7	96.1	96.8	93.6	98.3	98.5	97.3	97.8	94.7
Weighted Solar Fraction (%)	76.3	82.6	84.6	83.0	83.7	81.3	83.6	85.5	84.3	84.7	82.3
Average Solar Collector Efficiency (incl. Solar loop losses) (%)	31.9	32.1	32.0	32.5	31.3	30.7	31.2	31.4	32.0	30.9	30.4
STTS losses (GJ)	112	134	128	128	126	126	143	135	133	131	129
BTES losses (GJ)	1106	1282	1133	1066	1051	967	1170	1050	993	990	915

*Reference model using updated parameters for the solar and BTES pumps

Table A2.2: Control parameters for reference case*

Control parameter	Value for years 4 to 14
Winter Charge Factor	3.5
Winter Discharge Factor	1.0

*Reference model using updated parameters for the solar and BTES pumps

Table A2.3: Results for CTBO optimization

Item/Year	4	5	6	7	8	9	10	11	12	13	14
Total Incident Solar Energy (GJ)	12480	12919	13286	13941	12692	12498	12922	13265	13946	12699	12505
NET Total Solar Energy Collected (incl. loop losses) (GJ)	3867	3978	4092	4394	3867	3733	3906	4015	4345	3828	3704
Total Solar Energy Delivered to STTS (GJ)	3846	3959	4069	4370	3843	3710	3887	3992	4322	3805	3681
Energy Delivered to BTES (GJ)	2273	2469	2019	2243	2192	2159	2383	1945	2185	2144	2129
Energy Extracted from BTES (GJ)	1230	879	1233	1153	1228	1362	886	1264	1204	1254	1399
Solar Energy Delivered to District Loop (GJ)	2546	2038	2982	2982	2576	2630	2050	3002	3024	2606	2660
Total Gas Energy Used (GJ)	366	65	102	195	155	272	51	77	150	123	239
Boiler Thermal Energy Delivered to the District Loop (GJ)	329	58	92	176	139	245	46	69	135	111	215
Total Energy Delivered to District Loop (GJ)	2875	2097	3074	3157	2715	2876	2096	3070	3159	2717	2876
Electricity used by Pumps (GJ)	130	101	134	139	120	123	100	132	138	119	122
Gas + 3*Electricity (GJ)	754	368	505	612	515	641	351	473	564	481	606
Solar Fraction (%)	88.6	97.2	97.0	94.4	94.9	91.5	97.8	97.8	95.7	95.9	92.5
Weighted Solar Fraction (%)	77.1	84.7	85.5	83.0	83.3	80.4	85.4	86.4	84.3	84.4	81.4
Average Solar Collector Efficiency (incl. loop losses) (%)	31.0	30.8	30.8	31.5	30.5	29.9	30.2	30.3	31.2	30.1	29.6
STTS losses (GJ)	110	125	119	117	115	117	131	124	121	118	120
BTES losses (GJ)	1075	1201	1041	983	977	911	1089	960	913	920	864

Table A2.4: Control parameters for CTBO optimization

Parameter/Year	4	5	6	7	8	9	10	11	12	13	14
Winter Charge Factor	*0.5*	*0.5*	*0.5*	*0.5*	*0.5*	*0.5*	*0.5*	*0.5*	*0.5*	*0.5*	*0.5*
Winter Discharge Factor	*9.0*	*9.0*	*9.0*	*9.0*	*9.0*	*9.0*	*9.0*	*9.0*	*9.0*	*9.0*	*9.0*
minUE_L_L: Min. Usable Solar Energy for [STTS_L,BTES_L] scenario	3.0	2.2	2.1	3.0	3.0	3.0	2.2	2.1	3.0	3.0	3.0
minUE_L_H : STTS_L,BTES_H	2.1	1.8	2.2	1.2	0.6	0.4	1.8	2.2	1.2	0.6	0.4
maxL_L_L: Max. District Load for [STTS_L,BTES_L] scenario	10.0	10.3	10.0	10.0	17.5	10.0	10.3	10.0	10.0	17.5	10.0
maxL_L_H: STTS_L,BTES_H	12.5	13.0	13.8	13.0	11.0	11.5	13.0	13.8	13.0	11.0	11.5
max_L for STTS_M and BTES_L/H	13.0	13.0	13.0	13.0	13.5	13.0	13.0	13.0	13.0	13.5	13.0
Delta T for STTS_L (ΔT_L)	16.3	20.0	20.0	19.8	20.0	19.0	20.0	20.0	19.8	20.0	19.0
Delta T for STTS_M (ΔT_M)	18.0	25.0	25.0	25.0	23.8	25.0	25.0	25.0	25.0	23.8	25.0
Delta T for STTS_H (ΔT_H)	22.5	25.0	25.0	25.0	24.5	24.5	25.0	25.0	25.0	24.5	24.5
Delta T for summer-mode (ΔT_S)	23.8	25.0	25.0	21.0	23.5	16.5	25.0	25.0	21.0	23.5	16.5
Min. STTS ACL case 1 (ACLmin1)	*0.0*	*0.0*	*0.0*	*0.0*	*0.0*	*0.0*	*0.0*	*0.0*	*0.0*	*0.0*	*0.0*
Max. STTS ACL case 1 (ACLmax1)	1.2	1.2	1.2	1.2	1.2	1.2	1.2	1.2	1.2	1.2	1.2
ACLmin2	0.8	1.6	0.8	1.0	1.3	0.8	1.6	0.8	1.0	1.3	0.8
ACLmax2	*2.4*	*2.4*	*2.4*	*2.4*	*2.4*	*2.4*	*2.4*	*2.4*	*2.4*	*2.4*	*2.4*
Future Load Limit (FLL)	*15.5*	*15.5*	*15.5*	*15.5*	*15.5*	*15.5*	*15.5*	*15.5*	*15.5*	*15.5*	*15.5*

Note: Italic indicates the parameter is set to a constant value during the optimization

Table A2.5: Results for CLO optimization

Item/Year	4	5	6	7	8	9	10	11	12	13	14
Total Incident Solar Energy (GJ)	12480	12919	13286	13941	12692	12498	12922	13265	13946	12699	12505
NET Total Solar Energy Collected (incl. loop losses) (GJ)	3884	4032	4150	4424	3888	3747	3952	4072	4385	3848	3717
Total Solar Energy Delivered to STTS (GJ)	3862	4013	4126	4401	3864	3725	3933	4048	4360	3824	3693
Energy Delivered to BTES (GJ)	2287	2488	1994	2209	2191	2146	2385	1913	2142	2139	2105
Energy Extracted from BTES (GJ)	1229	842	1163	1107	1227	1349	845	1188	1143	1249	1384
Solar Energy Delivered to District Loop (GJ)	2547	2040	2993	3002	2594	2647	2053	3013	3045	2626	2680
Total Gas Energy Used (GJ)	364	63	91	172	135	253	48	64	127	102	218
Boiler Thermal Energy Delivered to the District Loop (GJ)	328	57	81	155	121	228	43	57	114	92	196
Total Energy Delivered to District Loop (GJ)	2875	2097	3074	3157	2715	2876	2096	3070	3159	2717	2876
Electricity used by Pumps (GJ)	131	105	139	142	123	125	104	137	142	122	124
Gas + 3*Electricity (GJ)	758	379	508	598	503	627	361	475	553	468	589
Solar Fraction (%)	88.6	97.3	97.3	95.1	95.5	92.1	97.9	98.1	96.4	96.6	93.2
Weighted Solar Fraction (%)	77.1	84.3	85.5	83.4	83.8	80.8	85.1	86.4	84.6	84.9	82.0
Average Solar Collector Efficiency (incl. loop losses) (%)	31.1	31.2	31.2	31.7	30.6	30.0	30.6	30.7	31.4	30.3	29.7
STTS losses (GJ)	111	127	122	120	118	118	134	128	124	122	121
BTES losses (GJ)	1079	1222	1067	1001	991	918	1109	987	935	935	870

Table A2.6: Control parameters for CLO optimization

Parameter/Year	4	5	6	7	8	9	10	11	12	13	14
Winter Charge Factor	*0.5*	*0.5*	*0.5*	*0.5*	*0.5*	*0.5*	*0.5*	*0.5*	*0.5*	*0.5*	*0.5*
Winter Discharge Factor	*9.0*	*9.0*	*9.0*	*9.0*	*9.0*	*9.0*	*9.0*	*9.0*	*9.0*	*9.0*	*9.0*
minUE_L_L: Min. Usable Solar Energy for [STTS_L,BTES_L] scenario	3.7	3.1	3.7	3.2	3.2	3.2	3.2	3.2	3.2	3.2	3.2
minUE_L_H : STTS_L,BTES_H	2.1	1.0	1.7	1.8	1.8	1.1	1.1	1.1	1.1	1.1	1.1
maxL_L_L: Max. District Load for [STTS_L,BTES_L] scenario	12.5	12.0	12.5	12.0	12.3	12.3	12.3	12.3	12.3	12.3	12.3
maxL_L_H: STTS_L,BTES_H	13.5	13.0	13.8	13.8	14.0	13.5	13.5	13.5	13.5	13.5	13.5
max_L for STTS_M and BTES_L/H	13.5	13.5	13.5	13.5	13.5	13.5	13.5	13.5	13.5	13.5	13.5
Delta T for STTS_L (ΔT_L)	17.5	18.0	18.0	18.0	17.8	17.8	17.8	17.8	17.8	17.8	17.8
Delta T for STTS_M (ΔT_M)	17.0	20.5	21.0	22.3	21.5	20.5	20.5	20.5	20.5	20.5	20.5
Delta T for STTS_H (ΔT_H)	23.0	23.5	23.5	23.5	23.5	23.3	23.3	23.3	23.3	23.3	23.3
Delta T for summer-mode (ΔT_S)	16.0	23.5	23.0	23.0	22.5	23.3	23.3	23.3	23.3	23.3	23.3
Min. STTS ACL case 1 (ACLmin1)	*0.0*	*0.0*	*0.0*	*0.0*	*0.0*	*0.0*	*0.0*	*0.0*	*0.0*	*0.0*	*0.0*
Max. STTS ACL case 1 (ACLmax1)	*1.3*	*1.3*	*1.3*	*1.3*	*1.3*	*1.3*	*1.3*	*1.3*	*1.3*	*1.3*	*1.3*
ACLmin2	1.0	1.1	1.0	1.0	1.2	1.0	1.0	1.0	1.0	1.0	1.0
ACLmax2	*2.4*	*2.4*	*2.4*	*2.4*	*2.4*	*2.4*	*2.4*	*2.4*	*2.4*	*2.4*	*2.4*
Future Load Limit (FLL)	*15.5*	*15.5*	*15.5*	*15.5*	*15.5*	*15.5*	*15.5*	*15.5*	*15.5*	*15.5*	*15.5*

Note: Italic indicates the parameter is set to a constant value during the optimization